

**RELIABILITY AND CONDITION-BASED MAINTENANCE
ANALYSIS OF DETERIORATING SYSTEMS SUBJECT TO
GENERALIZED MIXED SHOCK MODEL**

A Dissertation Presented to
the Faculty of the Department of Industrial Engineering
University of Houston

In Partial Fulfillment
of the Requirements for the Degree of
Doctor of Philosophy
in Industrial Engineering

By
Koosha Rafiee Darmian

August 2014

Reliability and Condition-based Maintenance Analysis of Deteriorating Systems subject to Generalized Mixed Shock Model

Koosha Rafiee Darmian

Approved:

Chair of the Committee
Qianmei Feng, Associate Professor
Industrial Engineering

Committee Members:

Gino Lim, Associate Professor
Industrial Engineering

David W. Coit, Professor
Industrial and Systems Engineering
Rutgers University

Marvin Karson, Adjunct Professor
Industrial Engineering

Zhu Han, Associate Professor
Electrical and Computer Engineering

Suresh K. Khator, Associate Dean,
Cullen College of Engineering

Gino Lim, Associate Professor and
Chairman, Industrial Engineering

Acknowledgements

I would have never been able to finish my Ph.D. dissertation without the guidance of my advisor and my committee members, the help from my friends, and the support from my family.

First, I would like to express my deep gratitude to my advisor, Dr. Qianmei Feng, for her excellent guidance and continuing encouragement ever since I joined her research group. She generously shared her ideas about different research topics with me. Otherwise, I would not be able to broaden the scope of my research.

I wish to express my appreciation to the Chair of Industrial Engineering Department, Dr. Gino Lim, for his unconditional support through my Ph.D. study. I am also very grateful to Dr. David W. Coit, for his detailed and constructive comments, and for his important support throughout this work. My sincere thanks are due to other committee members, Dr. Marvin Karson, Dr. Zhu Han, and Dr. Erhun Kundakcioglu, for their detailed review, constructive criticism and excellent advice during the preparation of this dissertation.

I also wish to extend my warmest thanks to Mrs. Sharon D. Hall and all those who have helped me in the Department of Industrial Engineering, University of Houston.

I owe my loving thanks to my family. They have lost a lot due to my research abroad. Without their encouragement and understanding it would have been impossible for me to finish this work.

Financial support from the University of Houston and National Science Foundation under grant No. 0970140 is gratefully acknowledged.

**RELIABILITY AND CONDITION-BASED MAINTENANCE
ANALYSIS OF DETERIORATING SYSTEMS SUBJECT TO
GENERALIZED MIXED SHOCK MODEL**

An Abstract of a
Dissertation Presented to
the Faculty of the Department of Industrial Engineering
University of Houston

In Partial Fulfillment
of the Requirements for the Degree of
Doctor of Philosophy
in Industrial Engineering

By
Koosha Rafiee Darmian

August 2014

Abstract

For successful commercialization of evolving devices (e.g., micro-electro-mechanical systems, and biomedical devices), there must be new research focusing on reliability models and analysis tools that can assist manufacturing and maintenance of these devices. These advanced systems may experience multiple failure processes that compete against each other. Two major failure processes are identified to be deteriorating or degradation processes (e.g., wear, fatigue, erosion, corrosion) and random shocks. When these failure processes are dependent, it is a challenging problem to predict reliability of complex systems. This research aims to develop reliability models by exploring new aspects of dependency between competing risks of degradation-based and shock-based failure considering a generalized mixed shock model, and to develop new and effective condition-based maintenance policies based on the developed reliability models.

In this research, different aspects of dependency are explored to accurately estimate the reliability of complex systems. When the degradation rate is accelerated as a result of withstanding a particular shock pattern, we develop reliability models with a changing degradation rate for four different shock patterns. When the hard failure threshold reduces due to changes in degradation, we investigate reliability models considering the dependence of the hard failure threshold on the degradation level for two different scenarios. More generally, when the degradation rate and the hard failure threshold can simultaneously transition multiple times, we propose a rich reliability model for a new generalized mixed shock model that is a combination of extreme shock model, δ -shock model and run shock model. This general assumption reflects complex behaviors

associated with modern systems and structures that experience multiple sources of external shocks.

Based on the developed reliability models, we introduce new condition-based maintenance strategies by including various maintenance actions (e.g., corrective replacement, preventive replacement, and imperfect repair) to minimize the expected long-run average maintenance cost rate. The decisions for maintenance actions are made based on the health condition of systems that can be observed through periodic inspection. The reliability and maintenance models developed in this research can provide timely and effective tools for decision-makers in manufacturing to economically optimize operational decisions for improving reliability, quality and productivity.

Table of Contents

Acknowledgements	iv
Abstract.....	vi
Table of Contents	viii
List of Figures.....	xii
List of Tables	xv
Acronyms	xvi
Chapter 1 Introduction	1
1.1. Dependent Competing Risks of Degradation and Shocks	1
1.2. Condition-based Maintenance	4
1.3. Problem Statement	5
1.4. Objectives and Contributions.....	7
1.5. Organization of the Dissertation	9
Chapter 2 Literature Review	13
2.1. Random Shock Models	13
2.1.1. Classification of Shock Models According to Arrival Time	13
2.1.2. Classification of Shock Models According to Impact	15
2.2. Degradation Models.....	18
2.2.1. Classification of Degradation Models According to Trend	18
2.2.2. Classification of Degradation Models According to Variation	18
2.2.3. Classification of Degradation Models According to Modeling Approach ...	19
2.3. Multiple Competing Failure Processes of Degradation and Random Shocks	22
2.3.1. Independence between Degradation and Random Shocks	23
2.3.2. Dependence between Degradation and Random Shocks	25
2.4. Condition-based Maintenance Policy	27

Chapter 3 Reliability Modeling for Dependent Competing Failure Processes with Changing Degradation Rate.....	30
3.1. Introduction.....	30
3.2. System Description	32
3.2.1. Modeling of Hard Failure Due to Shocks	34
3.2.2. Modeling of Soft Failure Due to Degradation and Shocks.....	35
3.3. Reliability Analysis Considering Changing Degradation Rate	37
3.3.1. Case 1: Generalized Extreme Shock Model	38
3.3.2. Case 2: Generalized δ -Shock Model.....	39
3.3.3. Case 3: Generalized m-Shock Model	42
3.3.4. Case 4: Generalized Run Shock Model	44
3.4. Numerical Examples and Results	47
3.4.1. Reliability Analysis for Case 1	49
3.4.2. Reliability Analysis for Case 2	50
3.4.3. Reliability Analysis for Case 3	51
3.4.4. Reliability Analysis for Case 4	52
3.5. Conclusion	53
Chapter 4 Reliability Assessment of Competing Risks with Generalized Mixed Shock Model	55
4.1. Introduction.....	55
4.2. Reliability Modeling with Generalized Mixed Shock Model.....	57
4.2.1. Transition Process	60
4.2.2. Shock Process and Hard Failure	62
4.2.3. Degradation Process and Soft Failure.....	64
4.2.4. System Reliability Modeling	65
4.3. Probability of Trigger Shock Count in the Generalized Mixed Shock Model	66

4.3.1.	Applicability of Different Shock Models	66
4.3.2.	Probability of Trigger Shock Count.....	68
4.3.3.	Probability of no Transition in Remaining Shocks.....	70
4.4.	Numerical Examples	72
4.5.	Conclusion	75
Chapter 5 Reliability Analysis and Condition-based Maintenance for Multiple Failure Processes under Degradation-dependent Hard Failure Threshold		76
5.1.	Introduction.....	76
5.2.	Reliability Analysis with Decreasing Hard Failure Threshold	78
5.2.1.	Modeling Soft Failure	80
5.2.2.	Modeling Hard Failure.....	82
5.2.3.	System Reliability Analysis.....	85
5.3.	Condition-based Maintenance Based on Failure Limit Policy	88
5.4.	Numerical Examples.....	91
5.4.1.	Reliability Analysis for Case 1	92
5.4.2.	Reliability Analysis for Case 2	93
5.4.3.	Optimal Maintenance Policy.....	94
5.5.	Conclusion	96
Chapter 6 Condition-based Replacement Analysis for Multi-stent Systems		98
6.1.	Introduction.....	98
6.2.	Analysis of Two Failure Processes for Stents.....	100
6.3.	Reliability Function of Multi-stent Systems	102
6.4.	Condition-based Replacement with Warning Limit	104
6.5.	Numerical Examples.....	110
6.6.	Conclusion	111

Chapter 7 A Condition-based Maintenance Strategy for Repairable Deteriorating Systems subject to Generalized Mixed Shock Model	113
7.1. Introduction.....	113
7.2. System Failure Modeling.....	115
7.2.1. Degradation-based Failure Modeling	116
7.2.2. Shock-based Failure Modeling	118
7.2.3. System Reliability Function.....	122
7.3. Condition-based Maintenance Strategy	122
7.3.1. Probability of Performing Imperfect Repair	124
7.3.2. Probability of Performing Preventive Replacement	125
7.3.3. Probability of Performing Corrective Replacement	127
7.3.4. Probability Density Functions of T_w and T_p	129
7.3.5. Expected Cost Rate	130
7.4. Illustrative Examples	131
7.5. Conclusions.....	134
Chapter 8 Conclusions and Summary	135
References	138
Appendices.....	152
Appendix I: The Probability of no Hard Failure given $S_1 \leq N(t) = i$ in Section 4.2.3..	152
Appendix II: The Probability of no Soft Failure given $S_1 \leq N(t) = i$ in Section 4.2.4..	152
Appendix III: List of Publications	153

List of Figures

Figure 1.1: Flow diagram to illustrate the contributions of this study in terms of the new aspects of dependency between shock process and degradation process	9
Figure 1.2: Flow diagram to illustrate the contributions of this study in terms of new condition-based maintenance policies	9
Figure 3.1: Two dependent competing failure modes: a) soft failure, b) hard failure	33
Figure 3.2: Generalized extreme shock model	38
Figure 3.3: Generalized δ -shock model ($B_4 < \delta$).....	40
Figure 3.4: Generalized m -shock model ($m = 2$)	42
Figure 3.5: Generalized run shock model ($n = 2$).....	45
Figure 3.6: Plot of $R(t)$ for Case 1.....	49
Figure 3.7: Sensitivity analysis of $R(t)$ on D_0 / D_1 for Case 1	50
Figure 3.8: Sensitivity analysis of $R(t)$ on $\mu_{\beta 2} / \mu_{\beta 1}$ for Case 1.....	50
Figure 3.9: Plot of $R(t)$ for Case 2.....	50
Figure 3.10: Sensitivity analysis of $R(t)$ on δ for Case 2	51
Figure 3.11: Sensitivity analysis of $R(t)$ on $\mu_{\beta 2} / \mu_{\beta 1}$ for Case 2.....	51
Figure 3.12: Plot of $R(t)$ for Case 3.....	51
Figure 3.13: Sensitivity analysis of $R(t)$ on D_0 / D_1 for Case 3	52
Figure 3.14: Sensitivity analysis of $R(t)$ on $\mu_{\beta 2} / \mu_{\beta 1}$ for Case 3.....	52
Figure 3.15: Plot of $R(t)$ for Case 4.....	53
Figure 3.16: Sensitivity analysis of $R(t)$ on D_0 / D_1 for Case 4.....	53
Figure 3.17: Sensitivity analysis of $R(t)$ on $\mu_{\beta 2} / \mu_{\beta 1}$ for Case 4.....	53
Figure 4.1: Two dependent competing failure processes: (a) soft failure, (b) hard failure	59

Figure 4.2: Plot of $R(t)$	74
Figure 4.3: Sensitivity analysis of $R(t)$ on D_e	74
Figure 4.4: Sensitivity analysis of $R(t)$ on δ	74
Figure 4.5: Sensitivity analysis of $R(t)$ on D_r	74
Figure 5.1: Two dependent competing failure modes for Case 1	79
Figure 5.2: Two dependent competing failure modes for Case 2	79
Figure 5.3: Condition-based maintenance policy	89
Figure 5.4: Plot of $R(t)$ for Case 1	93
Figure 5.5: Sensitivity analysis of $R(t)$ on D_1 / D_0 for Case 1	93
Figure 5.6: Plot of $R(t)$ for Case 2.....	93
Figure 5.7: Sensitivity analysis of $R(t)$ on α for Case 2	93
Figure 5.8: Plot of $C_A(\tau, H_R)$ on H_R and τ for Case 1	95
Figure 5.9: Plot of $C_A(\tau, H_R)$ on H_R and τ for Case 2	95
Figure 5.10: Sensitivity analysis of $C_A(\tau, H_R)$ on D_1 for Case 1	95
Figure 5.11: Sensitivity analysis of $C_A(\tau, H_R)$ on α for Case 2	95
Figure 6.1. Two failure processes of degradation and random shocks	102
Figure 6.2: Condition-based replacement policy	106
Figure 6.3: $C_A(\tau)$ versus τ	110
Figure 6.4: Sensitivity analysis of $C_A(\tau^*)$ and τ^* on a_{war}	111
Figure 6.5: Sensitivity analysis of $C_A(\tau^*)$ and τ^* on a_{th}	111
Figure 7.1: Two dependent competing failure processes:	116
(a) <i>degradation-based failure</i> , (b) <i>shock-based failure</i>	116
Figure 7.2: Proposed condition-based maintenance policy	122

Figure 7.3: Scenario 1 for performing preventive replacement at the i^{th} inspection	125
Figure 7.4: Scenario 2 for performing preventive replacement at the i^{th} inspection	126
Figure 7.5: Scenario 1 for performing corrective replacement at the i^{th} inspection	127
Figure 7.6: Scenario 2 for performing corrective replacement at the i^{th} inspection	128
Figure 7.7: Plot of $R(t)$	132
Figure 7.8: Sensitivity analysis of $R(t)$ on D_e	132
Figure 7.9: Sensitivity analysis of $R(t)$ on D_r	132
Figure 7.10: Sensitivity analysis of $R(t)$ on δ	132

List of Tables

Table 3.1: Parameter values	48
Table 4.1: Probability for occurrence of different shock patterns	68
Table 4.2: Probability of no transition after the l^{th} transition.....	71
Table 4.3: Parameter values	73
Table 5.1: Parameter values	92
Table 6.1. Parameter values for multi-component system reliability analysis	104
Table 7.1. Parameter values	131

Acronyms

Micro-electro-mechanical systems	MEMS
Dependent competing failure processes	DCFP
Degradation-threshold-shock	DTS
Condition-based maintenance	CBM
Condition-based replacement	CBR
Corrective maintenance	CM
Preventive maintenance	PM
Failure limit policy	FLP
Independent and identically distributed	<i>i.i.d.</i>
Cumulative distribution function	cdf
Probability density function	pdf
Nonlinear mixed-effect	NLME
First passage time distribution	FPTD
Stress-strength interference	SSI

Chapter 1

Introduction

This chapter introduces the research background about the reliability modeling and maintenance scheduling for systems subject to multiple failure processes. It is important to consider the dependence relationship between multiple failure processes to have an accurate estimation of the system reliability and an optimum maintenance policy. A detailed explanation about the importance of this research along with research objectives are presented in this chapter.

1.1. Dependent Competing Risks of Degradation and Shocks

In a highly competitive global market, emerging technologies and new products are challenged to compete to survive. Consumers appreciate high quality products that can bring ease and convenience to use on a daily base. When it comes to choosing a product, customers often compare alternatives based on their quality characteristics. One of the most valuable quality characteristics with which consumers are concerned is the reliability performance of products. Reliability is defined as the probability that a product functions for a desired period of time without failure under specified operating conditions (Elsayed 1996).

Typical quality characteristics such as dimensions, weight, etc. can be monitored during the production phase before delivering final products to consumers; however, the reliability is a time-dependent quality characteristic and it can only be estimated (Elsayed 2000). Therefore, researchers have focused on the development of probabilistic models to estimate reliability of complex systems. Predicting reliability of such systems is a

challenging problem due to interactions among components and environmental factors. To overcome this difficulty, it is necessary to explore the mechanisms that lead to the system failure.

System failures can be broadly classified into three categories (Meeker & Hamada 1995): infant mortality, external shocks/accidents, and unavoidable graceful degradation. Systems, especially mechanical devices, usually deteriorate and lose the intended functionality due to wear, fatigue, erosion, corrosion, and aging (Huynh et al. 2012). Systems can also stop functioning abruptly due to shocks, overloads, and other external stressors. Some systems may be affected by more than one failure process at a time. These processes compete against each other, and whichever occurs first can cause the system to fail. For example, a battery that supplies electrical power by chemical reaction weakens due to usage. On the other hand, a battery can suddenly fail under unusual environmental conditions or stressors, such as overheating and over-voltage. Due to the structure of complex systems, independence assumption of random shocks and degradation is unrealistic, and may lead to inaccurate estimation of the system reliability. Therefore, the dependence between these failure processes should not be neglected in reliability analysis of complex systems.

Generally, there are three aspects of a dependence relationship between competing failure risks of degradation and random shocks:

a) *Degradation toward shocks*: Most previous research assumes that the hard failure threshold remains a constant during the entire life of a device (Wang et al. 2008; Peng et al. 2010) or decreases according to different shock patterns (Jiang et al. 2012), which are appropriate assumptions for many design problems. However, due to the nature of

degradation for complex devices such as MEMS, a degraded system is more vulnerable to external forces and stresses during the operation. In other words, a device is more likely to fail against external shocks when it suffers more degradation. Few researchers considered the impact of degradation process toward shocks process. For instance, Fan et al. (2000) studied a multi-component system subject to the non-homogeneous Poisson process, while aging affects the magnitude of random shocks resulting in a higher failure rate. However, there is no research in the literature exploring the dependence of hard failure threshold on the degradation level.

b) *Shocks toward shocks*: When random shocks arrive, the system becomes more sensitive to future shocks. Jiang et al. (2012) assumed the hard failure threshold is not fixed, and can change due to different shock patterns (i.e., extreme shock model, m -shock model, and δ -shock model). The hard failure threshold shifts to a lower level when one of the shock patterns occurs.

c) *Shocks toward degradation*: In most studies on the competing failure processes, the degradation follows a linear path where the degradation rate is a random variable with known and fixed parameters (Wang et al. 2008; Peng et al. 2010), which is a valid assumption for many cases. However, for complex devices such as MEMS, the degradation rate can increase when the system becomes more prone to fatigue and deteriorates faster, as a result of withstanding shocks. The impact of shocks on the degradation process typically presents in two different ways: 1) an abrupt increment of the degradation level, and 2) increasing the degradation rate. For example, a component of a MEMS device becomes more susceptible to degradation/soft failure and degrades faster, after exposure to a significantly large shock (Tanner et al. 2000). When a device begins vibrating due to

impact of huge shocks, the deterioration rate of the device increases suddenly (Saassouh et al. 2007). Cha and Finkelstein (2009) assumed that random shocks may cause the catastrophic failure with probability $p(t)$, or may accelerate the wear process with probability $1 - p(t)$. Peng et al. (2010) proposed a reliability model for complex systems where the degradation is accumulated by continuous degradation over time and sudden increase due to shocks. However, there is a lack of research in the literature about the impact of different shock patterns on the degradation rate.

1.2. Condition-based Maintenance

Products deteriorate and finally break down because they are subject to load and stress while functioning in dynamic environments. Performing maintenance is an effective approach to achieve a satisfactory level of product reliability during its life. An effective maintenance plays an important role in mitigating the risk of system failure. Various maintenance policies have been proposed in the literature from corrective maintenance (CM), preventive maintenance (PM), to the recent condition-based maintenance (CBM). The early form of maintenance policies was unplanned maintenance (also called corrective maintenance), happening only at system failure. A later form of maintenance policies is planned or preventive maintenance that occurs to prevent system failures when the system is still functioning. In the traditional PM, maintenance actions are scheduled to be carried out at the predetermined intervals based on the historical life time data. The major problem that makes the PM approach less practical is that maintenance decision is made not based on the real health condition of the system, which may result in unnecessary maintenance actions and increase the maintenance cost. On the other hand, CBM, a recent approach of PM, is more effective because it takes into account the real health condition of the system

(i.e., degradation level) that can be observed through periodic inspection, continuous monitoring or the combination of both.

1.3. Problem Statement

In reality, there are many challenges that prevent the commercialization of new and evolving technologies such as micro-electro-mechanical systems (MEMS) and biomedical implant devices (e.g., stent). MEMS are a new technology that is composed of miniaturized mechanical and electro-mechanical components (i.e., actuators and sensors) that are made using micro-fabrication methods (Huang et al. 2012). MEMS devices have been used in many products such as accelerometers in automotive airbag deployment systems, and inkjet printer heads (Tanner 2009). They can also be applied in critical industries such as aerospace, nuclear, biological/medical and weapons due to cost efficiency, small size and weight, and high throughput (Peng et al. 2009). Stents, a small scaffold, are one of evolving bio-structures that are implanted in human arteries to counteract the effects of atherosclerosis (preventing the artery wall from collapsing). As reported in 2005, over one million stents are implanted in human arteries each year, and the market for endo- and cardiovascular stents was estimated to exceed \$7 billion annually (Marrey et al. 2006). However, one of the major challenges that have to be addressed for successful commercialization of advanced devices (e.g., MEMS and stents) is to improve reliability performance. It can assure that devices meet the required lifetime for commercial applications and defense-related products.

To address MEMS reliability issues, potential failure processes must be investigated for predicted usage conditions. MEMS may fail due to wear process or may break down due to shock loads caused by external sources. In the literature, these two

failure processes have been assumed to be independent, which is not a valid assumption. Complex structures of MEMS, due to both mechanical and electrical parts, and their interactions, make the wear process and shock process dependent. Therefore, conducting reliability research to explore new aspects of dependency between failure processes can help the commercialization of these products.

Traditionally, it has been assumed that a system fails as result of one large shock (i.e., extreme shock model), cumulative damages of smaller consecutive shocks (i.e., run shock model), or a short time lag between successive shocks (i.e., δ -shock model). However, in practice, it is common that a system fails due to more than one particular shock model (i.e., mixed shock model). The mixed shock models investigated in the literature are typically a combination of two classic shock models. There is a lack of research to incorporate three or more classic shock models into a generalized mixed shock model.

Another major challenge due to increasing product complexity is the high maintenance cost that has created a major expense for many industries. Therefore, a new maintenance approaches (e.g., CBM) must be introduced to handle this situation more efficiently. CBM is a technique that recommends maintenance actions according to the data collected through condition inspections (Jardine et al. 2006). CBM aims to prevent unnecessary maintenance actions by performing maintenance tasks only if an unusual system status is observed during inspections. The effective development and proper implementation of CBM policy is crucial, and can significantly cut maintenance costs through fewer PM actions. Most research about CBM modeling in the literature assumes that the system is non-repairable or the repair action is perfect, which is not a valid assumption for many cases. When the decision about a maintenance action is made based

on the actual health condition of a system, instead of the elapsed time or the number of inspections carried out since last action, there is a critical need for CBM policies to include different maintenance actions, such as corrective replacement, preventive replacement and imperfect repair.

1.4. Objectives and Contributions

The overall goals of this study are: 1) to develop reliability models by exploring new aspects of dependency between competing risks of soft failure due to degradation and hard failure due to shocks; and 2) to develop new and effective CBM policies based on the developed reliability modeling. We achieve these goals through five specific objectives:

Objective 1: Develop reliability models when the degradation rate increases according to a particular shock pattern. We assume the degradation rate shifts when a classic shock pattern occurs, including extreme shock model, δ -shock model, m -shock model and run shock model (Chapter 3).

Objective 2: Develop reliability models when the degradation rate and the hard failure threshold can simultaneously transition multiple times, whenever the condition for a generalized mixed shock model is satisfied. What distinguishes our new model from the previous research lies on this new assumption that the degradation rate and the hard failure threshold can *simultaneously* change *multiple times* given the condition for the *generalized mixed shock* model is satisfied (Chapter 4).

Objective 3: Investigate reliability models when the hard failure threshold is dependent on the degradation level. We assume that a system may suffer one time reduction in hard failure threshold as soon as the overall degradation reaches a critical value, or it may

undergo continuous reduction in hard failure threshold and the amount of reduction is proportional to the change in degradation (Chapter 5).

Objective 4: Explore a new generalized mixed shock model that can impact the degradation rate and hard failure threshold simultaneously, or lead to the failure of a system. We introduce a new shock model called generalized mixed shock model that is a combination of three classic shock models including extreme shock model, δ -shock model and run shock model (Chapters 4 and 7).

Objective 5: Develop new condition-based maintenance policies. Maintenance policies presented in Chapters 5 and 6 include preventive replacement and corrective replacement. Chapter 7 extends the proposed condition-based maintenance policy in previous chapters by adding imperfect repair action. The decisions for maintenance actions are made based on the system condition (e.g., degradation level) revealed at each inspection.

We use two figures to illustrate the contributions of this research. Figure 1.1 presents how this study distinguishes from the previous research, in terms of the new aspects of dependency between shock process and degradation process. Figure 1.2 represents how different CBM policies presented in this research are related to each other.

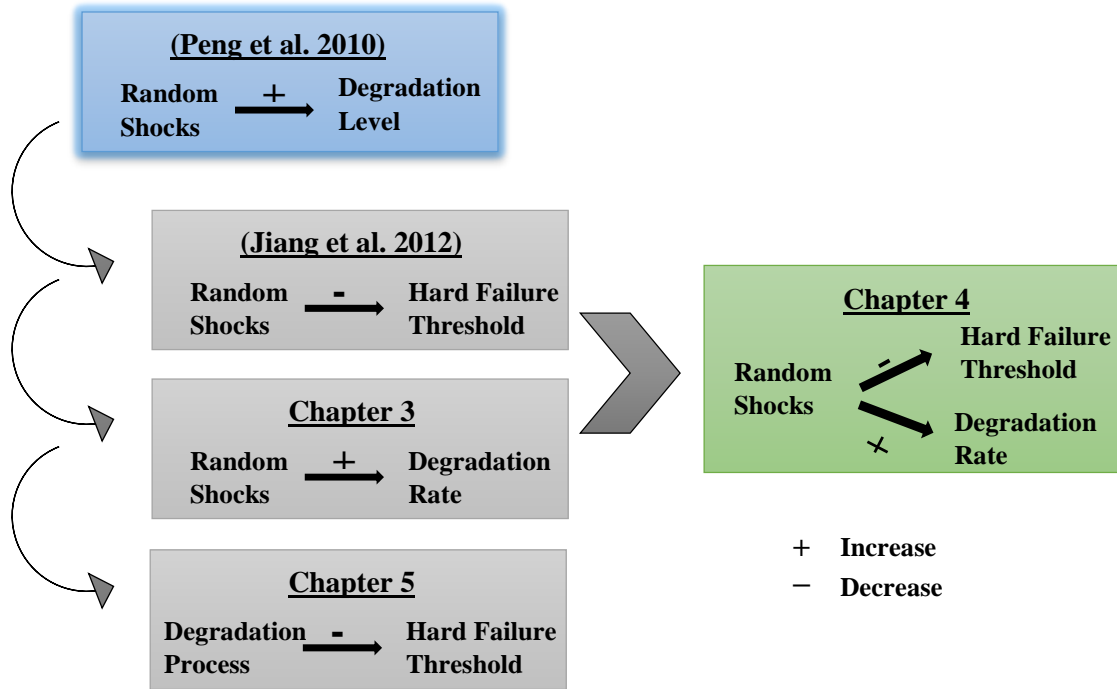


Figure 1.1: Flow diagram to illustrate the contributions of this study in terms of the new aspects of dependency between shock process and degradation process

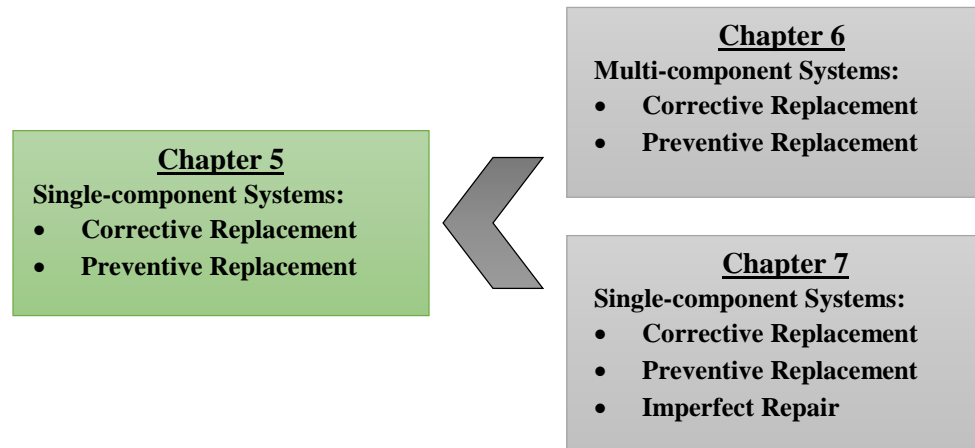


Figure 1.2: Flow diagram to illustrate the contributions of this study in terms of new condition-based maintenance policies

1.5. Organization of the Dissertation

The remaining dissertation is organized as follows. Chapter 2 presents literature reviews for shock models, degradation processes, competing failure processes, and CBM

policies. Chapter 3 presents reliability models for systems subject to multiple competing risks of soft failure and hard failure, with degradation rate transition. Soft failure occurs when the overall degradation (continuous degradation with additional abrupt damages caused by shocks) exceeds the soft failure threshold. Hard failure occurs when the magnitude of any shock is greater than the strength threshold. These two failure processes of soft failure and hard failure are dependent because: 1) each shock damages the system by increasing the degradation level; and 2) the degradation rate accelerates as soon as the condition for a particular shock model (extreme shock model, δ -shock model, m -shock model, or run shock model) is satisfied. Numerical results for MEMS are presented to illustrate the developed reliability models.

Chapter 4 develops a reliability model for complex systems subject to continuous degradation and random shocks under the impact from a generalized mixed shock model. The shock process contains fatal shocks that can cause hard failure instantaneously, and nonfatal shocks that impact the system in three different ways concurrently: 1) damage the unit by increasing the degradation instantaneously; 2) speed up the deterioration by accelerating the degradation rate; and 3) weaken the unit by reducing the hard failure threshold. While the first impact of non-fatal shocks comes from each individual shock, the other two impacts are realized when the condition for a generalized mixed shock model is satisfied, including the three classic shock models: extreme shock model, δ -shock model and run shock model. According to the proposed generalized mixed shock model, the degradation rate and the hard failure threshold shift simultaneously when at least one of these three shock models occurs. An example using MEMS devices illustrates the effectiveness of the proposed model with sensitivity analysis.

Chapter 5 introduces reliability analysis for systems subject to two competing failure risks of soft failure and hard failure, when the hard failure threshold depends on the degradation level. The system deterioration makes it more vulnerable to shocks by decreasing the strength threshold. We address two different scenarios of the changing hard failure threshold due to changes in degradation. In Case 1, the initial hard failure threshold value reduces to a lower level as soon as the overall degradation reaches a critical value. In Case 2, the hard failure threshold decreases continuously, and the amount of reduction is proportional to the change in degradation. A new CBM model derived from failure limit policy (FLP) is presented to ensure a device is functioning under a certain level of degradation. Finally, numerical examples are illustrated to explain the developed reliability and maintenance models along with sensitivity analysis.

Chapter 6 develops a condition-based replacement (CBR) models for a multi-component system of stents implanted in human arteries that is subject to both delayed and instantaneous failures. We develop a new CBR policy, in which the replacement is either a preventive or corrective action, performed depending on the condition of the system. Numerical examples using data from the literature are presented to investigate the effectiveness of the proposed CBR policy.

Chapter 7 proposes a CBM policy considering imperfect repair for complex systems subject to dependent competing risks of internal degradation and external shocks. External shocks can be divided into two classes: (1) *fatal shocks* that can cause the system to fail immediately, if a shock belongs to any of the three classic shock models (i.e., extreme shock model, run shock model, and δ -shock model), or the generalized mixed shock model; (2) *non-fatal shocks* that can damage the system by randomly increasing the

degradation level. Under the proposed CBM policy, the system is inspected at fixed time intervals and a decision for an appropriate maintenance action (i.e., no action, imperfect repair, preventive or corrective replacement) is made based on the actual health condition of the system detected through inspection. The imperfect repair impacts the system by lowering the degradation level to a certain level. The objective is to determine the optimal inspection interval that minimizes the expected long-run average maintenance cost rate. An MEMS example is used to evaluate the efficiency of developed reliability and CBM. Finally, conclusions for this research are given in Chapter 8.

Chapter 2

Literature Review

Literature reviews for random shock modeling, degradation modeling, multiple failure processes, and CBM policies are presented in this chapter.

2.1. Random Shock Models

Shock models are one of the most important subjects in reliability analysis, where a system is subject to shocks arriving at random times with random magnitudes. Many papers have studied the reliability of systems subject to shocks in a random environment, such as Wortman et al. (1994), Chelbi and Ait-Kadi (2000), Finkelstein and Zarudnij (2001), and Cirillo and Hüsler (2011). Mallor and Santos (2003) and Bai et al. (2006) surveyed the literature for shock models studied during the last three decades. According to their survey, shock models are classified according to their arrival time and their resulting effect on the system. In the first category, shock models are divided into four subcategories depending on how their arrival times are governed. In the second category, shock models are divided into five major models depending on how they can impact on the system.

2.1.1. *Classification of Shock Models According to Arrival Time*

1) *Homogeneous Poisson process*: The times between two successive shocks are independent, identically distributed (*i.i.d.*) exponential random variables. This model was first introduced by Esary et al. (1973). They proposed some models for the life distribution of a device subject to a sequence of shocks arriving randomly governed by a Poisson process. Li and Zhao (2007) investigated a general lifetime distribution for the δ -shock

model of complex systems consisting of n independent components where the shocks arrived according to homogeneous Poisson process. Finkelstein and Marais (2010) discussed the system failure and probabilities of failure-free performance of a system subject to a shock process that arrives according to a homogeneous Poisson process.

2) *Non-homogeneous Poisson process*: The probability of a shock in $(t, t + \Delta t]$ is $\lambda(t)\Delta t + o(\Delta t)$ based on a counting process with independent increments while the probability of more than one shock in $(t, t + \Delta t]$ is $o(\Delta t)$. Abdel-Hameed and Proschan (1973) introduced this model as an extension of the results obtained by Esary et al. (1973). They studied a device subject to shocks that arrive according to a nonhomogeneous Poisson process. Life distribution properties are related to the probability of failure after experiencing a given number of shocks. Li and Kong (2007) provided the analytical survival function, moment of any order, class properties and asymptotic behavior of a system for two cases: one with underlying homogeneous Poisson process and another case with underlying non-homogeneous Poisson process with periodic intensity $\lambda(t)$. Bai et al. (2012) analyzed the lifetime behavior of system subject to two types of shocks. The first type, called primary shocks that arrive according to a non-homogeneous Poisson process, causes a series of shocks called secondary shocks.

3) *Non-stationary pure birth process*: It is a Markov process where the probability of a shock in $(t, t + \Delta t]$ is $\lambda_j \lambda(t) \Delta t + o(\Delta t)$, given j shocks in $(0, t]$, while the probability of more than one shock in $(t, t + \Delta t]$ is $o(\Delta t)$. Abdel-Hameed and Proschan (1975) introduced this model by considering the life distribution of a device subject to a series of shocks arriving randomly according to a non-stationary pure birth process. They showed that various fundamental classes of life distributions can be obtained under appropriate

assumptions on λ_j and $\lambda(t)$. Sheu et al. (2012) studied a system subject to shocks that occur according to a non-stationary pure birth process. As shocks arrive, two types of failures may happen: *i*) minor failure that can be fixed by a general repair, and *ii*) catastrophic failure that leads to an unplanned replacement. The number of shocks that have occurred since the last replacement indicates the failure type based on some random mechanism.

4) *Renewal process*: The interval times between two successive shocks are *i.i.d.* random variables. Skoulakis (2000) investigated a reliability system subject to shocks generated by a renewal point process. Shocks arrive independently of each other with equal probabilities, and the shock arrival times are random drawn from a distribution. Sumita and Shanthikumar (1985) analyzed a class of cumulative shock models associated with a bivariate sequence $\{X_n, Y_n\}$ of correlated random variables. The $\{X_n\}$ denote the sizes of the shocks and the $\{Y_n\}$ denote the times between successive shocks that follows a renewal process. Two models, depending on whether the size of the n^{th} shock is correlated with the length of the interval since the last shock or with the length of the succeeding interval until the next shock, are considered.

2.1.2. Classification of Shock Models According to Impact

1) *Extreme shock model*: a system fails as soon as the magnitude of a shock exceeds some given threshold. Shanthikumar and Sumita (1983) developed an extreme shock model by considering a sequence of random shocks associated with a correlated pair (X_n, Y_n) , where X_n represents the magnitude of the n th shock and Y_n is the time lag between two successive shocks. Cha and Finkelstein (2013) generalized the classic extreme shock model to the history-dependent case, where the probability that a system survives each shock depending on the corresponding history of the shock process.

2) *Cumulative shock model*: a system breaks down when the accumulated magnitude of shocks exceeds some given threshold. Agrafiotis and Tsoukalas (1995) discussed a class of cumulative process with excess increments where the counting process is generated by the renewal sequence. The first passage time problem along with various asymptotic properties of the process was also obtained. Qian et al. (2003) analyzed maintenance and minimal repair policies for a system subject to an extended cumulative shock model where random shocks arrive according to a non-homogeneous Poisson process. The system undergoes the maintenance action every time that a shock occurs. Gut and Hüsler (2005) considered a cumulative shock model in which only the summation of the most recent shocks contribute to the system failure. Bai et al. (2012) studied a generalized cumulative shock model with a cluster shock structure. The system is subject to two kinds of shocks, called primary shocks and secondary shocks, where each primary shock causes a series of secondary shocks. They analyzed the lifetime behavior of the system with light-tailed and heavy-tailed distributed secondary shocks, while the primary shocks are governed by a non-homogeneous Poisson process.

3) *Run shock model*: a system works until the first run of n consecutive shocks greater than some given threshold. This model was defined by Mallor and Omey (2001) that studied random variables related to a shock reliability model. Their models can be used to study a system that breaks down when n consecutive shocks with critical magnitude arrive. They obtained characteristics of a distribution function of the random variables and limiting behaviors when n tends to infinity.

4) *δ -shock model*: a system fails when the time lag between two successive shocks falls into some critical region. Eryilmaz (2012) studied run-related generalization of the δ -

shock model such that the system breaks down when n consecutive interval times are less than a threshold δ . The survival function and the mean value of the failure time are derived when the shocks arrive according to a Poisson process. They also proposed a new combined shock model which considers both the magnitude of successive shocks and the interval times. Eryilmaz (2013) introduced a discrete time version of the shock model which has been studied previously for a continuous case. According to the model, a system fails when the interval time between two consecutive shocks is less than a pre-specified threshold, where the shocks occur according to a binomial process, i.e., the interval times between consecutive shocks follow a geometric distribution.

5) *Mixed shock model*: a system fails due to a mixture of different shock models. Traditionally, the mixed shock model studied in the literature is a combination of extreme shock model and cumulative shock model. This model was built by Gut (2001), in which the system is supposed to break down either because of one large shock, or as a result of many smaller ones. Cha and Finkelstein (2009) derived the survival function and corresponding failure rate function for systems subject to a specific shock process, which is a mixture of the extreme shock model and the cumulative shock model. Unlike traditional mixed shock models, Mallor et al. (2006) introduced the mixed shock model as a result of the combination of the run shock model and the cumulative shock model. They supposed that the system fails as soon as one of the following two events is presented: the accumulated damage exceeds a prefix level, or a critical run of specified length occurs. Eryilmaz (2012b) studied the survival function and mean time to failure of systems subject to a mixed shock model assuming that the shock magnitudes are random variable over discrete time periods.

2.2. Degradation Models

Reliability study based on degradation models has been focused on by a number of literature, such as Lu and Meeker (1993), Singpurwalla (1995), van Noortwijk and Pandey (2003), Pandey et al. (2005), Liao et al. (2006) and Yuan and Pandey (2009).

2.2.1. *Classification of Degradation Models According to Trend*

Degradation curves can be classified into three types (Meeker & Hamada 1995):

1) *Linear*: The degradation rate is constant over time. Linear degradation models can be used to model the increase of a resistance measurement over time (Suzuki et al. 1993) and to model lumen-output from florescent light bulbs over time (Taguchi 1987). The linear degradation also can be used to model wear degradation in advanced technology such as MEMS (Huang et al. 2012).

2) *Convex*: It is a non-linear degradation path where the degradation rate increases over time. In the literature, the convex-shape degradation path can be used to describe fatigue crack growth (Lu & Meeker 1993).

3) *Concave*: It is also a non-linear degradation path where the degradation rate tends to decrease over time. The concave degradation path can be used to model the degradation of electronic circuit boards (Meeker & LuValle 1995).

2.2.2. *Classification of Degradation Models According to Variation*

There are some factors impacting degradation-failure of systems, such as manufacturing, operating and environmental conditions. Depending on the degree of variability due to different factors, the degradation models can be categorized as follows (Meeker & Hamada 1995):

1) *Unit-to-unit variability*: The variability due to difference in the characteristics of individual units:

- *Initial degradation level*: The manufacturing process is not identical for all the units; therefore, it causes a unit-to-unit variability in the initial degradation level.
- *Degradation growth rate*: The variability in degradation growth rate is due to variability in material properties and component geometries or dimensions.
- *Degradation limit level*: The variability in the degradation threshold level is due to variability in material properties such as strength.

2) *Temporal variability due to operating and environmental conditions*: The variability in degradation-failure can be caused by operating and environmental conditions, called external noise (Taguchi 1986). Variability in operation conditions includes changes in the amount of stresses applied to components, and variability in environmental conditions includes different temperature, humidity, etc.

3) *Variability due to measurement errors*: Inspection tools and processes used to measure degradation amounts may have measurement errors associated with them and are not always error-free. Therefore, in order to determine the actual degradation, the measurement error should be considered in the measured degradation obtained by using an inspection device.

2.2.3. *Classification of Degradation Models According to Modeling Approach*

In the literature, there are three different approaches to model the degradation:

1) *Parametric method*: that is, using experimental data to estimate the degradation path parameters, also called the general path model. Lu and Meeker (1993) described a

two-stage method based on Monte Carlo simulation to estimate the parameters for the mixed-effect path. Wu and Shao (1999) studied the product reliability based on a nonlinear mixed-effect degradation model and the ordinary and weighted least squares method. A simulation was also run to assess the result obtained from the proposed method.

Yuan and Pandey (2009) presented an advanced a nonlinear mixed-effect (NLME) method to model and predict the degradation path. The NLME method considers unit-specific random effects and the potential correlation among repeated measurements, unlike traditional regression models. The method is applied to a nuclear pipe system example to predict degradation. Robinson and Crowder (2000) proposed a fully Bayesian approach to estimate the distribution function of failure time for both future units and those that are currently under test. In addition, fatigue crack growth data was used to illustrate the methods.

2) *Stochastic process method*: The degradation model is described as a stochastic process such as Brownian motion and gamma process. van Noortwijk et al. (1995) proposed a Bayesian approach of the failure model where the average degradation over a finite or an infinite time is defined by a prior density function. The probability of preventive repair and failure depends on the average deterioration. Xue and Yang (1995) generalized 2-state reliability parameters such as $R(t)$ to multi-state reliability parameters, $R(t, i)$ by combining a Markov process and a coherent multi-state system structure to transfer multi-state reliability dynamics to a set of 2-state reliability dynamics. The model was implemented for multi-state systems including series systems and parallel systems.

Ebrahimi (2001) assessed the failure time of a system by using a deterioration process and covariates. The survival and hazard functions for two semi-parametric models

are obtained by using the differential equation. Kharoufeh (2003) derived the the failure time distribution of a single-unit system by a Markov additive process where the cumulative damage over time follows a continuous wear process and depends on the external environment process. Kharoufeh and Cox (2005) developed a degradation based model to estimate the full and residual lifetime distributions for single-unit systems subject to a Markov environment by using a hybrid approach including two models: *i*) the degradation rate depends on the state of random environment that follows a homogeneous Markov process; and *ii*) the degradation rate is estimated by using the differential equation and clustering method.

Nicolai et al. (2007) focused on modeling the deterioration of an organic coating layer based on three stochastic processes including Brownian motion with non-linear drift, non-stationary gamma process, and two-stage hit-and-grow process. The model parameters were estimated by either the least-squares approach when the data set is based on expert judgment or the maximum likelihood when the data set is based on inspection results. The discrete degradation model can be utilized when the amount of degradation can be observed at the particular time points, e.g., the metal crack growth on an aircraft. Saassouh et al. (2007) proposed an online maintenance policy to maximize availability of a system with a two-mode stochastically deteriorating model. When the system is in the first mode, the deterioration level increases suddenly where the amount of increase follows a gamma process and the deterioration rate increases when the system transitions to the second mode. Hsieh et al. (2009) proposed a non-homogeneous compound Poisson process to model the discrete degradation. Then the first passage time distributions (FPTD) and the likelihood estimation of the model parameters are presented.

3) *Mixed parametric and stochastic process method*: that is, a combination of parametric and non-parametric methods, called statistical method. Bae and Kvam (2004) examined a nonlinear random coefficient model to predict the non-monotonic degradation path for highly reliable light displays. Performance of four different methods in approximating the log-likelihood function including Lindstrom-bates algorithm, adaptive Gaussian quadrature, adaptive importance sampling and first-order method were compared.

Huang and Dietrich (2005) proposed a new graphical approach for degradation reliability modeling considering the degradation path governed by a truncated Weibull distribution with a time-dependent shape parameter. A maximum likelihood method is derived to estimate the two parameters of Weibull distribution. Bae et al. (2007) investigated the relationship between the practitioner's selected degradation path function and the resulting lifetime distribution for two cases: in the first case, the additive function is used to model the degradation path; and in the second case, the multiplicative function is used. The result implies that the lifetime distribution is affected by the degradation path in terms of failure rate and distribution classes.

2.3. Multiple Competing Failure Processes of Degradation and Random Shocks

The failure of a system can be due to random shocks, or graceful degradation. Some systems may experience more than one failure process that compete against each other, and whichever occurs first causes the system to fail. Most of the papers in the literature assume that these two competing failure processes of random shocks and degradation are independent from each other, which is not a realistic assumption due to the structure of systems and may lead to inaccurate estimation of the system reliability. When they are

dependent, predicting the system reliability becomes a challenging problem. There are some aspects underlying the dependence assumption between these two failure processes: (1) random shocks cause abrupt increase in the degradation level; (2) random shocks accelerate the degradation rate; (3) random shocks make the system more vulnerable to upcoming shocks; and (4) the degradation makes the system more vulnerable to upcoming shocks.

2.3.1. Independence between Degradation and Random Shocks

Sim and Endrenyi (1993) proposed a Markov model for a system subject to deterioration and Poisson failures. In addition, the optimal maintenance policy including minimal repair, periodic minimal maintenance and major maintenance after a number of minimal maintenances was explored to minimize costs or unavailability. Ciampoli (1998) developed a probabilistic model to forecast the reliability of structural components where the deterioration process modeled by the stochastic differential equation is due to shocks created during regular operation and accidental events.

Hosseini et al. (2000) presented a generalized stochastic Petri net to formulate the maintenance policy for a system subject to deterioration process and shocks modulated by a homogeneous Poisson process. If the system fails due to deterioration failure, a major maintenance needs to be carried out to restore the system to “as good as new”; however, if the system breaks down due to shocks, a minimal maintenance needs to be performed to restore the system to an early stage. Chiang and Yuan (2001) developed a state-dependent maintenance policy for a multi-state continuous-time Markovian system subject to degradation and shocks. The system is inspected at scheduled time points. Depending on

the current state of the system, a further action is performed including do-nothing, repair and replacement.

Klutke and Yang (2002) derived the availability of a system that deteriorates due to random shocks that occur according to a Poisson process and graceful degradation that follows a linear path. The failure of the system is hidden and can be explored during periodical inspections. Huang and Askin (2004) extended the stress-strength interference (SSI) reliability model so that it can be applied for any non-homogeneous Poisson shock process and any type of strength degradation process. Wang and Zhang (2005) studied reliability of a system subject to two shock processes described by the extreme shock model and the δ -shock model. The failed system undergoes a repair to make it “as good as new”; however, repair times follow a stochastically-increasing geometric process. The optimal replacement policy determines the number of repairs before the system is being replaced, to minimize the long-run average cost.

Li and Pham (2005) extended the multi-state degraded system reliability when there is more than one failure process. They derived a generalized reliability model for a multi-state degraded system subject to two degradation processes and a cumulative shock process that are independent. Montoro-Cazorla and Pérez-Ocón (2006) presented a maintenance policy for a two-unit cold standby system, where the units are repairable. Two types of maintenance actions governed by phase-type distributions are considered: PM that restores the unit degradation to be operative and CM that replaces the failed unit. Chien et al. (2006) proposed a generalized maintenance policy for a system subject to random shocks that are modeled by a non-homogeneous Poisson process. The system is replaced as soon as: (i) the n^{th} minor failure occurs where the first $n - 1$ minor failures are rectified by minimal

repair; (ii) catastrophic failure occurs where its probability depends on the number of shocks since the last replacement; or (iii) the age of system exceeds T .

van der Weide et al. (2010) introduced a method to assess the reliability of systems subject to transient shocks and a degradation process which is modeled as a cumulative stochastic point process. Furthermore, a combined maintenance policy considering both condition-based and aged-based criteria was presented. Wang and Pham (2011) studied reliability and maintenance modeling for a system subject to competing risks of degradation wear and random shocks. Two kinds of random shocks are considered: 1) fatal shocks that can lead to sudden failures, and 2) nonfatal shocks that cause abrupt damage in the degradation level.

2.3.2. Dependence between Degradation and Random Shocks

Satow et al. (2000) put forward a replacement policy for a system that is damaged due to shocks or aging. The system is considered as failed as soon as the damage exceeds the threshold level K . To avoid failure, the system is inspected after each shock and replaced if the damage is beyond a lower threshold k . The optimum maintenance policy defines an optimal k^* that minimizes the expected cost rate. Chiodo and Mazzanti (2006) dealt with the stress-strength model for a system subject to repeated shocks while the system fails when the magnitude of a shock is greater than the remaining degradation resistance.

van Noortwijk et al. (2007) introduced a time-dependent reliability model for a structural component subject to two stochastic processes, which are the deteriorating resistance that follows a gamma process and the fluctuating load that is governed by a Poisson process. Wang et al. (2008) dealt with multi-state system reliability for a system

subject to dependent and competing risks of shocks and degradation process, when the transition time from state i to $i + 1$ is a random variable. The shocks that are generated by the system themselves during the operation have regular periods; however, the shocks that are imposed from the external environment are governed by a Poisson process. Frostig and Kenzin (2009) examined an availability model for a hidden-failure system that breaks down due to the cumulative shock model and degradation process according to two different scenarios. In the first scenario, the shocks and degradation process are independent of the external environment; in the second scenario, the shock arrival rate, the shock size and the degradation rate depend on the external environment that is modulated by a Markov process.

Lehmann (2009) focused on degradation-threshold-shock models (DTS) to discover how the survival function is affected when considering the relationship between failure time data and covariate data. Two types of DTS models are compared, including a general DTS where the degradation process and catastrophic failure are modeled based on stochastic processes, and the DTS with covariate where an external covariate process due to dynamic environment may affect soft failure and hard failure. Zhu et al. (2010) studied a maintenance model for a unit subject to the dependent competing risks of degradation and sudden failure. Every time that the unit breaks down, an immediate repair is carried out where the time associated with repair increases with the number of repairs. The proposed maintenance policy aims to maximize the unit availability given that the budget for repair cost is limited.

Huynh et al. (2011) compared a new CBM policy with traditional time-based block replacement policy for a system subject to two dependent competing risks of deterioration

and traumatic failure. Ye et al. (2011) introduced the single failure time model and the recurrent event model by using a Brown-Proschan model. The system subjects to shocks that arrive according to a non-homogeneous Poisson process and the degradation process, given that the amount of degradation and the magnitude of shocks are not observable. Chen et al. (2011) investigated reliability modeling for complex systems under dependent competing failures of degradation and shocks. In addition, the maintenance actions including inspection, PM and replacement are obtained to minimize the maintenance expected cost rate.

Wang and Pham (2011b) proposed a two-process combination model for a deteriorating system that fails due to multiple dependent competing risks of cumulative damage of shocks, where the multiple degradation processes include additive and multiplicative models. Furthermore, an imperfect PM policy was introduced to adopt inspection intervals and the total number of minimal repairs before replacement, in order to minimize the long-run average maintenance cost rate. Wang and Pham (2012) put forward a novel approach in the reliability modeling of systems subject to dependent competing risks of multiple degradation processes and random shocks by employing time-varying copulas. A time-scaled covariate factor is used to govern the dependent relationship between shocks and degradation processes.

2.4. Condition-based Maintenance Policy

Recently, there has been much research on the mathematical formulation of maintenance policies where the system undergoes a maintenance action such as corrective replacement, preventive replacement or imperfect repair according to the system condition. Liao et al. (2009) proposed a novel imperfect PM model to minimize the total maintenance

cost for a repairable system subject to both sudden failure and delayed failure. The aim of their sequential maintenance policy is to find (R^*, N^*) , where R^* is the optimum repair threshold (when the system reliability reaches R^* or an unexpected system failure occurs, a repair needs to be performed to restore the system to an earlier age), and N^* is the number of repairs that the system can be undergone before it is replaced. Zhao et al. (2010) discussed a CBM policy for a deteriorating system subject to environmental covariates that are modulated by a time-homogeneous Markov chain with finite state space. The optimum inspection interval and replacement policy is derived to minimize the average maintenance cost. Tan et al. (2010) investigated an imperfect maintenance policy for a repairable system that deteriorates according to a gamma process. The imperfect maintenance improves the system condition; however, the degradation level immediately after the repair is a random variable.

Fan et al. (2011) studied a predictive maintenance strategy for a repairable system subject to two dependent failure processes. The imperfect repair improves the system condition by impacting on the hazard rate function and effective age. The amount of age reduction depends on the resources allocated to perform maintenance. Fouladirad and Grall (2011) proposed a CBM strategy for a deteriorating system by using a detection algorithm. The deterioration is governed by a non-homogeneous gamma process, while at an unknown time the deterioration rate increases due to external factors. Li and Pham (2011) addressed a CBM policy for a system subject to degradation and cumulative shock damage. While the system is being inspected, the appropriate maintenance action can be performed, including PM, CM, or no actions. The optimum inspection interval and PM threshold are determined to minimize the long-run maintenance cost per unit time.

van and Bérenguer (2012) presented an imperfect PM strategy considering aspects of maintenance cost and productivity for a single-unit deteriorating system. The imperfect repair restores the system condition to “better than old”, but the repair actions can be performed for a limited number of times and the system will be replaced after. Taghipour and Banjevic (2012) studied a maintenance policy for a complex system including two types of components: the first type experiences hard failure that is self-announcing; and the second type experiences soft failure that is hidden and can only be detected during the inspection. The system can operate with soft failure, but its performance is declined. Even though the system is inspected periodically, the hard failure provides a chance for an unplanned inspection (opportunistic inspection). A minimal repair or corrective replacement is performed to remove both types of failure depending on the condition of system. Huynh et al. (2012) assessed the performance of degradation-based maintenance with minimal repairs. The minimal repair is carried out after a failure due to shocks to bring the system back to the same degradation level right before failure. A preventive replacement is performed when the degradation level exceeds a predetermined threshold.

Le and Tan (2013) studied inspection-maintenance schemes for a multi-state degradation system. The degradation follows a continuous-time Markov process where each degradation level is represented by a state. The aim of combining both inspection and continuous monitoring is to minimize the mean long-run cost rate by enhancing the system reliability and avoiding unnecessary inspection. Liu et al. (2013) developed a CBM policy for a continuously monitored degrading system subject to multiple failure modes. The degradation is a stochastic process and a corrective replacement is performed when the degradation level exceeds a pre-determined threshold.

Chapter 3

Reliability Modeling for Dependent Competing Failure Processes with Changing Degradation Rate

In this chapter, we propose reliability models for devices subject to dependent competing failure processes (DCFP) of degradation and random shocks with a changing degradation rate according to particular random shock patterns. In the literature, the degradation rate is commonly assumed to be fixed, which is an appropriate assumption for many design problems and reliability analyses. However, due to the nature of degradation for complex devices such as MEMS, the degradation rate can change when the system becomes more susceptible to fatigue, as a result of withstanding shocks. In this chapter, we consider four different cases of dependency between the shock process and the degradation rate. Numerical examples are presented to illustrate the developed reliability models, along with sensitivity analysis.

3.1. Introduction

In this chapter, we develop reliability models for a unit experiencing DCFP by considering the changing degradation rate due to the exposure to a particular pattern of shocks. We study two dependent failure processes: soft failure due to continuous degradation as well as sudden increases in degradation caused by random shocks, and hard failure due to the same shocks. These two failure processes are dependent because arriving random shocks affect both failure processes. Furthermore, in our new model, the shock process impacts the degradation rate: the exposure to a significant pattern of shocks or sufficiently large shocks can accelerate the degradation process by increasing the

degradation rate. In most studies on the competing failure processes, the degradation follows a linear path where the degradation rate is a random variable with known and fixed parameters (Wang et al. 2008; Peng et al. 2011), which is an appropriate assumption for many cases. However, due to the nature of degradation in complex devices such as MEMS, the degradation rate can increase when the system becomes more prone to fatigue and deteriorates faster, as a result of withstanding shocks. For example, a component of a MEMS device becomes more susceptible to degradation/soft failure and degrades faster, after exposure to a significantly large shock (Tanner et al. 2000). When a device begins vibrating due to impact of huge shocks, the deterioration rate of the device increases suddenly (Saassouh et al. 2007).

We focus on four shock models: extreme shock model, δ -shock model, m -shock model and run shock model, which are representatives among many different shock models explored in the literature. Our work can be readily extended to other shock models such as cumulative shock model. Specifically, the four different cases of dependency between the shock process and the degradation rate include (1) generalized extreme shock model: the degradation rate shifts when the first shock above a critical value is recorded, (2) generalized δ -shock model: the degradation rate changes when the inter-arrival time of two sequential shocks is less than a threshold δ , (3) generalized m -shock model: the degradation rate varies after m shocks greater than a critical level, and (4) generalized run shock model: the degradation rate transitions right after the first run of n consecutive shocks greater than a critical value. The reliability analysis with the changing degradation rate is a challenging problem, especially considering that the transition time for the degradation rate is unknown and random.

The developed reliability model is illustrated by using a realistic example of MEMS exposed to DCFP. Recently, there have been many studies performed on the reliability of MEMS to achieve wide acceptance of MEMS devices (Peng et al. 2009; Ye et al. 2012). Sandia National Laboratory has conducted reliability experiments to demonstrate failure processes and mechanisms for MEMS devices (Miller et al. 1998; Tanner et al. 2000; Tanner & Dugger 2003). The results of tests implied that, both soft failure due to wear degradation as well as random shocks and hard failure due to the same shock impact the reliability of MEMS.

The remainder of this chapter is organized as follows. Section 3.2 presents a brief description of reliability models for two dependent failure processes, along with the notations used in the reliability modeling. In Section 3.3, we propose the reliability models for a unit experiencing DCFP of degradation and random shocks with a changing degradation rate due to different shock patterns. Section 3.4 uses a numerical example to demonstrate the reliability models. Section 3.5 summarizes the article and concluding remarks are made.

3.2. System Description

As shown in Figure 3.1, the failure of a unit is due to two dependent yet competing failure processes: soft failure due to continuous degradation, in addition to sudden degradation increases caused by random shocks; and hard failure due to the same shock process. Whichever occurs first can cause the system failure. The dependence of these two failure processes are reflected in two different aspects:

- a) Because random shocks cause additional abrupt increases in the degradation level, the two competing failure processes are dependent due to shared exposure to random shocks.
- b) When a device sustains a series of shocks, it becomes more sensitive to degradation and degrades at a faster rate. The increase of the degradation rate occurs based on four different shock models: generalized extreme shock, δ -shock, m -shock, or run shock model.

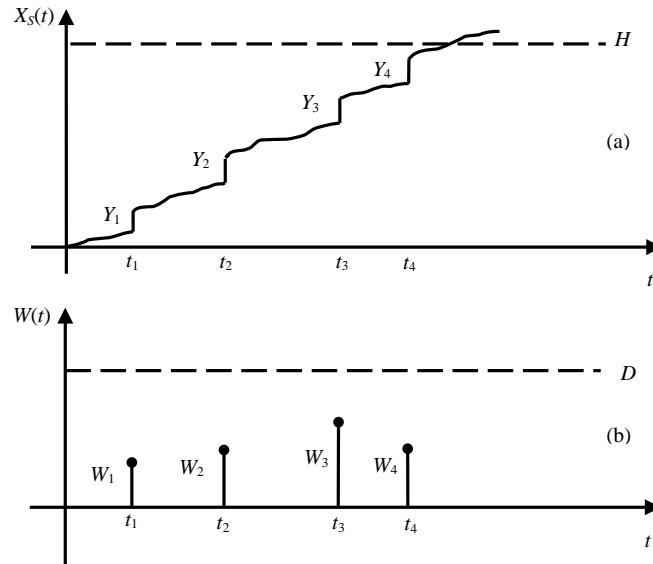


Figure 3.1: Two dependent competing failure modes: a) soft failure, b) hard failure

Notation

D_1	Threshold level for hard failure
D_0	Critical level on shock magnitude
$N(t)$	Number of random shocks arrived by time t
λ	Arrival rate of random shocks
W_k	Magnitude of the k^{th} shock load
$F_W(w)$	Cumulative distribution function (cdf) of W_{ki}
H	Threshold level for soft failure
$X(t)$	Amount of continuous degradation at time t
$X_S(t)$	Total degradation due to both continuous degradation and instantaneous damage at time t
φ	Initial level of degradation
β_1	Initial degradation rate

β_2	Changed degradation rate after the trigger shock in different cases
η	Amount of increase in initial degradation rate
Y_k	Damage size on degradation caused by the k^{th} random shock
$Z(t)$	Cumulative damage size by random shocks at time t
ε	Random error term in degradation path
$F_X(x, t)$	Cumulative distribution function (cdf) of $X_S(t)$
T_j	Arrival time of the j^{th} shock ($T_j \sim \text{gamma}(\lambda, j)$)
J	Shock count that causes a transition in the degradation rate (trigger shock)
T_J	Time at which the degradation rate changes (occurring at the J^{th} shock)
m	Required number of shocks that are greater than D_0 to change the degradation rate in the m -shock model
n	Required number of consecutive shocks that are greater than D_0 to change the degradation rate in the run shock model
U_i	Probability that by the i^{th} random shock, no run of n consecutive shocks that are greater than D_0 happens
\tilde{U}_j	Probability that by the j^{th} random shock, the first run of n consecutive shocks that are greater than D_0 occurs
B_k	Inter-arrival time between the $(k-1)^{th}$ and k^{th} shocks
δ	Minimum time lag between two consecutive shocks for δ -shock model
$R(t)$	Reliability function by time t

3.2.1. Modeling of Hard Failure Due to Shocks

Hard failure occurs as soon as the magnitude of a random shock is greater than the strength of material or the threshold level D_1 , which implies an extreme shock model. Arriving random shocks occur according to Poisson process with a rate of λ . The size of the k^{th} random shock denoted by W_k is an *i.i.d.* random variable with the cdf of $F_W(w)$. Therefore, the probability that the hard failure does not occur by time t , given number of shocks arrived by that time, $N(t)$, is

$$R_H(t) = P\left(\bigcap_{k=1}^{N(t)} \{W_k < D_1\}\right) = [F_W(D_1)]^{N(t)}. \quad (3.1)$$

3.2.2. Modeling of Soft Failure Due to Degradation and Shocks

Soft failure occurs when the total degradation exceeds the threshold level H . The overall degradation, $X_S(t)$, is accumulated by continuous degradation and abrupt damage caused by shocks (based on cumulative shock model). The continuous degradation is assumed to follow a degradation path $X(t) = \varphi + \beta t + \varepsilon$, where the initial degradation φ and the degradation rate β (the slope of degradation path) are random variables, capturing the unit-to-unit variability. The random error term ε following a normal distribution $\varepsilon \sim N(0, \sigma^2)$, is added to model temporal variability. The initial degradation rate β_1 can increase to β_2 if the condition for one of the four cases is satisfied, where $\beta_2 = \beta_1 + \eta$, and η is a positive random variable and independent of the initial degradation rate.

We define the first shock that triggers the change in the degradation rate as the *trigger shock*, occurring at the J^{th} shock where J is a random variable. The time at which the degradation rate changes (i.e., the arrival time of the J^{th} shock) is called *transition time*, denoted as T_J , which is a random variable with an unknown J . The trigger shock may or may not occur by time t . Therefore, the degradation by time t in this new model is expressed as

$$X(t) = \begin{cases} \varphi + \beta_1 T_J + \beta_2 (t - T_J) + \varepsilon, & J \leq N(t) \\ \varphi + \beta_1 t + \varepsilon, & J > N(t) \end{cases}, \quad (3.2)$$

where $N(t)$ is the total number of shocks arrived by time t . In this chapter, the degradation rate is allowed to change only once, as soon as the condition for the specified shock model is satisfied. That is, the increased degradation rate remains the same, even if the condition for the same shock model is repetitively satisfied after the trigger shock.

In addition, the degradation can accumulate damage instantaneously when a shock arrives. The abrupt shift in the overall degradation described as the shock damage size, Y_k ,

for $k = 1, 2, \dots, N(t)$, is an *i.i.d.* random variable. The total damage size caused by random shocks by time t , $Z(t)$, is

$$Z(t) = \begin{cases} \sum_{k=1}^{N(t)} Y_k, & N(t) > 0 \\ 0, & N(t) = 0 \end{cases}. \quad (3.3)$$

The overall degradation consists of both degradation and shock damage, $X_S(t) = X(t) + Z(t)$. In order for a unit to survive, the total degradation must be less than the threshold H . Therefore, the probability of no soft failure by time t is

$$R_S(t) = \sum_{i=0}^{\infty} \sum_{j=0}^{\infty} R_S(t | J = j, N(t) = i) P(J = j | N(t) = i) P(N(t) = i), \quad (3.4)$$

where $P(J = j | N(t) = i)$ is the conditional probability that the j^{th} shock is the trigger shock given i shocks by time t . Conditioning on the values of $N(t)$ and J , the probability of surviving against soft failure at time t is

$$R_S(t | J = j, N(t) = i) = \begin{cases} P\left(\varphi + \beta_1 T_j + \beta_2 (t - T_j) + \varepsilon + \sum_{k=1}^i Y_k < H\right), & j \leq i \\ P\left(\varphi + \beta_1 t + \varepsilon + \sum_{k=1}^i Y_k < H\right), & j > i \end{cases}. \quad (3.5)$$

It is essential to investigate the distribution for the transition time of the degradation rate, T_j , in (3.5). Random shocks arrive according to a Poisson process; therefore, given a value of $J = j$, the transition time of the degradation rate, T_j (i.e., the arrival time of the j^{th} shock), follows a gamma distribution with the scale parameter of j , and the shape parameter of λ . Therefore, the probability density function (pdf) for the transition time, given a value of $J = j$, is

$$f_{T_j}(t_j) = \frac{\lambda^j}{(j-1)!} t_j^{j-1} e^{-\lambda t_j}, \quad (3.6)$$

where the probability that the trigger shock occurs at the j^{th} shock can be calculated based on the specific case considered. Then the conditional probability in (3.5) can be calculated as

$$R_S(t|J=j, N(t)=i) = \begin{cases} \int_0^t P\left(\varphi + \beta_1 t_j + \beta_2(t-t_j) + \varepsilon + \sum_{k=1}^i Y_k < H\right) f_{T_j}(t_j) dt_j, & j \leq i \\ P\left(\varphi + \beta_1 t + \varepsilon + \sum_{k=1}^i Y_k < H\right), & j > i \end{cases} \quad (3.7)$$

The model presented in (3.7), is general and can accommodate many distributional assumptions. In a specific case, we assume that φ is a constant, Y_k, β_1 and η are normally-distributed, i.e., $Y_k \sim N(\mu_Y, \sigma_Y^2)$, $\beta_1 \sim N(\mu_{\beta_1}, \sigma_{\beta_1}^2)$, and $\eta \sim N(\mu_\eta, \sigma_\eta^2)$; consequently, β_2 is also normally-distributed, $\beta_2 \sim N(\mu_{\beta_1} + \mu_\eta, \sigma_{\beta_1}^2 + \sigma_\eta^2)$ or $\beta_2 \sim N(\mu_{\beta_2}, \sigma_{\beta_2}^2)$. We assume that $\mu_\eta \gg 3\sigma_\eta$ to ensure $\beta_2 > \beta_1$. The probability in (3.7) for this special case is

$$R_S(t|J=j, N(t)=i) = \begin{cases} \int_0^t \Phi\left(\frac{H - (\varphi + \mu_{\beta_1} t_j + \mu_{\beta_2}(t-t_j) + i\mu_Y)}{\sqrt{\sigma_{\beta_1}^2 t_j^2 + \sigma_{\beta_2}^2 (t-t_j)^2 + i\sigma_Y^2 + \sigma^2}}\right) f_{T_j}(t_j) dt_j, & j \leq i \\ \Phi\left(\frac{H - (\varphi + \mu_{\beta_1} t + i\mu_Y)}{\sqrt{\sigma_{\beta_1}^2 t^2 + i\sigma_Y^2 + \sigma^2}}\right), & j > i \end{cases} \quad (3.8)$$

3.3. Reliability Analysis Considering Changing Degradation Rate

In this section, reliability analysis is investigated for four different cases of random shock patterns. The reliability at time t for a device that experiences two DCFP is

$$\begin{aligned} R(t) &= \sum_{i=0}^{\infty} \sum_{j=0}^{\infty} R(t|J=j, N(t)=i) P(J=j|N(t)=i) P(N(t)=i) \\ &= \sum_{i=0}^{\infty} \sum_{j=0}^{\infty} R_H(t|J=j, N(t)=i) R_S(t|J=j, N(t)=i) P(J=j|N(t)=i) P(N(t)=i). \end{aligned} \quad (3.9)$$

The conditional independence between the events $R_H(t)$ and $R_S(t)$ is due to the assumption that the shock damage size Y_i is independent of the shock load W_i .

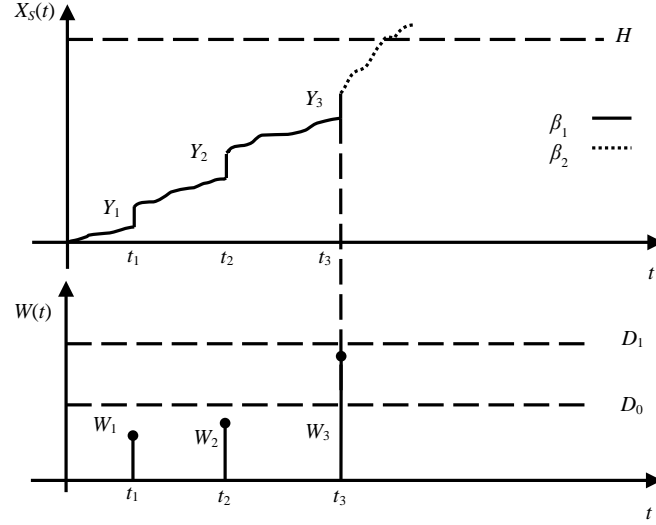


Figure 3.2: Generalized extreme shock model

3.3.1. Case 1: Generalized Extreme Shock Model

Figure 3.2 shows a generalized extreme shock model; that is, the degradation rate changes from β_1 to β_2 when the first shock greater than D_0 is recorded.

By considering the following situations, the reliability is derived further.

i) When no shocks occur by time t , or $N(t) = 0$:

$$R(t | N(t) = 0) = P(\varphi + \beta_1 t + \varepsilon < H). \quad (3.10)$$

ii) When at least one shock occurs by time t , or $N(t) > 0$, there are two different situations for the unit to work without failure, and the probability of those mutually exclusive scenarios must be added together for every possible $N(t) > 0$.

a. All the shocks are less than D_0 , or $J > N(t)$:

$$R(t | J > N(t) = i > 0) = P\left(\varphi + \beta_1 t + \varepsilon + \sum_{k=1}^i Y_k < H\right) P\left(\bigcap_{k=1}^i \{W_k < D_0\}\right). \quad (3.11)$$

b. At least a random shock is greater than D_0 , or $J = j \leq N(t)$, and $j = \min\{k; W_k > D_0\}$:

$$R(t|0 < J = j \leq N(t) = i) = \sum_{j=1}^i \left(\int_0^t P \left(\varphi + \beta_1 t_j + \beta_2 (t - t_j) + \varepsilon + \sum_{k=1}^i Y_k < H \right) f_{T_j}(t_j) dt_j \right) \times P \left(\bigcap_{k=1}^{j-1} \{W_k < D_0\}, D_0 < W_j < D_1, \bigcap_{k=j+1}^i \{W_k < D_1\} \right). \quad (3.12)$$

Now by summing them all, the system reliability at time t is derived to be

$$\begin{aligned} R(t) &= P(\varphi + \beta_1 t + \varepsilon < H) P(N(t) = 0) \\ &+ \sum_{i=1}^{\infty} P \left(\varphi + \beta_1 t + \varepsilon + \sum_{k=1}^i Y_k < H \right) P \left(\bigcap_{k=1}^i \{W_k < D_0\} \right) P(N(t) = i) \\ &+ \sum_{i=1}^{\infty} \sum_{j=1}^i \left(\int_0^t P \left(\varphi + \beta_1 t_j + \beta_2 (t - t_j) + \varepsilon + \sum_{k=1}^i Y_k < H \right) f_{T_j}(t_j) dt_j \right) \\ &\times P \left(\bigcap_{k=1}^{j-1} \{W_k < D_0\}, D_0 < W_j < D_1, \bigcap_{k=j+1}^i \{W_k < D_1\} \right) P(N(t) = i). \end{aligned} \quad (3.13)$$

The reliability function for the specific case of constant φ and normally-distributed Y_k , β_1 and η , can be expressed as

$$\begin{aligned} R(t) &= \Phi \left(\frac{H - (\varphi + \mu_{\beta_1} t)}{\sqrt{\sigma_{\beta_1}^2 t^2 + \sigma^2}} \right) e^{-\lambda t} + \sum_{i=1}^{\infty} \Phi \left(\frac{H - (\varphi + \mu_{\beta_1} t + i \mu_Y)}{\sqrt{\sigma_{\beta_1}^2 t^2 + i \sigma_Y^2 + \sigma^2}} \right) [F_w(D_0)]^i \frac{e^{-\lambda t} (\lambda t)^i}{i!} \\ &+ \sum_{i=1}^{\infty} \sum_{j=1}^i \left[\int_0^t \Phi \left(\frac{H - (\varphi + \mu_{\beta_1} t_j + \mu_{\beta_2} (t - t_j) + i \mu_Y)}{\sqrt{\sigma_{\beta_1}^2 t_j^2 + \sigma_{\beta_2}^2 (t - t_j)^2 + i \sigma_Y^2 + \sigma^2}} \right) \frac{\lambda^j}{(j-1)!} t_j^{j-1} e^{-\lambda t_j} dt_j \right] \\ &\times [F_w(D_0)]^{j-1} [F_w(D_1) - F_w(D_0)] [F_w(D_1)]^{i-j} \frac{e^{-\lambda t} (\lambda t)^i}{i!}. \end{aligned} \quad (3.14)$$

3.3.2. Case 2: Generalized δ -Shock Model

As shown in Figure 3.3, in the generalized δ -shock model, the degradation rate changes from β_1 to β_2 when the time interval of two sequential shocks is less than δ . Since the arrival of random shocks follows a Poisson process with parameter λ , the inter-arrival time of two consecutive shocks follows an exponential distribution with the same

parameter λ . We define B_k as the time between the occurrences of the $(k - 1)^{th}$ and k^{th} random shocks, or $B_k = T_k - T_{k-1}$.

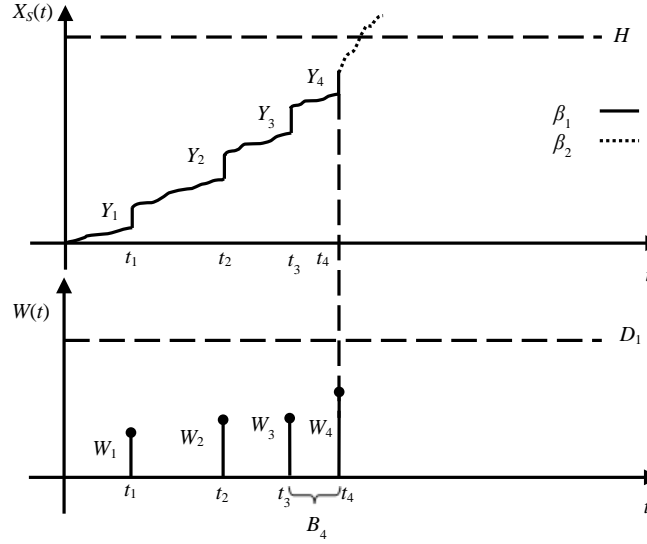


Figure 3.3: Generalized δ -shock model ($B_4 < \delta$)

By considering the following situations, it is derived further.

i) When no shocks occur by time t , or $N(t) = 0$,

$$R(t|N(t) = 0) = P(\varphi + \beta_1 t + \varepsilon < H). \quad (3.15)$$

ii) When there is just one random shock by time t , or $N(t) = 1$:

$$R(t|N(t) = 1) = P(\varphi + \beta_1 t + \varepsilon + Y_1 < H) P(W_1 < D_1). \quad (3.16)$$

iii) When there are more than one shock by time t , or $N(t) > 1$, the degradation rate may or

may not shift from β_1 to β_2 depending on if B_k is less than δ or not.

a. There is no $B_k < \delta$ for $k = 2, \dots, i$, or $J > N(t)$:

$$\begin{aligned} R(t|J > N(t) = i, 2 \leq i \leq \lfloor t/\delta \rfloor + 1) &= P\left(\varphi + \beta_1 t + \varepsilon + \sum_{k=1}^i Y_k < H\right) \\ &\times P\left(\bigcap_{k=2}^i \{B_k > \delta\}\right) P\left(\bigcap_{k=1}^i \{W_k < D_1\}\right). \end{aligned} \quad (3.17)$$

For all time lags to be larger than or equal to δ , the maximum number of shocks occurred by time t is $\lfloor t / \delta \rfloor + 1$, where $\lfloor t / \delta \rfloor$ is the integer part of t/δ , and it is the maximum number of inter-arrival times by time t given that all time lags are larger than or equal to δ .

- b. There is at least one $B_k < \delta$ for $k = 2, \dots, i$, or $J = j \leq N(t)$, and $j = \min\{k ; B_k < \delta\}$.

The ratio t/δ can be either an integer or not. When t/δ is an integer, $j - 1$ must be less than or equal to $\lfloor t / \delta \rfloor - 1$, or $j \leq \lfloor t / \delta \rfloor = \lceil t / \delta \rceil$. However, when t/δ is not an integer, $j - 1$ must be less than or equal to $\lfloor t / \delta \rfloor$, or $j \leq \lceil t / \delta \rceil$, where

$$L = \min\{\lceil t / \delta \rceil, i\}:$$

$$\begin{aligned} R(t | 2 \leq J = j \leq N(t) = i) &= \sum_{j=2}^L P\left(\bigcap_{k=1}^i \{W_k < D_1\}\right) P\left(\bigcap_{k=2}^{j-1} \{B_k > \delta\}, B_j < \delta\right) \\ &\quad \times \left(\int_0^t P\left(\varphi + \beta_1 t_j + \beta_2(t - t_j) + \varepsilon + \sum_{k=1}^i Y_k < H\right) f_{T_j}(t_j) dt_j \right), \end{aligned} \quad (3.18)$$

Now by summing them all, the system reliability at time t is derived to be:

$$\begin{aligned} R(t) &= P(\varphi + \beta_1 t + \varepsilon < H) P(N(t) = 0) \\ &\quad + P(\varphi + \beta_1 t + \varepsilon + Y_1 < H) P(W_1 < D_1) P(N(t) = 1) \\ &\quad + \sum_{i=2}^{\infty} P\left(\varphi + \beta_1 t + \varepsilon + \sum_{k=1}^i Y_k < H\right) P\left(\bigcap_{k=2}^i \{B_k > \delta\}\right) P\left(\bigcap_{k=1}^i \{W_k < D_1\}\right) P(N(t) = i) \\ &\quad + \sum_{i=2}^{\infty} \sum_{j=2}^L \left(\int_0^t P\left(\varphi + \beta_1 t_j + \beta_2(t - t_j) + \varepsilon + \sum_{k=1}^i Y_k < H\right) f_{T_j}(t_j) dt_j \right) \\ &\quad \times P\left(\bigcap_{k=1}^i \{W_k < D_1\}\right) P\left(\bigcap_{k=2}^{j-1} \{B_k > \delta\}, B_j < \delta\right) P(N(t) = i). \end{aligned} \quad (3.19)$$

Since B_k follows an exponential distribution, the reliability function for specific case where φ is a constant, Y_k , β_1 and η are normally distributed can be expressed as

$$\begin{aligned}
R(t) = & \Phi\left(\frac{H - (\varphi + \mu_{\beta_1} t)}{\sqrt{\sigma_{\beta_1}^2 t^2 + \sigma^2}}\right) e^{-\lambda t} + \Phi\left(\frac{H - (\varphi + \mu_{\beta_1} t + \mu_Y)}{\sqrt{\sigma_{\beta_1}^2 t^2 + \sigma_Y^2 + \sigma^2}}\right) F_W(D_1) e^{-\lambda t} \lambda t \\
& + \sum_{i=2}^{\infty} \Phi\left(\frac{H - (\varphi + \mu_{\beta_1} t + i \mu_Y)}{\sqrt{\sigma_{\beta_1}^2 t^2 + i \sigma_Y^2 + \sigma^2}}\right) [F_W(D_1)]^i e^{-\lambda \delta(i-1)} \frac{e^{-\lambda t} (\lambda t)^i}{i!} \\
& + \sum_{i=2}^{\infty} \sum_{j=2}^L \left[\int_0^t \Phi\left(\frac{H - (\varphi + \mu_{\beta_1} t_j + \mu_{\beta_2} (t - t_j) + i \mu_Y)}{\sqrt{\sigma_{\beta_1}^2 t_j^2 + \sigma_{\beta_2}^2 (t - t_j)^2 + i \sigma_Y^2 + \sigma^2}}\right) \frac{\lambda^j}{(j-1)!} t_j^{j-1} e^{-\lambda t_j} dt_j \right] \\
& \times [F_W(D_1)]^i e^{-\lambda \delta(j-1)} (1 - e^{-\lambda \delta}) \frac{e^{-\lambda t} (\lambda t)^i}{i!}.
\end{aligned} \tag{3.20}$$

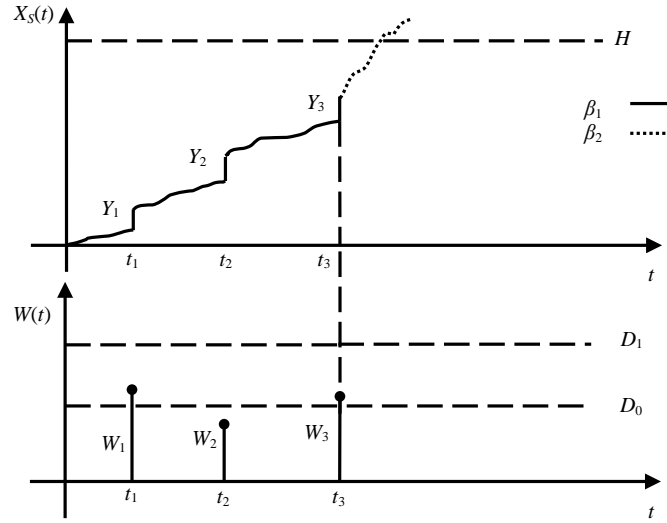


Figure 3.4: Generalized m -shock model ($m = 2$)

3.3.3. Case 3: Generalized m -Shock Model

Figure 3.4 shows a generalized m -shock model; that is, the degradation rate changes from β_1 to β_2 immediately following m shocks that are larger than a threshold D_0 .

By considering the following situations, it can be derived further.

i) When no shocks occur by time t , or $N(t) = 0$:

$$R(t|N(t) = 0) = P(\varphi + \beta_1 t + \varepsilon < H). \tag{3.21}$$

ii) When number of shocks by time t is between 1 and $m - 1$, or $N(t) = i$, $1 \leq i \leq m - 1$:

$$R(t|0 < N(t) = i < m) = P\left(\varphi + \beta_1 t + \varepsilon + \sum_{k=1}^i Y_k < H\right) P\left(\bigcap_{k=1}^i \{W_k < D_1\}\right). \quad (3.22)$$

iii) When the number of shocks is greater than or equals to m , the degradation rate may or may not shift from β_1 to β_2 :

a. There are less than m shocks greater than D_0 , or $J > N(t)$:

$$\begin{aligned} R(t|J > N(t) = i \geq m) &= \sum_{l=0}^{m-1} \binom{i}{l} P\left(\varphi + \beta_1 t + \varepsilon + \sum_{k=1}^i Y_k < H\right) \\ &\times P\left(\bigcap_{k=1}^l \{D_0 < W_k < D_1\}, \bigcap_{k=l+1}^i \{W_k < D_0\}\right), \end{aligned} \quad (3.23)$$

where number of shocks greater than D_0 is denoted by l , for $l = 0, 1, 2, \dots, m-1$.

To derive the reliability that the system survives by time t , all possible combinations of l out of the total number of shocks i must be considered. Since all the shock sizes are independent and identically distributed, the formula remains unchanged for each of the combinations.

b. There are at least m shocks greater than the critical level D_0 , or $J = j \leq N(t)$:

$$\begin{aligned} R(t|m \leq J = j \leq N(t) = i) &= \sum_{j=m}^i \left(\int_0^t P\left(\varphi + \beta_1 t_j + \beta_2 (t - t_j) + \varepsilon + \sum_{k=1}^i Y_k < H\right) f_{T_j}(t_j) dt_j \right) \\ &\left(\binom{j-1}{m-1} P\left(\bigcap_{k=1}^{j-m} \{W_k < D_0\}, \bigcap_{k=j-m+1}^j \{D_0 < W_k < D_1\}, \bigcap_{k=j+1}^i \{W_k < D_1\}\right) \right), \end{aligned} \quad (3.24)$$

where the m^{th} shock that is greater than D_0 is the trigger shock j , for $j = m, m+1, m+2, \dots, N(t)$. Therefore, there are $m-1$ shocks larger than the critical level by the $(j-1)^{th}$ shock. To derive the probability that the system survives by time t , all possible combinations of $m-1$ out of $j-1$ shocks must be considered.

Now by summing them all, the system reliability at time t is derived to be

$$\begin{aligned}
R(t) &= P(\varphi + \beta_1 t + \varepsilon < H) P(N(t) = 0) \\
&+ \sum_{i=1}^{m-1} P\left(\varphi + \beta_1 t + \varepsilon + \sum_{k=1}^i Y_k < H\right) P\left(\bigcap_{k=1}^i \{W_k < D_1\}\right) P(N(t) = i) \\
&+ \sum_{i=m}^{\infty} \sum_{l=0}^{m-1} \binom{i}{l} P\left(\varphi + \beta_1 t + \varepsilon + \sum_{k=1}^i Y_k < H\right) P\left(\bigcap_{k=1}^l \{D_0 < W_k < D_1\}, \bigcap_{k=l+1}^i \{W_k < D_0\}\right) \\
&\times P(N(t) = i) + \sum_{i=m}^{\infty} \sum_{j=m}^i \binom{j-1}{m-1} \left(\int_0^t P\left(\varphi + \beta_1 t_j + \beta_2(t-t_j) + \varepsilon + \sum_{k=1}^i Y_k < H\right) f_{T_j}(t_j) dt_j \right) \\
&\times P\left(\bigcap_{k=1}^{j-m} \{W_k < D_0\}, \bigcap_{k=j-m+1}^j \{D_0 < W_k < D_1\}, \bigcap_{k=j+1}^i \{W_k < D_1\}\right) P(N(t) = i).
\end{aligned} \tag{3.25}$$

The reliability function for the specific case that φ is a constant, Y_k , β_1 and η are normally distributed can be expressed as

$$\begin{aligned}
R(t) &= \Phi\left(\frac{H - (\varphi + \mu_{\beta_1} t)}{\sqrt{\sigma_{\beta_1}^2 t^2 + \sigma^2}}\right) e^{-\lambda t} + \sum_{i=1}^{m-1} \Phi\left(\frac{H - (\varphi + \mu_{\beta_1} t + i\mu_Y)}{\sqrt{\sigma_{\beta_1}^2 t^2 + i\sigma_Y^2 + \sigma^2}}\right) [F_W(D_1)]^i \frac{e^{-\lambda t} (\lambda t)^i}{i!} \\
&+ \sum_{i=m}^{\infty} \sum_{l=0}^{m-1} \binom{i}{l} \Phi\left(\frac{H - (\varphi + \mu_{\beta_1} t + i\mu_Y)}{\sqrt{\sigma_{\beta_1}^2 t^2 + i\sigma_Y^2 + \sigma^2}}\right) [F_W(D_1) - F_W(D_0)]^l [F_W(D_0)]^{i-l} \frac{e^{-\lambda t} (\lambda t)^i}{i!} \\
&+ \sum_{i=m}^{\infty} \sum_{j=m}^i \binom{j-1}{m-1} \left[\int_0^t \Phi\left(\frac{H - (\varphi + \mu_{\beta_1} t_j + \mu_{\beta_2}(t-t_j) + i\mu_Y)}{\sqrt{\sigma_{\beta_1}^2 t_j^2 + \sigma_{\beta_2}^2 (t-t_j)^2 + i\sigma_Y^2 + \sigma^2}}\right) \frac{\lambda^j}{(j-1)!} t_j^{j-1} e^{-\lambda t_j} dt_j \right] \\
&\times [F_W(D_0)]^{j-m} [F_W(D_1) - F_W(D_0)]^m [F_W(D_1)]^{i-j} \frac{e^{-\lambda t} (\lambda t)^i}{i!}.
\end{aligned} \tag{3.26}$$

3.3.4. Case 4: Generalized Run Shock Model

As shown in Figure 3.5, in a run shock model, the degradation rate changes from β_1 to β_2 immediately following the first run of n consecutive shocks larger than a threshold D_0 .

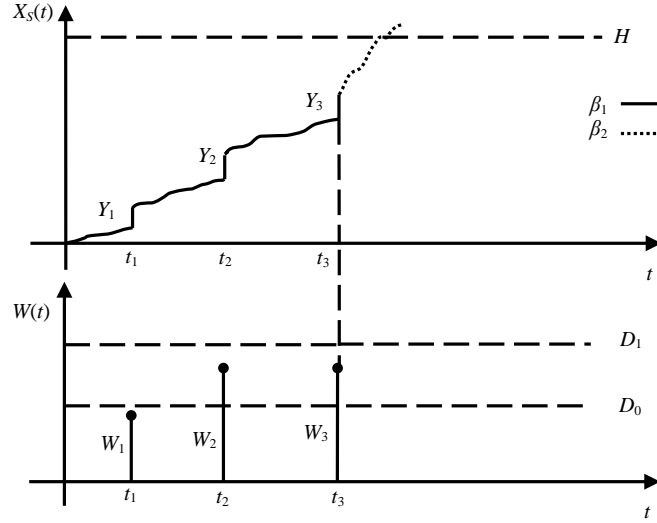


Figure 3.5: Generalized run shock model ($n = 2$)

By considering the following situations, it can be derived further.

i) When no shocks occur by time t , or $N(t) = 0$:

$$R(t | N(t) = 0) = P(\varphi + \beta_1 t + \varepsilon < H). \quad (3.27)$$

ii) When at least one shock occurs by time t , or $N(t) > 0$, the degradation rate may or may not shift from β_1 to β_2 :

a. There is no run of n consecutive shocks (CS) that are greater than a critical value D_0 , or $J > N(t)$:

$$R(t | J > N(t) = i > 0) = U_i P\left(\varphi + \beta_1 t + \varepsilon + \sum_{k=1}^i Y_k < H\right) P\left(\bigcap_{k=1}^i \{W_k < D_1\}\right). \quad (3.28)$$

b. There is at least one run of n CS greater than D_0 , or $J = j > N(t)$. The first run of n CS greater than D_0 can happen at the j^{th} random shock for $j = n, n + 1, n + 2, \dots, i$:

$$\begin{aligned} R(t | n \leq J = j \leq N(t) = i) &= \sum_{j=n}^i \tilde{U}_j P\left(\bigcap_{k=1}^i \{W_k < D_1\}\right) \\ &\times \left(\int_0^t P\left(\varphi + \beta_1 t_j + \beta_2 (t - t_j) + \varepsilon + \sum_{k=1}^i Y_k < H\right) f_{T_j}(t_j) dt_j \right). \end{aligned} \quad (3.29)$$

Now the reliability function by time t is

$$\begin{aligned}
R(t) = & PP(\varphi + \beta_1 t + \varepsilon < H) P(N(t) = 0) \\
& + \sum_{i=1}^{\infty} U_i P\left(\varphi + \beta_1 t + \varepsilon + \sum_{k=1}^i Y_k < H\right) P\left(\bigcap_{k=1}^i \{W_k < D_1\}\right) P(N(t) = i) \\
& + \sum_{i=n}^{\infty} \sum_{j=n}^i \left(\int_0^t P\left(\varphi + \beta_1 t_j + \beta_2(t - t_j) + \varepsilon + \sum_{k=1}^i Y_k < H\right) f_{T_j}(t_j) dt_j \right) \\
& \times \tilde{U}_j P\left(\bigcap_{k=1}^i \{W_k < D_1\}\right) P(N(t) = i),
\end{aligned} \tag{3.30}$$

where U_i is the probability that by the i^{th} random shock, no run of n CS that are greater than D_0 has occurred, or $U_i = P(J > i | N(t) = i)$; and \tilde{U}_j is the probability that, by the j^{th} random shock, the first run of n CS greater than D_0 occurs, or $P(J = j \leq i | N(t) = i)$. We propose Lemma 3.1 to derive U_i and \tilde{U}_j .

Lemma 3.1: We define U_N to be the probability that no n consecutive successes occur in N trials, and \tilde{U}_N to be the probability that the first run of n consecutive successes occurs at the N^{th} trial:

$$\begin{aligned}
U_N &= \Pr\{\text{no } n \text{ consecutive successes in } N \text{ trials}\} \\
\tilde{U}_N &= \Pr\{\text{the first run of } n \text{ consecutive successes occurs at the } N^{\text{th}} \text{ trial}\}
\end{aligned}$$

In general, U_N has been shown to satisfy the recursive equation (Krieger, 1984):

$$U_N = qU_{N-1} + pqU_{N-2} + p^2qU_{N-3} + \dots + p^{n-1}qU_{N-n}, \tag{3.31}$$

where p is the probability of success, and $q = 1 - p$. In addition, we have $U_k = 1$ for $0 \leq k \leq n - 1$, and $U_n = 1 - p^n$. To have the first run of n consecutive successes occurring at the N^{th} trial, the last n trials must be successes, the $(N - n)^{\text{th}}$ trial must be a failure, and no consecutive n successes occur in the first $N - n - 1$ trials. Therefore, we have

$$\tilde{U}_N = \begin{cases} p^n & \text{if } N = n \\ U_{N-n-1}qp^n & \text{if } N > n \end{cases}. \quad (3.32)$$

□

For our model, we define a success as a shock being greater than the critical value D_0 , given it is not beyond the failure threshold value D_1 . Then we have

$$p = P(W_i > D_0 | W_i < D_1) = \frac{P(D_0 < W_i < D_1)}{P(W_i < D_1)} = \frac{F_w(D_1) - F_w(D_0)}{F_w(D_1)} \quad (3.33a)$$

$$q = 1 - p = P(W_i < D_0 | W_i < D_1) = \frac{P(W_i < D_0)}{P(W_i < D_1)} = \frac{F_w(D_0)}{F_w(D_1)}. \quad (3.33b)$$

We use t_j to denote the time that the degradation rate changes from β_1 to β_2 , i.e., the first time that a run of n CS that are greater than D_0 happens. If we assume that φ is a constant, and Y_k, β_1 and η are normally distributed, the reliability function for this specific case is

$$\begin{aligned} R(t) = & \Phi\left(\frac{H - (\varphi + \mu_{\beta_1}t)}{\sqrt{\sigma_{\beta_1}^2 t^2 + \sigma^2}}\right) e^{-\lambda t} + \sum_{i=1}^{\infty} U_i \times \Phi\left(\frac{H - (\varphi + \mu_{\beta_1}t + i\mu_Y)}{\sqrt{\sigma_{\beta_1}^2 t^2 + i\sigma_Y^2 + \sigma^2}}\right) [F_w(D_1)]^i \frac{e^{-\lambda t} (\lambda t)^i}{i!} \\ & + \sum_{i=n}^{\infty} \sum_{j=n}^i \tilde{U}_j \times \left[\int_0^t \Phi\left(\frac{H - (\varphi + \mu_{\beta_1}t_j + \mu_{\beta_2}(t-t_j) + i\mu_Y)}{\sqrt{\sigma_{\beta_1}^2 t_j^2 + \sigma_{\beta_2}^2 (t-t_j)^2 + i\sigma_Y^2 + \sigma^2}}\right) \frac{\lambda^j}{(j-1)!} t_j^{j-1} e^{-\lambda t_j} dt_j \right] [F_w(D_1)]^i \frac{e^{-\lambda t} (\lambda t)^i}{i!}. \end{aligned} \quad (3.34)$$

3.4. Numerical Examples and Results

A micro-engine includes orthogonal comb-drive actuators and a rotating gear that are mechanically joined to each other. The linear displacement of the comb-drives is transferred to the gear through pin joints. Operation of a micro-engine over time leads to visible wear on the rubbing surface between the gear and the pin joint, and finally the growth of the wear results in a broken pin joint, which is the most frequent reason for

micro-engine failure. The major source of wear is degradation process. However, the results from shock tests on micro-engines demonstrate that shocks themselves can create wear debris between the pin joint and the gear, and cause the spring fracture (Tanner et al. 2000). Therefore, a micro-engine fails due to two competing failure processes: (1) soft failure as the result of aging degradation and debris caused by shocks, and (2) hard failure because of spring fracture from the same shocks. In addition, a micro-engine becomes more susceptible to wear degradation and the wear volume accumulates faster, after exposure to a certain pattern of shocks or a significantly large shock. We implement our new reliability models to the application of micro-engines. The corresponding values of the parameters for the reliability analysis are given in Table 3.1.

Table 3.1: Parameter values

Parameters	Values	Sources
H	$0.00125 \mu\text{m}^3$	(Tanner & Dugger, 2003)
D_1	1.5 Gpa	(Tanner & Dugger, 2003)
D_0	1.2 Gpa	Assumption
φ	0	(Tanner & Dugger, 2003)
μ_{β_1}	$8.4823 \times 10^{-9} \mu\text{m}^3$	(Tanner & Dugger, 2003)
σ_{β_1}	$6.0016 \times 10^{-10} \mu\text{m}^3$	(Tanner & Dugger, 2003)
μ_{η}	$2.4823 \times 10^{-9} \mu\text{m}^3$	Assumption
σ_{η}	$1.0016 \times 10^{-10} \mu\text{m}^3$	Assumption
σ	$10^{-10} \mu\text{m}^3$	Assumption
λ	5×10^{-5} / revolutions	Assumption
μ_W	1.2 Gpa	Assumption
σ_W	0.2 Gpa	Assumption
μ_Y	$1.0 \times 10^{-4} \mu\text{m}^3$	Assumption
σ_Y	$2 \times 10^{-5} \mu\text{m}^3$	Assumption
δ	2.0×10^3 revolutions	Assumption
m	2	Assumption
n	2	Assumption

In reality, only one shock pattern may exist for a certain device. However, for the purpose of illustration, we use this application of micro-engines to demonstrate the four

different cases. By using a similar set of parameter values for all four cases (other than the model-specific parameters), it also enables comparison among different shock models.

3.4.1. Reliability Analysis for Case 1

For the described extreme shock model with increasing degradation rate, the reliability function $R(t)$ in (3.13) is plotted in Figure 3.6, and a sensitivity analysis is performed to measure the effects of the ratios D_0 / D_1 and $\mu_{\beta_2} / \mu_{\beta_1}$ on the reliability function (Figure 3.7-3.8).

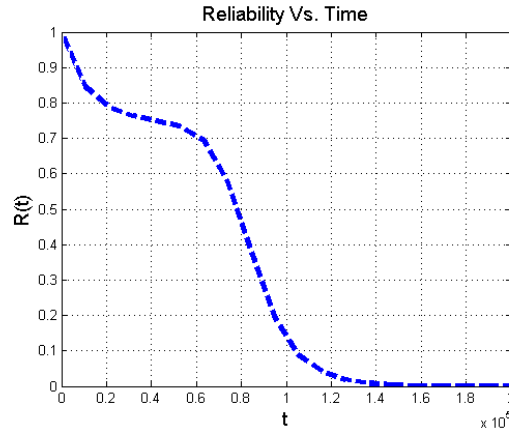


Figure 3.6: Plot of $R(t)$ for Case 1

As you can see in Figure 3.7, the ratio between the critical threshold and hard failure threshold (D_0 / D_1) has a significant impact on the reliability of the system. By increasing the ratio (D_1 is fixed at 1.5 Gpa and D_0 increases from 1.2 Gpa to 1.5 Gpa), $R(t)$ shifts to right. It can be inferred that reliability of system improves by approaching D_0 to D_1 , and finally when $D_0 = D_1$, the system performs without the change of degradation rate. In Figure 3.8, we can observe that $R(t)$ is susceptible to the ratio between the increased degradation rate and the initial degradation rate, $\mu_{\beta_2} / \mu_{\beta_1}$. When the ratio reduces, $R(t)$ shifts to right. Therefore, units with a smaller ratio $\mu_{\beta_2} / \mu_{\beta_1}$ have a better reliability performance.

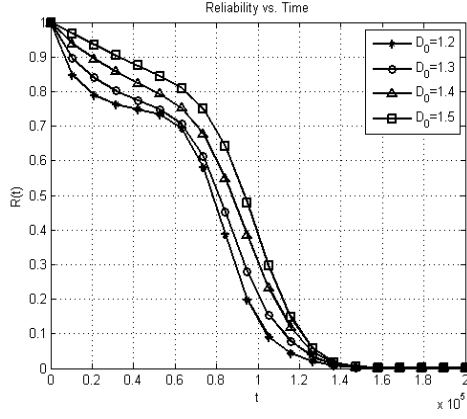


Figure 3.7: Sensitivity analysis of $R(t)$ on D_0 / D_1 for Case 1

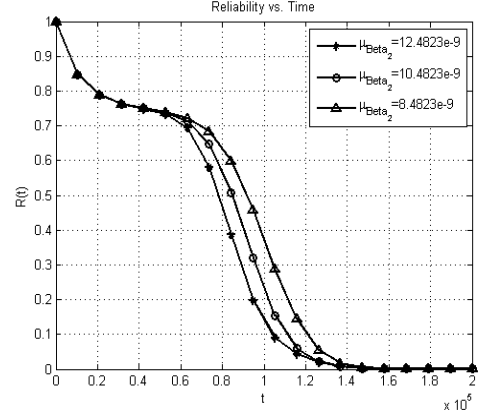


Figure 3.8: Sensitivity analysis of $R(t)$ on $\mu_{\beta_2} / \mu_{\beta_1}$ for Case 1

3.4.2. Reliability Analysis for Case 2

Figure 3.9 presents the reliability plot for the generalized δ -shock model in (3.19). Figure 3.10 and Figure 3.11, show that sensitivity analysis was performed to observe how the parameters δ and $\mu_{\beta_2} / \mu_{\beta_1}$ affect system reliability, respectively.

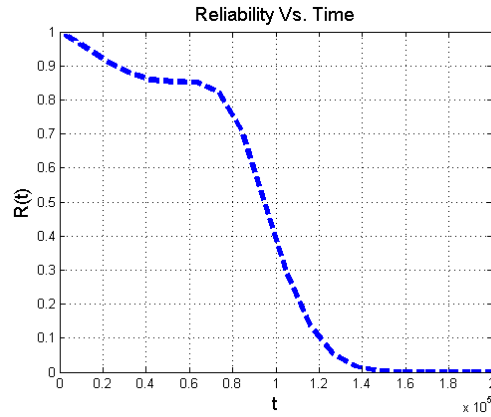


Figure 3.9: Plot of $R(t)$ for Case 2

As can be observed in Figure 3.10, the inter-arrival time threshold δ affects the reliability function. By increasing δ from 0.5×10^3 revolutions to 2.0×10^3 revolutions, $R(t)$ shifts slightly to the right at the time that degradation rate changes. It indicates that reliability performance is better for the smaller value of δ . Figure 3.11 shows that $R(t)$ is significantly dependent on the ratio between the increased degradation rate and the initial

degradation rate, $\mu_{\beta_2} / \mu_{\beta_1}$. When the ratio reduces, $R(t)$ moves to right. Therefore, the device with a smaller ratio $\mu_{\beta_2} / \mu_{\beta_1}$ is more likely to survive.

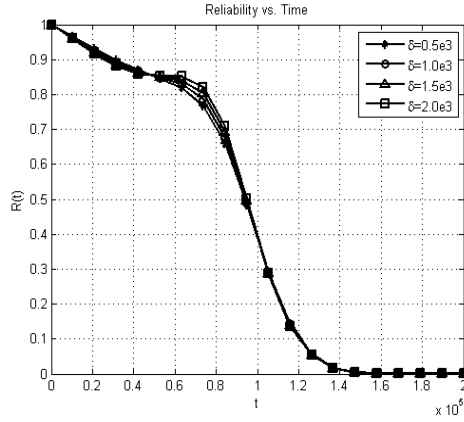


Figure 3.10: Sensitivity analysis of $R(t)$ on δ for Case 2

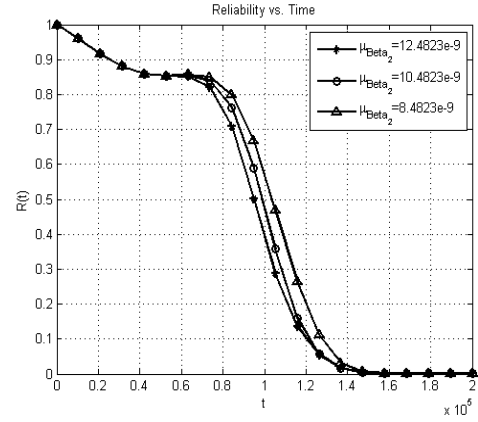


Figure 3.11: Sensitivity analysis of $R(t)$ on $\mu_{\beta_2} / \mu_{\beta_1}$ for Case 2

3.4.3. Reliability Analysis for Case 3

The reliability function for the generalized m -shock model in (3.25) is plotted in Figure 3.12. Sensitivity analyses were also conducted to assess impact of the ratio D_0 / D_1 and $\mu_{\beta_2} / \mu_{\beta_1}$ on the system reliability, respectively (Figure 3.13-3.14).

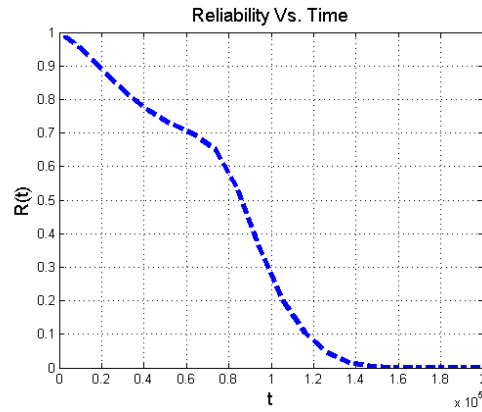


Figure 3.12: Plot of $R(t)$ for Case 3

From Figure 3.13, one can understand the great effect of the ratio between the critical threshold and hard failure threshold (D_0 / D_1) on the reliability of the system. When the ratio increases (D_1 is fixed at 1.5 Gpa and D_0 increases from 1.2 Gpa to 1.5 Gpa), the

$R(t)$ shifts to right. This implies that a system with a higher ratio (D_0 / D_1) has better performance. In Figure 3.14, we can see that $\mu_{\beta_2} / \mu_{\beta_1}$ has a large impact on $R(t)$. When the ratio reduces, $R(t)$ shifts to right. Therefore, units with a smaller ratio of $\mu_{\beta_2} / \mu_{\beta_1}$ can have a better reliability performance.

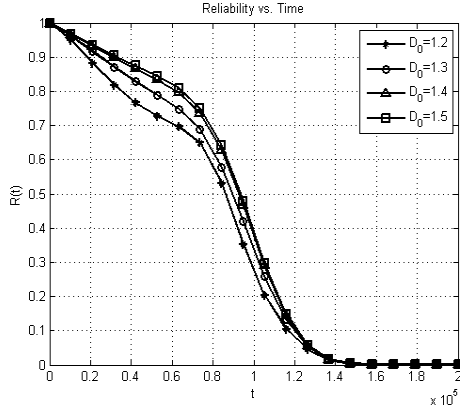


Figure 3.13: Sensitivity analysis of $R(t)$ on D_0 / D_1 for Case 3

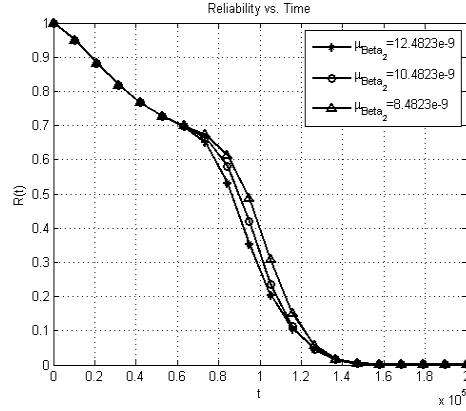


Figure 3.14: Sensitivity analysis of $R(t)$ on $\mu_{\beta_2} / \mu_{\beta_1}$ for Case 3

3.4.4. Reliability Analysis for Case 4

For the generalized run shock model, we plot the reliability function in Figure 3.15. In addition, we perform sensitivity analyses to study how $R(t)$ in (3.30) responds to the ratios D_0 / D_1 and $\mu_{\beta_2} / \mu_{\beta_1}$, respectively (Figure 3.16-3.17). Figure 3.16 shows that system reliability is sensitive to the ratio D_0 / D_1 . Increasing D_0 / D_1 (D_1 is fixed at 1.5 Gpa and D_0 increases from 1.2Gpa to 1.5 Gpa), causes $R(t)$ to shift to right. When D_0 approaches the value of D_1 , $R(t)$ becomes closer to the basic system reliability with a fixed degradation rate. It has been shown in Figure 3.17, that $R(t)$ is responsive to the change in the ratio between the increased degradation rate and the initial degradation rate, $\mu_{\beta_2} / \mu_{\beta_1}$. When the ratio reduces, $R(t)$ shifts to right. Therefore, units with a smaller ratio $\mu_{\beta_2} / \mu_{\beta_1}$ have a better reliability performance.

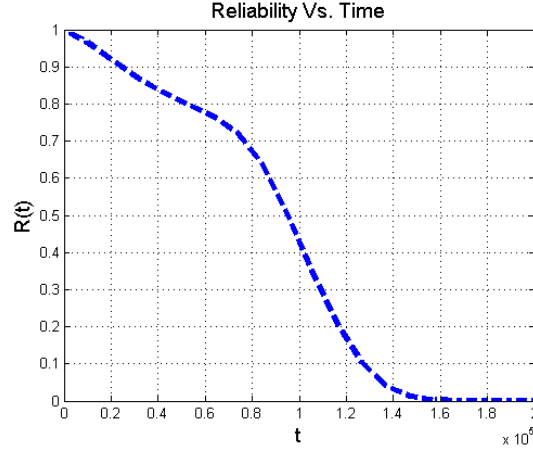


Figure 3.15: Plot of $R(t)$ for Case 4

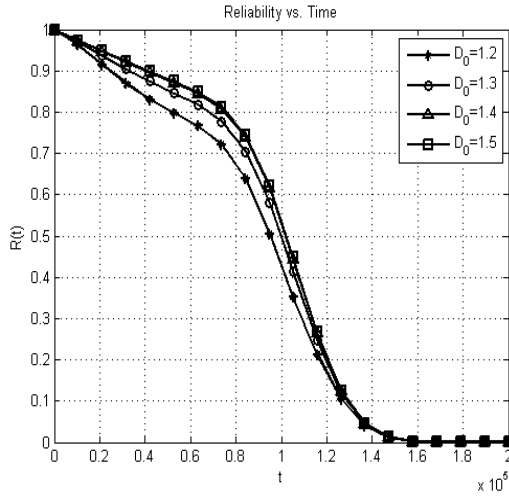


Figure 3.16: Sensitivity analysis of $R(t)$ on D_0 / D_1 for Case 4

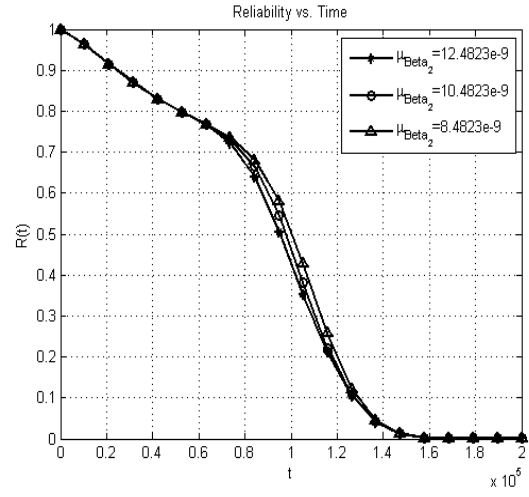


Figure 3.17: Sensitivity analysis of $R(t)$ on $\mu_{\beta_2} / \mu_{\beta_1}$ for Case 4

3.5. Conclusion

In this chapter, we introduced new reliability models for a complex system experiencing DCFP with a changing degradation rate according to different shock patterns. This study represents entirely new research for a device with DCFP. The two dependent failure processes are soft failure due to continuous wear degradation, and sudden increases in degradation caused by random shocks, and hard failure due to same shocks. These two failure processes are dependent because arriving random shocks affect both failure processes and the shock processes impact on the degradation rate. Four cases of

dependency between the shock process and the wear degradation rate are studied: 1) the degradation rate changes when the first shock is recorded above a critical value, or a generalized extreme shock model; 2) the degradation rate shifts when the inter-arrival time of two sequential shocks is less than a threshold, or a generalized δ -shock model; 3) the degradation rate shifts to a higher level right after m shocks greater than a threshold, or a generalized m -shock model; and 4) the degradation rate changes right after the first run of n consecutive shocks larger than a critical value, or generalized run shock model. Then the developed reliability models are demonstrated for these four cases by using a micro-engine example.

Chapter 4

Reliability Assessment of Competing Risks with Generalized Mixed Shock Model

This chapter investigates reliability modeling for systems subject to dependent competing risks considering the impact from a new generalized mixed shock model. Two dependent competing risks are soft failure due to a degradation process, and hard failure due to random shocks. Unlike most existing mixed shock models that consider a combination of two shock patterns, our new generalized mixed shock model includes three classic shock patterns: extreme shock model, δ -shock model, and run shock model. According to the proposed generalized mixed shock model, the degradation rate and the hard failure threshold can simultaneously shift multiple times, whenever the condition for one of these three shock patterns is satisfied. An example using MEMS devices illustrates the effectiveness of the proposed modeling approach with sensitivity analysis.

4.1. Introduction

Recently, there have been many studies devoted to reliability analysis for systems subject to multiple DCFP (Wang et al. 2008; Lehmann 2009; Jiang et al. 2012). For complex systems such as MEMS, the dependence between the two competing risks of degradation and shocks can lead to complex behavior, which can be considered in a variety of different analytical perspectives. When a system withstands shocks, it becomes more vulnerable to upcoming shocks, while the shock process can also damage the system and accelerate the deterioration process (Tanner et al. 2000). This chapter aims to extend the previous models (Jiang et al. 2012; Rafiee et al. 2014a; Rafiee et al. 2014b) by

incorporating multiple sources of dependence between competing risks into a rich reliability model.

Recent research has started to consider the impacts of shocks on the degradation process in dependent competing risks. Wang et al. (2011) investigated reliability modeling when the degradation and shocks are involved. Each shock impacts degradation in two forms: a sudden increase in the degradation rate, and an abrupt damage. Peng et al. (2010) proposed a reliability model for systems with two dependent failure processes: soft failure due to degradation that is accumulated by continuous degradation over time and sudden increase due to shocks, and hard failure caused by the same shocks. To extend the study in Peng et al. (2010), Jiang et al. (2012) considered the case where the system resistance to failure weakens when withstanding shocks. Therefore, the hard failure threshold is not fixed, and can change due to different shock patterns, i.e., extreme shock model, m -shock model, and δ -shock model. The hard failure threshold shifts to a lower level when one of the shock patterns occurs. Rafiee et al. (2014b) extended the model in Peng et al. (2010) by introducing new reliability models where the degradation rate can accelerate due to different shock patterns. As a result of withstanding shocks, the degradation rate is not a constant when the system becomes more prone to fatigue. By considering the declining hard failure threshold according to changes in degradation, Rafiee et al. (2014a) introduced reliability models for a device with two dependent failure processes: soft failure due to degradation, and hard failure due to random shocks.

However, none of the existing research considers the integration or combination of these impacts of shocks on the system in one general model. The new model proposed in this chapter takes care of three different impacts of shocks on the system: 1) abrupt damage

on degradation, 2) increasing the degradation rate, and 3) shifting the hard failure threshold. What distinguishes our model from the previous research lies on this new assumption that the degradation rate and the hard failure threshold can *simultaneously* change *multiple times*, given the condition for the *generalized mixed shock model* is satisfied. This general assumption reflects the more complex behavior associated with modern systems and structures that experience multiple sources of external shocks.

Compared to existing studies (Jiang et al. 2012; Rafiee et al. 2014a; Rafiee et al. 2014b), the main contributions of this chapter are considered to be:

1. The degradation rate and the hard failure threshold can shift/transition *simultaneously*.
2. A transition is triggered by three shock models in a new *generalized mixed shock model*, instead of only one shock model.
3. The transition can occur *multiple times*, whenever the condition for the generalized mixed shock model is satisfied.

This chapter is organized as follows. Section 4.2 describes two dependent failure processes of hard failure and soft failure, and derives the reliability model for a system subject to a generalized mixed shock model. In Section 4.3, we derive the probability of trigger shock count in the generalized mixed shock model. Section 4.4 presents a numerical example and evaluates the effects of model parameters. Section 4.5 summarizes the chapter and concluding remarks are made.

4.2. Reliability Modeling with Generalized Mixed Shock Model

We propose a new reliability model for systems subject to dependent competing risks under the impact from a generalized mixed shock model. Two dependent competing

risks are soft failure due to a degradation process, and hard failure due to shocks. The shock process contains fatal shocks that can cause the hard failure instantaneously, and nonfatal shocks that simultaneously impact the system in three different ways: 1) damage the unit by increasing the degradation level instantaneously, 2) speed up the deterioration by accelerating the degradation rate, and 3) weaken the unit strength by reducing the hard failure threshold. While the first impact of nonfatal shocks comes from each individual shock, the other two impacts are realized when the condition for the generalized mixed shock model is satisfied. Unlike most existing mixed shock models that consider a combination of two shock patterns, our generalized mixed shock model includes three classic shock patterns: extreme shock model, δ -shock model and run shock model.

Figure 4.1 depicts two dependent failure processes: soft failure due to a degradation process and hard failure due to random shocks. A soft failure occurs when the overall degradation level exceeds a predetermined threshold H . The continuous degradation by time t , $X(t)$, is monotonically increasing, which is assumed to be a linear path, expressed as $X(t) = \varphi + \beta t$, where φ is the initial degradation level and β is degradation rate. This linear path function can be applied to a wide range of degradation models.

Hard failure can be caused by fatal shocks that have a magnitude larger than D_j ($j = 1, 2, 3$). Nonfatal shocks impact the systems in three different ways: sudden increment in the degradation level at each shock z , Y_z , and the simultaneous transitions in the hard failure threshold D_j and the degradation rate β_j , whenever the conditions of the generalized mixed shock model is satisfied. For example, the first transition occurs when the magnitude of the shock arrived at time t_2 is greater than the critical level for the extreme shock model

increased degradation rate from β_1 to β_2 .

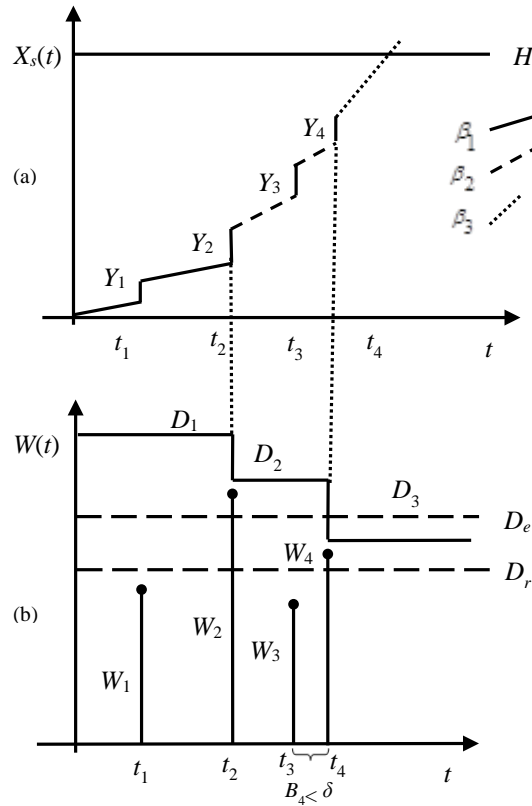


Figure 4.1: Two dependent competing failure processes: (a) soft failure, (b) hard failure

Notation

D_e	Critical level for extreme shock model
D_r	Critical level for run shock model
D_j	Hard failure threshold after the $j-1^{th}$ transition, $j=1, 2, \dots$
d	Amount of reduction in hard failure threshold after a transition
$N(t)$	Number of shocks arrived by time t
λ	Arrival rate of shocks
W_z	Magnitude of the shock load
$F_W(w)$	Cumulative distribution function (cdf) of W
H	Threshold level for soft failure
$X(t)$	Amount of continuous degradation at time t
$X_S(t)$	Degradation due to continuous degradation and abrupt damage at time t
φ	Initial level of degradation
β_j	Degradation rate after the $j-1^{th}$ transition
η	Amount of increase in degradation rate after a transition
Y_z	Damage size on degradation caused by the shocks

$Z(t)$	Cumulative damage size by shocks at time t
n	Required number of consecutive shocks that are greater than D_r in the run shock model
B_z	Inter-arrival time between two consecutive shocks
δ	Minimum time lag between two consecutive shocks for the δ -shock model
T_j	The j^{th} transition time
L	Maximum number of possible transitions for a system
$R(t)$	Reliability function by time t
$R_H(t)$	Probability of no hard failure by time t
$R_S(t)$	Probability of no soft failure by time t
S_j	Shock count that triggers the j^{th} transition
S_j^e	Shock count that triggers the j^{th} transition according to extreme shock model
S_j^r	Shock count that triggers the j^{th} transition according to run shock model
S_j^δ	Shock count that triggers the j^{th} transition according to δ -shock model

4.2.1. Transition Process

According to the proposed generalized mixed shock model, the degradation rate and the hard failure threshold shift simultaneously, if 1) a shock is above a critical value D_e in the extreme shock model, 2) a time lag between two sequential shocks is less than δ in the δ -shock model, or 3) a run of n consecutive shocks are greater than a critical level D_r ($D_r < D_e$) in the run shock model. These three classic shock models are competing against each other, and whichever occurs first causes the shift in the hard failure threshold and the degradation rate. Every time that a transition occurs, the condition of the system worsens. In practice, the system can only undergo a limited number of transitions, after which any transition can cause the system to fail. The maximum number of possible transitions for a system, L , is predetermined based on the device characteristics. Some important assumptions regarding the transitions include:

1. If more than one shock pattern takes place at the same time, they do not amplify the effects on the hard failure threshold and the degradation rate.

2. The transition is not a onetime event, and can happen multiple times whenever the condition for the generalized mixed shock model is satisfied.
3. After each transition, prior shocks are not taken into account for the next generalized mixed shock model.
4. The trigger shock count and the transition time are being reset after each transition.

The degradation rate increases from β_j to β_{j+1} when the system experiences the j^{th} transition for $j = 1, \dots, l$, where l is the total number of transitions actually occurred before failure, and $l \leq L$. The $\boldsymbol{\beta}$ representing the degradation rate vector is

$$\boldsymbol{\beta} = [\beta_1 \quad \cdots \quad \beta_j \quad \cdots \quad \beta_{l+1}], \quad (4.1)$$

where the j^{th} element (β_j) is the degradation rate after the $(j-1)^{th}$ transition. We define $\beta_{j+1} = \beta_j + \eta$ where η is an *i.i.d.* positive random variable and independent of β_j .

Similarly, the hard failure threshold declines from D_j to D_{j+1} after the j^{th} transition for $j = 1, \dots, l$. We use \mathbf{D} to represent the hard failure threshold vector as

$$\mathbf{D} = [D_1 \quad \cdots \quad D_j \quad \cdots \quad D_{l+1}], \quad (4.2)$$

where the j^{th} element (D_j) is the hard failure threshold after the $(j-1)^{th}$ transition. We define $D_{j+1} = D_j - d$ where d is an *i.i.d.* positive random variable that is independent of D_j .

The shock that triggers a transition is called the trigger shock. The time lag between two successive transitions is defined as the transition time. To facilitate the evaluation of reliability for a system subject to changing hard failure threshold and changing degradation rate according to multiple competing shock patterns, we investigate each transition separately from others. Consequently, the trigger shock count (the number of shocks leading to a transition) and the transition time are being reset after each transition. The number of shocks leading to the j^{th} transition is denoted as S_j after the last transition, which

is an unknown random variable. The time lag between the $(j-1)^{th}$ and the j^{th} trigger shocks is called the j^{th} transition time, T_j , which is also a random variable. We use \mathbf{T} to denote the transition time vector including T_j for $j = 1, \dots, l$:

$$\mathbf{T} = [T_1 \quad \cdots \quad T_j \quad \cdots \quad T_l \quad T_{l+1}], \quad (4.3)$$

where $T_{l+1} = t - \sum_{j=1}^l T_j$ represents the remaining time after the last transition. After the random transition times are realized, the vector \mathbf{T} transfers to be a vector composed of known values of transition times:

$$\tilde{\mathbf{t}} = [t_1 \quad \cdots \quad t_j \quad \cdots \quad t_l \quad t_{l+1}]. \quad (4.4)$$

4.2.2. Shock Process and Hard Failure

Random shocks arrive according to a homogeneous Poisson process with rate λ , and it is independent of the degradation process. The total number of shocks by time t , $N(t)$, follows a Poisson distribution:

$$P(N(t) = i) = \frac{e^{-\lambda t} (\lambda t)^i}{i!}, \quad i = 0, 1, 2, \dots \quad (4.5)$$

The magnitude of a shock is denoted by W_z for $z = 1, 2, \dots$, a sequence of *i.i.d.* non-negative random variables with a common cumulative distribution $F_W(w) = P(W_z < w)$. In this chapter, the traditional extreme shock model is employed for traumatic failure. It means that the unit fails as soon as the size of any shock is greater than the corresponding hard failure threshold at the time of shock arrival. The probability that a unit survives after exposing to a single shock is

$$P(W_z < D_j) = F_W(D_j), \quad \text{for } z = 1, 2, \dots; \quad j = 1, \dots, \text{or } l+1. \quad (4.6)$$

In order for a unit not to experience hard failure by time t , it needs to survive all the shocks by that time. By considering the following two scenarios, the probability of no hard failure by time t , $R_H(t)$, can be derived further.

- i) No transition occurs by time t , or the shock count for the first transition is larger than $N(t)$, $S_1 > N(t) = i$. The magnitude of each shock must be less than the initial hard failure threshold, D_1 . The probability of surviving against hard failure given that no transition occurs by time t is

$$R_H(t | S_1 > N(t) = i) = P\left(\bigcap_{z=1}^i \{W_z < D_1\}\right) = F_W(D_1)^i. \quad (4.7)$$

- ii) At least one transition occurs by time t , or the shock count for the first transition is less than or equal to $N(t)$, $S_1 \leq N(t) = i$. The magnitude of each shock must be less than the corresponding hard failure threshold at the time of shock arrival. We use $I_{j+1} = i - \sum_{k=1}^j S_k$, for $j = 1, \dots, l$, to denote the number of remaining shocks after the j^{th} transition, which is a random variable. After the value for shock counts are realized, it becomes $i_{j+1} = i - \sum_{k=1}^j s_k$. The probability of no hard failure given $S_1 \leq N(t) = i$ is (see

Appendix D)

$$R_H(t | S_1 = s_1 \leq N(t) = i) = \sum_{s_1=1}^{i_1} \cdots \sum_{s_2=1}^{i_2} \sum_{l=1}^L \left[\prod_{j=1}^l F_W(D_j)^{s_j} \right] F_W(D_{l+1})^{i_{l+1}} \times P(S_{l+1} > i_{l+1}) \left[\prod_{j=2}^l P(S_j = s_j) \right]. \quad (4.8)$$

We present the further derivation of $P(S_j = s_j)$, the probability that the j^{th} transition occurs at the s_j^{th} shock after the last transition, and $P(S_{l+1} > i_{l+1})$, the probability that no transition occurs in the remaining shocks after the very last transition in Section 4.3.

4.2.3. Degradation Process and Soft Failure

A soft failure occurs when the overall degradation exceeds a predetermined threshold H . As aforementioned, we model the degradation process as a linear path, expressed as $X(t) = \varphi + \beta t$, where φ is the initial degradation level that is a random variable (due to variability in manufacturing and delivering processes) and β is degradation rate that is a random variable and varies from part to part.

The shock process impacts the degradation in two ways: causing a sudden increment to the degradation by each nonfatal shock, and increasing the degradation rate according to a generalized mixed shock model. We denote the damage from each shock by Y_z for $z = 1, 2, \dots$, where Y_z is an *i.i.d.* non-negative random variable. The overall degradation including both continuous degradation and instantaneous damage induced by nonfatal shocks can be expressed as

$$X_s(t) = X(t) + Z(t) = X(t) + \sum_{z=1}^{N(t)} Y_z, \quad (4.9)$$

where $Z(t)$ represents the cumulative damage by nonfatal random shocks.

By considering the following two situations, the probability of no soft failure by time t , $R_s(t)$, can be derived further.

- i) No transition occurs by time t , or the shock count for the first transition is larger than $N(t)$, $S_1 > N(t) = i$. Given no transition by time, the initial degradation rate is fixed and the probability of no soft failure by time t is

$$R_s(t | S_1 > N(t) = i) = P(X_s(t) < H | S_1 > N(t) = i) = P\left(\varphi + \beta_1 t + \sum_{z=1}^i Y_z < H\right). \quad (4.10)$$

- ii) At least one transition occurs by time t , or the shock count for the first transition is less than or equal to $N(t)$, $S_1 \leq N(t) = i$. When a system experiences a transition, the

degradation rate shifts; therefore, the degradation progresses at an increased degradation rate. The probability of no soft failure given at least one transition and the total number of shocks occurred by time t is (see Appendix II)

$$R_s(t|S_1 = s_1 \leq N(t) = i) = \sum_{s_1=1}^{i_1} \cdots \sum_{s_2=1}^{i_2} \sum_{l=1}^L P\left(\varphi + \sum_{j=1}^l \beta_j T_j + \beta_{l+1} T_{l+1} + \sum_{z=1}^i Y_z < H\right) \times P(S_{l+1} > i_{l+1}) \left[\prod_{j=2}^l P(S_j = s_j) \right]. \quad (4.11)$$

In a homogeneous Poisson process, the time for the j^{th} transition T_j , given a value of $S_j = s_j$, follows a gamma distribution with the scale parameter of s_j , and the shape parameter of λ :

$$f_{T_j}(t_j) = \frac{\lambda^{s_j}}{(s_j - 1)!} t_j^{s_j-1} e^{-\lambda t_j}, \quad \text{for } j = 1, \dots, l. \quad (4.12)$$

The probability that the j^{th} transition occurs at the s_j^{th} shock after the last transition, $P(S_j = s_j)$, changes based on which shock pattern occurs. Let $t'_j = t - \sum_{k=1}^{j-1} t_k$ denote the remaining time after the j^{th} transition for $j = 1, \dots, l$. Then the probability in (4.11) can be calculated as

$$R_s(t|S_1 = s_1 \leq N(t) = i) = \sum_{s_1=1}^{i_1} \cdots \sum_{s_2=1}^{i_2} \sum_{l=1}^L P(S_{l+1} > i_{l+1}) \left[\prod_{j=2}^l P(S_j = s_j) \right] \times \left(\int_0^t \cdots \left(\int_0^{t'_l} P\left(\varphi + \sum_{j=1}^l \beta_j t_j + \beta_{l+1} t_{l+1} + \sum_{z=1}^i Y_z < H\right) f_{T_l}(t_l) dt_l \right) \cdots f_{T_1}(t_1) dt_1 \right). \quad (4.13)$$

4.2.4. System Reliability Modeling

We investigate the reliability model for a system subject to the generalized mixed shock model that can cause multiple transitions in both the degradation rate and the hard failure threshold. Given the number of shocks by time t , the soft failure and hard failure

processes are conditionally independent, due to the assumption that the shock damage size Y_z is independent of the shock load W_z . Considering situations when there is no transition, only one transition, and more than one transition by time t , the reliability at time t for a system that experiences two DCFP is derived based on Eqs. (4.8) and (4.13):

$$\begin{aligned}
R(t) = & P(\varphi + \beta_1 t < H) \times e^{-\lambda t} + \sum_{i=1}^{\infty} P\left(\varphi + \beta_1 t + \sum_{z=1}^i Y_z < H\right) F_W(D_1)^i P(S_1 > i) \frac{e^{-\lambda t} (\lambda t)^i}{i!} \\
& + \sum_{i=1}^{\infty} \sum_{s_1=1}^{i_1} \cdots \sum_{s_2=1}^{i_2} \sum_{s_1=1}^i \sum_{l=1}^L \left(\int_0^t \cdots \int_0^{t_l'} P\left(\varphi + \sum_{j=1}^l \beta_j t_j + \beta_{l+1} t_{l+1} + \sum_{z=1}^i Y_z < H\right) f_{T_l}(t_l) dt_l \right) \cdots f_{T_1}(t_1) dt_1 \\
& \times \left[\prod_{j=1}^l F_W(D_j)^{s_j} \right] F_W(D_{l+1})^{i_{l+1}} P(S_{l+1} > i_{l+1}) \left[\prod_{j=1}^l P(S_j = s_j) \right] \frac{e^{-\lambda t} (\lambda t)^i}{i!}.
\end{aligned} \tag{4.14}$$

4.3. Probability of Trigger Shock Count in the Generalized Mixed Shock Model

The probabilities related to S_j (the trigger shock count for the j^{th} transition) in (4.14) are derived in the following sections. First section discussed the applicability of different shock models, and last two sections derive the probability of trigger shock count and no transition consecutively.

4.3.1. Applicability of Different Shock Models

A transition occurs when the condition is satisfied for at least one of three shock patterns in the generalized mixed shock model: extreme shock model, δ -shock model, and run shock model. It is likely that the conditions for two or more shock patterns are satisfied at the same shock. For example, a shock with a size greater than D_e (extreme shock pattern) can have a time lag that is shorter than δ (δ -shock pattern). In a transition, the hard failure threshold is assumed to shift to a lower level. If the resulting hard failure threshold D_j is less than D_e in the extreme shock model or D_r in the run shock model, the corresponding

shock pattern is not applicable in the generalized mixed shock model anymore. For example, when D_j is less than D_e , a shock larger than D_j leads to a hard failure even before it is considered in the extreme shock model for triggering a transition.

Depending on the applicability of different shock patterns, we derive the probability of the j^{th} transition occurring at the s_j^{th} shock (after the last transition), $P(S_j = s_j)$, in the following. Due to the independence between the arriving time and the shock magnitude, the occurrence of δ -shock model is probabilistically independent from the occurrence of extreme shock model and run shock model.

1. If the hard failure threshold is greater than the critical level of extreme shock model ($D_j > D_e > D_r$), all three shock patterns are applicable. Then we have

$$\begin{aligned}
 P(S_j = s_j) &= P(S_j^e = s_j \cup S_j^r = s_j \cup S_j^\delta = s_j) \\
 &= P(S_j^e = s_j) + P(S_j^r = s_j) + P(S_j^\delta = s_j) \\
 &\quad - P(S_j^r = s_j | S_j^e = s_j) P(S_j^e = s_j) - P(S_j^e = s_j) P(S_j^\delta = s_j) \\
 &\quad - P(S_j^r = s_j) P(S_j^\delta = s_j) + P(S_j^r = s_j | S_j^e = s_j) P(S_j^e = s_j) P(S_j^\delta = s_j).
 \end{aligned} \tag{4.15}$$

2. If the hard failure threshold is between the critical levels of extreme shock model and run shock model ($D_e > D_j > D_r$), the extreme shock model is not applicable. Then we have

$$P(S_j = s_j) = P(S_j^r = s_j \cup S_j^\delta = s_j) = P(S_j^r = s_j) + P(S_j^\delta = s_j) - P(S_j^r = s_j) P(S_j^\delta = s_j). \tag{4.16}$$

3. If the hard failure threshold is less than the critical level of run shock model ($D_r > D_j$), only δ -shock model is applicable:

$$P(S_j = s_j) = P(S_j^\delta = s_j). \tag{4.17}$$

4.3.2. Probability of Trigger Shock Count

The probabilities for different shock patterns occurring at the s_j^{th} shock in Eqs. (4.15-4.17) are derived and presented in Table 4.1. The first column lists different shock patterns that can cause the j^{th} transition, and the second column presents the probabilities of the corresponding shock patterns.

Table 4.1: Probability for occurrence of different shock patterns

Shock models that cause the j^{th} transition at the s_j^{th} shock		Probability
1) Extreme shock pattern at the s_j^{th} shock		$P(S_j^e = s_j) = P\left(\bigcap_{z=1}^{s_j-1} \{W_z < D_e\}, W_{s_j} \geq D_e \mid \bigcap_{z=1}^{s_j} \{W_z < D_j\}\right)$ $= \frac{F_W(D_e)^{s_j-1} (F_W(D_j) - F_W(D_e))}{F_W(D_j)^{s_j}}$
2) δ -shock pattern at the s_j^{th} shock		$P(S_j^\delta = s_j) = P\left(\bigcap_{z=1}^{s_j-1} \{B_z < \delta\}, B_{s_j} \leq \delta\right) = e^{-(s_j-1)\lambda\delta} (1 - e^{-\lambda\delta})$
3) Run shock pattern at the s_j^{th} shock	$s_j < n$	$P(S_j^r = s_j) = 0$
	$s_j = n$	$P(S_j^r = s_j) = P\left(\bigcap_{z=1}^n \{W_z \geq D_r\} \mid \bigcap_{z=1}^n \{W_z < D_j\}\right) = \frac{(F_W(D_j) - F_W(D_r))^n}{F_W(D_j)^n}$
	$s_j > n$	$P(S_j^r = s_j) = P(S_j^r > s_j - n - 1) P\left(W_{s_j-n} < D_r, \bigcap_{z=s_j-n+1}^{s_j} \{W_z \geq D_r\} \mid \bigcap_{z=s_j-n}^{s_j} \{W_z < D_j\}\right)$ $= P(S_j^r > s_j - n - 1) \frac{F_W(D_r) (F_W(D_j) - F_W(D_r))^n}{F_W(D_j)^{n+1}}$
4) Run shock pattern at the s_j^{th} shock given concurrent extreme shock pattern	$s_j < n$	$P(S_j^r = s_j \mid S_j^e = s_j) = 0$
	$s_j = n$	$P(S_j^r = s_j \mid S_j^e = s_j) = P\left(\bigcap_{z=1}^n \{D_r \leq W_z\} \mid \bigcap_{z=1}^{n-1} \{W_z < D_e\}, W_n \geq D_e\right)$ $= \frac{(F_W(D_e) - F_W(D_r))^{n-1}}{F_W(D_e)^{n-1}}$
	$s_j > n$	$P(S_j^r = s_j \mid S_j^e = s_j) = P\left(S_j^r > s_j - n - 1 \mid \bigcap_{z=1}^{s_j-n-1} \{W_z < D_e\}\right)$ $\times P\left(W_{s_j-n} < D_r, \bigcap_{z=s_j-n+1}^{s_j} \{D_r \leq W_z\} \mid \bigcap_{z=s_j-n}^{s_j-1} \{W_z < D_e\}, W_{s_j} \geq D_e\right)$ $= P\left(S_j^r > s_j - n - 1 \mid \bigcap_{z=1}^{s_j-n-1} \{W_z < D_e\}\right) \frac{F_W(D_r) (F_W(D_e) - F_W(D_r))^{n-1}}{F_W(D_e)^n}$

When the run shock model is involved, we have three subcases based on the relationship between s_j and n , as presented in Table 4.1. In general, we defined V_{s_j} to be the probability that no run of n consecutive successes (a success is defined as a shock greater than D_r) occur in a set of s_j shocks, and V'_{s_j} to be the probability that the first run of n consecutive successes occurs at the s_j^{th} shock. We have (Krieger 1984):

$$V_{s_j} = \begin{cases} 1, & \text{if } 0 \leq s_j < n \\ 1 - p^n, & \text{if } s_j = n, \\ qV_{s_j-1} + \dots + qp^{n-1}V_{s_j-n}, & \text{if } s_j > n \end{cases} \quad (4.18)$$

where p is the probability of success, and $q = 1 - p$. In addition, we have

$$V'_{s_j} = \begin{cases} 0, & \text{if } 0 \leq s_j < n \\ p^n, & \text{if } s_j = n. \\ qp^nV_{s_j-n-1}, & \text{if } s_j > n \end{cases} \quad (4.19)$$

When $s_j > n$, to have the first run of n consecutive successes occurring at the s_j^{th} trial, the last n trials must be successes, the $(s_j - n)^{th}$ trial must be a failure, and no consecutive n successes occur in the first $s_j - n - 1$ trials.

The derivation of the four cases in Table 1 is described as follows:

- 1) Extreme shock pattern: the probability is derived for the situation when the s_j^{th} shock is the first shock with a magnitude greater than D_e , and the prior $s_j - 1$ shocks are less than D_e , given that the magnitudes of all shocks are less than D_j to ensure no occurrence of hard failure.
- 2) δ -shock pattern: the probability is derived for the situation when the time lag between the $s_j - 1^{th}$ shock and the s_j^{th} shock is shorter than δ , while the prior $s_j - 1$ time lags are longer than δ .

- 3) Run shock pattern: the probability is derived based on the relationship between s_j and n . Eq. (4.19) is used in three different subcases to derive the probability of the first run of n consecutive shocks greater than D_r occurs at the s_j^{th} shock, with the probability of success $p = (W_z \geq D_r \mid W_z < D_j)$.
- 4) Run shock pattern given concurrent occurrence of extreme shock pattern at the s_j^{th} shock: according to Eq. (4.19), when the run shock model is among shock patterns that can cause a transition, we have three subcases based on the relationship between s_j and n , with the probability of success $p = (W_z \geq D_r \mid W_z < D_e)$.

4.3.3. Probability of no Transition in Remaining Shocks

When the number of transitions by time t is l , it implies that there is no transition in the remaining i_{l+1} shocks after the l^{th} transition, or the shock count for the $l + 1$ transition is larger than i_{l+1} . The probability of no transition in the last i_{l+1} shocks depends on the relationship between the final hard failure threshold D_{l+1} and the critical levels for extreme shock pattern (D_e) and run shock pattern (D_r):

1. If the hard failure threshold after the l^{th} transition is greater than the critical level of extreme shock model ($D_{l+1} > D_e > D_r$), all three shock patterns are applicable. Then the probability of no transition in the last i_{l+1} shocks is

$$\begin{aligned} P(S_{l+1} > i_{l+1}) &= P(S_{l+1}^e > i_{l+1} \cap S_{l+1}^r > i_{l+1} \cap S_{l+1}^\delta > i_{l+1}) = \\ &= P(S_{l+1}^r > i_{l+1} \mid S_{l+1}^e > i_{l+1}) P(S_{l+1}^e > i_{l+1}) P(S_{l+1}^\delta > i_{l+1}). \end{aligned} \quad (4.20)$$

2. If the hard failure threshold after the l^{th} transition is between the critical levels of extreme shock model and run shock model ($D_e > D_{l+1} > D_r$), the extreme shock model is not applicable. Then we have

$$P(S_{l+1} > i_{l+1}) = P(S_{l+1}^r > i_{l+1} \cap S_{l+1}^\delta > i_{l+1}) = P(S_{l+1}^r > i_{l+1}) P(S_{l+1}^\delta > i_{l+1}). \quad (4.21)$$

3. If the hard failure threshold after the l^{th} transition is less than the critical level of run shock model ($D_r > D_{l+1}$), only δ -shock model is applicable:

$$P(S_{l+1} > i_{l+1}) = P(S_{l+1}^\delta > i_{l+1}). \quad (4.22)$$

The probabilities of no transition after the l^{th} transition in the remaining i_{l+1} shocks, or $P(S_{l+1} > i_{l+1})$, for different scenarios in Eqs. (4.20)-(4.22) are derived and presented in Table 4.2.

Table 4.2: Probability of no transition after the l^{th} transition

Shock models that can cause the $l+1^{th}$ transition in remaining i_{l+1} shocks		Probability
1) No extreme shock pattern in remaining i_{l+1} shocks		$P(S_{l+1}^e > i_{l+1}) = P\left(\bigcap_{z=1}^{i_{l+1}} \{W_z < D_e\} \mid \bigcap_{z=1}^{i_{l+1}} \{W_z < D_{l+1}\}\right) = \frac{F_W(D_e)^{i_{l+1}}}{F_W(D_{l+1})^{i_{l+1}}}$
2) No δ -shock pattern in remaining i_{l+1} shocks		$P(S_{l+1}^\delta > i_{l+1}) = P\left(\bigcap_{z=1}^{i_{l+1}} \{B_z > \delta\}\right) = e^{-i_{l+1}\lambda\delta}$
3) No run shock pattern in remaining i_{l+1} shocks	$i_{l+1} < n$	$P(S_{l+1}^r > i_{l+1}) = 1$
	$i_{l+1} = n$	$P(S_{l+1}^r > i_{l+1}) = 1 - P\left(\bigcap_{z=1}^{i_{l+1}} \{W_z \geq D_r\} \mid \bigcap_{z=1}^{i_{l+1}} \{W_z < D_{l+1}\}\right) \\ = 1 - \frac{(F_W(D_{l+1}) - F_W(D_r))^n}{F_W(D_{l+1})^n}$
	$i_{l+1} > n$	$P(S_{l+1}^r > i_{l+1}) = (S_{l+1}^r > i_{l+1} - 1)P(W_{i_{l+1}} < D_r \mid W_{i_{l+1}} < D_{l+1}) + \dots \\ \dots + P(S_{l+1}^r > i_{l+1} - n)P\left(W_{i_{l+1}-n+1} < D_r, \bigcap_{z=i_{l+1}-n+2}^{i_{l+1}} \{W_z \geq D_r\} \mid \bigcap_{z=i_{l+1}-n+1}^{i_{l+1}} \{W_z < D_{l+1}\}\right) \\ = P(S_{l+1}^r > i_{l+1} - 1) \frac{F_W(D_r)}{F_W(D_{l+1})} + \dots \\ \dots + P(S_{l+1}^r > i_{l+1} - n) \frac{F_W(D_r)(F_W(D_{l+1}) - F_W(D_r))^{n-1}}{F_W(D_{l+1})^n}$
4) No run shock pattern in remaining i_{l+1} shocks given no extreme shock pattern	$i_{l+1} < n$	$P(S_{l+1}^r > i_{l+1} - 1 \mid S_{l+1}^e > i_{l+1} - 1) = 1$
	$i_{l+1} = n$	$P(S_{l+1}^r > i_{l+1} - 1 \mid S_{l+1}^e > i_{l+1} - 1) = 1 - P\left(\bigcap_{z=1}^n \{D_r \leq W_z\} \mid \bigcap_{z=1}^n \{W_z < D_e\}\right) \\ = 1 - \frac{(F_W(D_e) - F_W(D_r))^n}{F_W(D_e)^n}$

	$i_{l+1} > n$	$P\left(S_{l+1}^r > i_{l+1} - 1 \mid S_{l+1}^e > i_{l+1} - 1\right) = P\left(S_{l+1}^r > i_{l+1} - 1 \mid \bigcap_{z=1}^{i_{l+1}-1} \{W_z < D_e\}\right)$ $\times P\left(W_{i_{l+1}} < D_r \mid W_{i_{l+1}} < D_e\right) + \dots + P\left(S_{l+1}^r > i_{l+1} - n \mid \bigcap_{z=1}^{i_{l+1}-n} \{W_z < D_e\}\right)$ $\times P\left(W_{i_{l+1}-n+1} < D_r, \bigcap_{z=i_{l+1}-n+2}^{i_{l+1}} \{W_z \geq D_r\} \mid \bigcap_{z=i_{l+1}-n+1}^{i_{l+1}} \{W_z < D_e\}\right)$ $= P\left(S_{l+1}^r > i_{l+1} - 1 \mid \bigcap_{z=1}^{i_{l+1}-1} \{W_z < D_e\}\right) \frac{F_W(D_r)}{F_W(D_e)} + \dots$ $\dots + P\left(S_{l+1}^r > i_{l+1} - n \mid \bigcap_{z=1}^{i_{l+1}-n} \{W_z < D_e\}\right) \frac{F_W(D_r)(F_W(D_e) - F_W(D_r))^{n-1}}{F_W(D_e)^n}$
--	---------------	---

- 1) No extreme shock pattern: the probability is derived for the situation when the magnitude of all i_{l+1} shocks are less than D_e , given that the magnitudes of all shocks are less than D_{l+1} to ensure no occurrence of hard failure.
- 2) No δ -shock pattern: the probability is derived for the situation when the time lags between any two successive shocks must be longer than δ .
- 3) No run shock pattern: the probability is derived based on the relationship between i_{l+1} and n . Eq. (4.18) is used to further derive the probability of no transition for three different subcases with the probability of success $p = (W_z \geq D_r \mid W_z < D_e)$.
- 4) No run shock pattern given no extreme shock pattern in the remaining i_{l+1} shocks: Eq. (4.18) is used to further derive the probability of no set of n consecutive shocks that are greater than D_r (no run shock pattern), given that the magnitudes of all shocks are less than D_e (no extreme shock pattern) for three subcases.

4.4. Numerical Examples

The developed reliability model is illustrated by using a realistic example of MEMS. Emerged in the late 1980s, MEMS devices are composed of (a) micro mechanical-structures, (b) micro-sensors, (c) micro-electronics, and (d) micro-actuators, all placed into the same device at micro-scale. They have been widely used in many applications such as

medical, aerospace, military, etc. (Ye et al. 2012). We implement our new reliability models to the application of micro-engines, because a micro-engine fails due to two competing failure processes: (1) soft failure as the result of aging degradation and debris caused by shocks, and (2) hard failure because of spring fracture from the same shocks. In addition, a micro-engine becomes more susceptible to shocks and the wear volume accumulates faster, after exposure to a certain pattern of shocks or a significantly large shock. The corresponding value for each parameter is presented in Table 4.3.

Table 4.3: Parameter values

Parameters	Values	Sources
H	$0.00125\mu\text{m}^3$	(Tanner & Dugger 2003)
D_1	1.5Gpa	(Tanner & Dugger 2003)
μ_d	0.2Gpa	Assumption
σ_d	0.01Gpa	Assumption
D_e	1.4Gpa	Assumption
D_r	1.2Gpa	Assumption
ϕ	0	(Tanner & Dugger 2003)
$\mu_{\beta 1}$	$8.4823 \times 10^{-9} \mu\text{m}^3$	(Tanner & Dugger 2003)
$\sigma_{\beta 1}$	$6.0016 \times 10^{-10} \mu\text{m}^3$	(Tanner & Dugger 2003)
$\mu_{\eta 1}, \mu_{\eta 2}$	$2.4823 \times 10^{-9} \mu\text{m}^3$	Assumption
$\sigma_{\eta 1}, \sigma_{\eta 2}$	$1.0016 \times 10^{-10} \mu\text{m}^3$	Assumption
λ	5×10^{-5} / revolutions	Assumption
μ_W	1.2Gpa	Assumption
σ_W	0.2Gpa	Assumption
μ_Y	$1.0 \times 10^{-4} \mu\text{m}^3$	Assumption
σ_Y	$2 \times 10^{-5} \mu\text{m}^3$	Assumption
δ	2.0×10^3 revolutions	Assumption

For the proposed generalized mixed shock model with increasing degradation rate and decreasing hard failure threshold, the reliability function $R(t)$ in (4.14) is plotted in Figure 4.2, and sensitivity analysis is performed to measure the effects of the parameters D_e , δ and D_r on the reliability function (Figure 4.3-4.5).

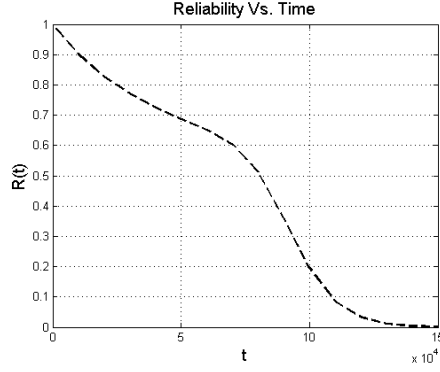


Figure 4.2: Plot of $R(t)$

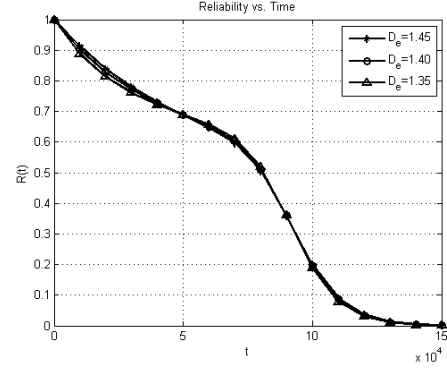


Figure 4.3: Sensitivity analysis of $R(t)$ on D_e

As can be observed in Figure 4.3, the critical threshold for extreme shock model (D_e) has a significant impact on the reliability of the system. By increasing the threshold (D_e increases from 1.35 Gpa to 1.45 Gpa), $R(t)$ shifts to right. It can be inferred that the reliability of system improves by increasing D_e . As you can see in Figure 4.4, the time lag threshold δ affects the reliability function. By increasing δ from 0.5×10^3 revolutions to 2.0×10^3 revolutions, $R(t)$ shifts slightly to the left. It indicates that the reliability performance is better for the smaller value of δ .

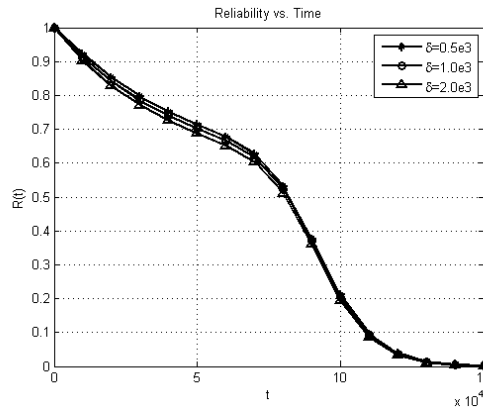


Figure 4.4: Sensitivity analysis of $R(t)$ on δ

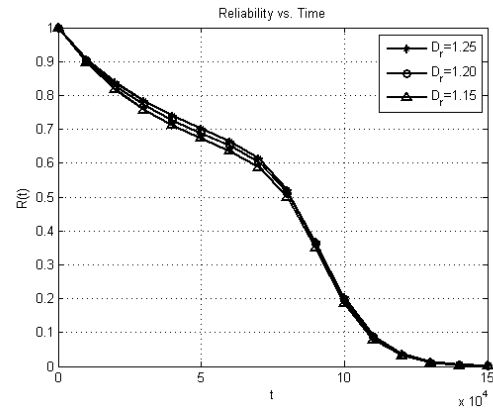


Figure 4.5: Sensitivity analysis of $R(t)$ on D_r

Figure 4.5 shows that the system reliability is sensitive to the critical threshold for run shock model (D_r). Increasing D_r from 1.15Gpa to 1.25 Gpa, causes $R(t)$ to shift to right. When D_0 approaches D_1 , $R(t)$ shifts to right that indicates a more reliable system.

4.5. Conclusion

This chapter studies a new reliability model for a system subject to dependent competing risks under the impact from a generalized mixed shock model. Two dependent failure risks are soft failure due to degradation process, and hard failure due to shocks. A soft failure occurs when the overall degradation level accumulated by continuous degradation and sudden increment caused by shocks exceeds a predetermined threshold. The hard failure occurs when the size of a fatal shock is beyond the hard failure threshold level that can change over time. A device fails as soon as either one of the failure mechanisms occurs. These two failure processes are competing yet dependent, because 1) the shocks damage the unit by increasing the degradation instantaneously, 2) the shock process may speed up the deterioration by accelerating the degradation rate, and 3) the shock process may weaken the unit by reducing the hard failure threshold. While the first impact of nonfatal shocks comes from each individual shocks, the other two impacts are realized when the condition for a generalized mixed shock model is satisfied. The proposed generalized mixed shock model happens if 1) a shock is above a critical value in extreme shock model, 2) a time lag between two sequential shocks is less than δ in δ -shock model, or 3) a run of n consecutive shocks is greater than a threshold in run shock model. When the condition for the generalized mixed shock model is satisfied, the degradation rate increases and the hard failure threshold decreases simultaneously. An example using MEMS devices illustrates the effectiveness of the proposed model with sensitivity analysis.

Chapter 5

Reliability Analysis and Condition-based Maintenance for Multiple Failure Processes under Degradation-dependent Hard Failure Threshold

In this chapter, we introduce reliability models for a device with two dependent failure processes: soft failure due to degradation, and hard failure due to random shocks, by considering the declining hard failure threshold according to changes in degradation. Previous research assumes that the hard failure threshold is a constant during the entire life of a device or decreases according to different shock models, which are appropriate assumptions for many applications. However, due to the nature of degradation for complex devices such as MEMS, a degraded system is more vulnerable to force and stress during operation. A new CBM model derived from failure limit policy (FLP) is presented to ensure that a device is functioning under a certain level of degradation. Finally, numerical examples are illustrated to explain the developed reliability and maintenance models, along with sensitivity analysis.

5.1. Introduction

For a system with two dependent failure processes: soft failure and hard failure, this chapter investigates a new problem on the decreasing hard failure threshold *due to changes in degradation level* that creates a direct dependence between hard failure and soft failure. Most previous research assumes that the hard failure threshold remains a constant during the entire life of a device (Wang et al. 2008; Peng et al. 2010) or decreases according to different shock models (Jiang et al. 2012), which are appropriate assumptions for many

design problems. However, due to the nature of degradation for complex devices such as MEMS, a degraded system can be more vulnerable to external force and stress during the operation. In other words, a device is more susceptible to failure due to external shocks when it has suffered more degradation. This observation motivates us to study the reliability of a device given that the hard failure threshold is not fixed, but decreases according to changes in degradation.

We investigate two different scenarios including (1) *one-time reduction* in hard failure threshold, where hard failure threshold decreases to a lower level instantaneously when the overall degradation exceeds a critical level; and (2) *continuous reduction* in hard failure threshold, where hard failure threshold gradually reduces from an initial value, and the amount of reduction is linearly proportional to changes in degradation. This new problem is related to but fundamentally different from the work in Jiang et al. (2012), where the hard failure threshold shifts due to the exposure to various shock patterns, rather than due to the changes in degradation. Our problem is more challenging in modeling the unknown random transition time in Case 1, and the continuously declining hard failure threshold in Case 2.

Based on the reliability models developed for these two cases, we propose a new CBM model derived from FLP, under which parts are preventively replaced when some reliability index reaches a predetermined level. Under FLP, parts are replaced preventively when the failure rate or other reliability indices reach a predetermined level. FLP can assure that a unit functions above a minimum acceptable level of reliability (Wang 2002). Bergman (1978) studied a FLP, in which replacement is performed according to an assessment of some changing state variable, e.g., wear, accumulated damage, or

accumulated stress. They proved that the optimal maintenance rule, based on the average long-run cost, is to replace units instantly at failure or when the state variable exceeds a critical threshold, whichever occurs first. In this chapter, we extend Bergman's FLP to a CBM policy by inspecting the part at the prearranged times. Based on what the inspection reveals, preventive replacement is performed if the degradation is beyond a cut-off limit, or corrective replacement is performed if the part has failed.

The remainder of this chapter is organized as follows. Section 5.2 proposes the reliability models for devices subject to degradation and random shocks with a decreasing hard failure threshold due to the changing degradation. In Section 5.3, we introduce a new maintenance policy based on FLP. Section 5.4 presents a numerical example to assess the reliability models and maintenance policy. Section 5.5 summarizes the chapter and concluding remarks are made.

5.2. Reliability Analysis with Decreasing Hard Failure Threshold

As shown in both Figure 5.1 and Figure 5.2, we consider two competing dependent failure processes: (i) soft failure happens when the total level of degradation, the result of continuous degradation in addition to abrupt damages due to random shocks, exceeds a threshold level H_0 ; and (ii) hard failure occurs when the magnitude of a shock is above a changing threshold level. In the previous research, the hard failure threshold is either fixed (Peng et al. 2010) or changing due to different shock patterns (Jiang et al. 2012). In this new model, we address the problem of the decreasing hard failure threshold due to the changes in degradation. When a device deteriorates, it is more likely to fail due to shocks. For example, a component of a MEMS device becomes more susceptible to hard failure after it wears out over time (Tanner et al. 2000).

The dependence between two failure processes is reflected in two respects.

- 1) The two competing failure processes are dependent due to shared exposure to random shocks: random shocks cause additional abrupt increasing in degradation level.
- 2) The hard failure threshold reduces according to the changes in degradation. In Case 1 (Figure 5.1), it lowers to a reduced level when the degradation amount reaches a specified critical value; and in Case 2 (Figure 5.2), it gradually decreases when the system is degrading.

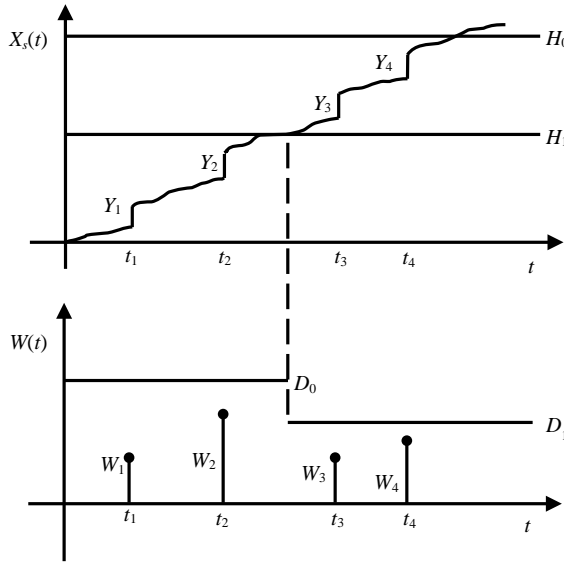


Figure 5.1: Two dependent competing failure modes for Case 1

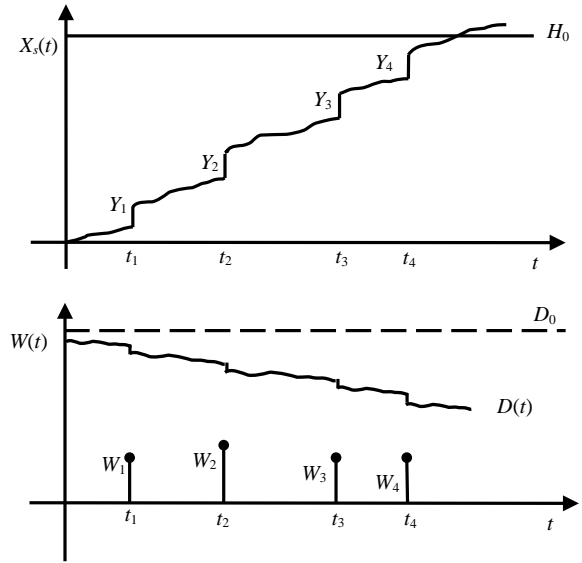


Figure 5.2: Two dependent competing failure modes for Case 2

The dependence between two failure processes is reflected in two respects.

- 3) The two competing failure processes are dependent due to shared exposure to random shocks: random shocks cause additional abrupt increasing in degradation level.
- 4) The hard failure threshold reduces according to the changes in degradation. In Case 1 (Figure 5.1), it lowers to a reduced level when the degradation amount reaches a specified critical value; and in Case 2 (Figure 5.2), it gradually decreases when the system is degrading.

Notation

D_0	Initial hard failure threshold
D_1	Reduced hard failure threshold in Case 1
$D(t)$	Hard failure threshold at time t in Case 2
λ	Arrival rate of random shocks
α	Coefficient in continuously decreasing hard failure threshold in Case 2
W_k	Magnitude of the k^{th} shock load
H_0	Soft failure threshold
H_1	Degradation level for the hard failure threshold transition in Case 1
$X(t)$	Amount of continuous degradation at time t
$X_S(t)$	Degradation due to continuous degradation and shock damages at time t
φ	Initial level of degradation
β	Degradation rate
Y_k	Damage size caused by the k^{th} random shock
T_k	Arrival time of the k^{th} shock in Case 2
$Z(t)$	Cumulative damage size by random shocks at time t
$R_H(t)$	Probability of no hard failure by time t
$R_S(t)$	Probability of no soft failure by time t
$R(t)$	System reliability by time t
$C_A(\tau, H_R)$	Average maintenance cost rate
$C(t)$	Cumulative maintenance cost by time t
C_I	Inspection cost
C_R	Replacement cost
C_F	Penalty cost per unit of time for an undetected failure
C_T	Total maintenance cost incurred in a renewal cycle
L	Length of a renewal cycle
ρ	System down time (time from system failure to the next inspection)
τ	Length of inspection interval
T	Failure time
N_I	Number of inspection before replacement
H_R	Cut-off limit on degradation for preventive replacement
$R(t H)$	System reliability by time t given the soft failure threshold is H
N_{PR}	Count of inspection at which the preventive replacement is performed
N_{CR}	Count of inspection at which the corrective replacement is performed

5.2.1. Modeling Soft Failure

Soft failure occurs when the overall degradation exceeds the threshold value H_0 .

The total degradation expressed as $X_S(t)$ is accumulated by continuous degradation over time and instantaneous damage caused by shocks. The degradation over time follows a

path $X(t) = \varphi + \beta t + \varepsilon$, where the initial value φ and the degradation rate β (the slope of degradation path) are random variables, capturing the unit-to-unit variability. The random error term ε following a normal distribution $\varepsilon \sim N(0, \sigma^2)$, is added to model temporal variability. In addition, degradation accumulates instantaneously when a shock arrives. The abrupt shifts in degradation measured as shock damage size, Y_k , for $k = 1, 2, \dots, N(t)$, are assumed to be *i.i.d.* random variables. The total damage size caused by random shocks by time t , $Z(t)$, is

$$Z(t) = \begin{cases} \sum_{k=1}^{N(t)} Y_k, & N(t) > 0 \\ 0, & N(t) = 0 \end{cases}, \quad (5.1)$$

where $N(t)$ is the total number of shocks that have arrived by time t . The degradation, consisting of both degradation and accumulated shock damages, is $X_S(t) = X(t) + Z(t)$.

For a unit not to experience a soft failure, the total degradation should be less than the threshold H_0 . Therefore the probability of surviving against soft failure, $R_S(t)$, is

$$\begin{aligned} R_S(t) &= \sum_{i=0}^{\infty} R_S(t|N(t)=i) P(N(t)=i) = \sum_{i=0}^{\infty} P(X_S(t) < H_0 | N(t)=i) P(N(t)=i) \\ &= P(X(t) < H_0) P(N(t)=0) + \sum_{i=1}^{\infty} P\left(X(t) + \sum_{k=1}^i Y_k < H_0\right) P(N(t)=i). \end{aligned} \quad (5.2)$$

If we denote $F_X(x, t)$ to be the cdf of the continuous degradation, $X(t)$, and $f_Z(z)$ to be the pdf of the accumulated damage caused by shocks, $Z(t)$, then the cdf of $X_S(t)$, $F_{X_S}(x, t)$, can be derived using a convolution integral:

$$F_{X_S}(x, t) = F_X(x, t) e^{-\lambda t} + \sum_{i=1}^{\infty} \left(\int_0^x F_X(x-u, t) f_Z(u) du \right) \frac{e^{-\lambda t} (\lambda t)^i}{i!}, \quad (5.3)$$

and we have $R_S(t) = F_{X_S}(H_0, t)$.

The model in (5.3) is general and can accommodate different distributional assumptions. In a specific case, we assume that φ is a constant, β and Y_k are normally distributed, i.e., $\beta \sim N(\mu_\beta, \sigma_\beta^2)$ and $Y_k \sim N(\mu_Y, \sigma_Y^2)$. For this specific case, the resulting total degradation, $X_S(t)$, follows a normal distribution. Then the probability in (5.2) can be expressed as

$$R_S(t) = F_{X_S}(H_0, t) = \sum_{i=0}^{\infty} \Phi \left(\frac{H_0 - (\varphi + \mu_\beta t + i\mu_Y)}{\sqrt{\sigma_\beta^2 t^2 + \sigma^2 + i\sigma_Y^2}} \right) \frac{e^{-\lambda t} (\lambda t)^i}{i!}, \quad (5.4)$$

where $\Phi(\cdot)$ is the cdf of a standard normal random variable.

5.2.2. Modeling Hard Failure

Random shocks arrive according to Poisson process with a rate λ . The size of the k^{th} random shock, denoted by W_k , and they are *i.i.d.* random variables with cdf $F_W(w)$. The system fails due to hard failure as soon as the size of a random shock exceeds the corresponding threshold. The initial threshold for hard failure is D_0 ; however, it may decrease due to the changes in degradation by considering two different cases.

Case 1: One time reduction in hard failure threshold

When the degradation reaches the transition level H_1 , it causes the hard failure threshold to reduce to D_1 . We denote the first time that the degradation exceeds H_1 , or the transition time, to be Θ , which is a random variable defined as

$$\Theta = \inf \{t : X_S(t) \geq H_1\}. \quad (5.5)$$

The number of shocks before the degradation exceeds H_1 , $N(\Theta)$, is also a random variable. The degradation may or may not reach the transition level H_1 by time t . Then the probability that the system survives against hard failure by time t , $R_H(t)$, is

$$\begin{aligned}
R_H(t) &= \sum_{i=0}^{\infty} R_H\left(t \mid X_S(t) \geq H_1 \cap N(t) = i\right) P\left(X_S(t) \geq H_1 \mid N(t) = i\right) P(N(t) = i) \\
&+ \sum_{i=0}^{\infty} R_H\left(t \mid X_S(t) < H_1 \cap N(t) = i\right) P\left(X_S(t) < H_1 \mid N(t) = i\right) P(N(t) = i) \\
&= \sum_{i=0}^{\infty} P\left(\bigcap_{k=1}^{N(\Theta)} \{W_k < D_0\}, \bigcap_{k=N(\Theta)+1}^i \{W_k < D_1\}\right) P\left(X(t) + \sum_{k=1}^i Y_k \geq H_1\right) P(N(t) = i) \\
&+ \sum_{i=0}^{\infty} P\left(\bigcap_{k=1}^i \{W_k < D_0\}\right) P\left(X(t) + \sum_{k=1}^i Y_k < H_1\right) P(N(t) = i) \\
&= \sum_{i=0}^{\infty} \sum_{j=0}^i P\left(\bigcap_{k=1}^{N(\Theta)} \{W_k < D_0\}, \bigcap_{k=N(\Theta)+1}^i \{W_k < D_1\} \mid N(\Theta) = j\right) \\
&\times P(N(\Theta) = j) P\left(X(t) + \sum_{k=1}^i Y_k \geq H_1\right) P(N(t) = i) \\
&+ \sum_{i=0}^{\infty} P\left(\bigcap_{k=1}^i \{W_k < D_0\}\right) P\left(X(t) + \sum_{k=1}^i Y_k < H_1\right) P(N(t) = i) \\
&= \sum_{i=0}^{\infty} \sum_{j=0}^i F_W(D_0)^j F_W(D_1)^{i-j} P\left(X(t) + \sum_{k=1}^i Y_k \geq H_1\right) \\
&\times \left(\int_0^t P(N(\theta) = j) f_{\Theta}(\theta \mid N(\theta) = j) d\theta\right) P(N(t) = i) \\
&+ \sum_{i=0}^{\infty} F_W(D_0)^i P\left(X(t) + \sum_{k=1}^i Y_k < H_1\right) P(N(t) = i). \tag{5.6}
\end{aligned}$$

To derive the conditional pdf of Θ , $f_{\Theta}(\theta \mid N(\theta) = j)$, we employ the cdf of $X_S(t)$ in Eq. (5.3) to find the cdf of Θ given the number of shocks by that time, $F_{\Theta}(\theta \mid N(\theta) = j)$.

Similar to defining the probability of no soft failure by time t , we have

$$F_{\Theta}(\theta \mid N(\theta) = j) = 1 - F_{X_S}(H_1, \theta \mid N(\theta) = j) = 1 - \int_0^{H_1} F_X(H_1 - u, \theta \mid N(\theta) = j) f_Z(u) du. \tag{5.7}$$

For the specific case when β and $Z(t)$ follow normal distributions,

$$F_{\Theta}(\theta \mid N(\theta) = j) = 1 - F_{X_S}(H_1, \theta \mid N(\theta) = j) = 1 - \Phi\left(\frac{H_1 - (\varphi + \mu_{\beta}\theta + j\mu_Y)}{\sqrt{\sigma_{\beta}^2\theta^2 + \sigma^2 + j\sigma_Y^2}}\right). \tag{5.8}$$

Then the pdf of Θ is derived as follows:

$$\begin{aligned}
f_{\Theta}(\theta|N(\theta)=j) &= \frac{dF_{\Theta}(\theta|N(\theta)=j)}{d\theta} \\
&= -\frac{dF_{X_s}(H_1, \theta|N(\theta)=j)}{d\theta} = -\phi\left(\frac{H_1 - (\varphi + \mu_{\beta}\theta + j\mu_Y)}{\sqrt{\sigma_{\beta}^2\theta^2 + \sigma^2 + j\sigma_Y^2}}\right) \\
&\quad \times \left(\frac{-\mu_{\beta}(\sigma_{\beta}^2\theta^2 + \sigma^2 + j\sigma_Y^2) - \sigma_{\beta}^2\theta(H_1 - (\varphi + \mu_{\beta}\theta + j\mu_Y))}{(\sigma_{\beta}^2\theta^2 + \sigma^2 + j\sigma_Y^2)^{\frac{3}{2}}}\right),
\end{aligned} \tag{5.9}$$

where $\phi(\cdot)$ is the pdf of a standard normal random variable.

Case 2: Continuous reduction in hard failure threshold

A unit fails if the size of random shock exceeds the corresponding threshold $D(t)$, which is a function of the degradation at time t . The rationale is that a device is weakening when the total degradation continuously increases. Therefore, it becomes more sensitive to shocks, as reflected in the form that the hard failure threshold drops gradually. We assume that the change in $D(t)$ is inversely proportional to the change in $X_s(t)$:

$$D(t) = D_0 - \alpha(X_s(t) - X_s(0)). \tag{5.10}$$

The probability a device survives against hard failure by time t , $R_H(t)$, is

$$\begin{aligned}
R_H(t) &= \sum_{i=0}^{\infty} R_H(t|N(t)=i)P(N(t)=i) = \sum_{i=0}^{\infty} P\left(\bigcap_{k=1}^i \{W_k < D(T_k)\}\right)P(N(t)=i) \\
&= \sum_{i=0}^{\infty} \left(\prod_{k=1}^i P(W_k < D(T_k))\right)P(N(t)=i) \\
&= \sum_{i=0}^{\infty} \int_{t_{i-1}}^t \cdots \int_0^t \left(\prod_{k=1}^i P(W_k < D(t_k))f_{T_k}(t_k)dt_k\right)P(N(t)=i) \\
&= \sum_{i=0}^{\infty} \int_{t_{i-1}}^t \cdots \int_0^t \left(\prod_{k=1}^i P(\bar{W}_k < D_0)f_{T_k}(t_k)dt_k\right)P(N(t)=i) \\
&= \sum_{i=0}^{\infty} \int_{t_{i-1}}^t \cdots \int_0^t \left(\prod_{k=1}^i F_{\bar{W}_k}(D_0)f_{T_k}(t_k)dt_k\right)P(N(t)=i),
\end{aligned} \tag{5.11}$$

where $\bar{W}_k = W_k + \alpha(X_S(t_k) - X_S(0))$ is a random variable with cdf $F_{\bar{W}_k}(\bar{w})$, and T_k is the arrival time of the k^{th} shock, for $k = 1, \dots, N(t)$. Given k , T_k follows a gamma distribution with the scale parameter of k , and the shape parameter of λ :

$$f_{T_k}(t_k | k) = \frac{\lambda^k}{(k-1)!} t_k^{k-1} e^{-\lambda t_k}. \quad (5.12)$$

In a specific case where the W_k and $X_S(t_k)$ are assumed to follow normal distributions, it can be shown that \bar{W}_k is also a normal variable. Therefore, the probability of no hard failure by time t is

$$R_H(t) = \sum_{i=0}^{\infty} \int_{t_{i-1}}^t \dots \int_0^t \left(\prod_{k=1}^i \Phi \left(\frac{D_0 - (\mu_W + \alpha(\mu_\beta t_k + k\mu_Y))}{\sqrt{\sigma_W^2 + \alpha^2(\sigma_\beta^2 t_k^2 + k\sigma_Y^2)}} \right) \frac{\lambda^k}{(k-1)!} t_k^{k-1} e^{-\lambda t_k} dt_k \right) P(N(t) = i). \quad (5.13)$$

For numerical computation, a practical upper-bound can be used for the number of random shocks, instead of infinity.

5.2.3. System Reliability Analysis

The reliability at time t for a device that experiences two DCFP is formulated as

$$R(t) = \sum_{i=0}^{\infty} R_S(t | N(t) = i) R_H(t | N(t) = i) P(N(t) = i). \quad (5.14)$$

Given the number of shocks by time t , the soft failure and hard failure processes are conditionally independent, due to the assumption that the shock damage size Y_k is independent of the shock load W_k .

Case 1: One time reduction in hard failure threshold

The reliability in (5.14) is derived further by considering the following situations:

i) When no shocks occur by time t , or $N(t)=0$,

$$R(t|N(t)=0) = R_S(t|N(t)=0)R_H(t|N(t)=0) = P(X(t) < H_0). \quad (5.15)$$

ii) At least one shock occurs by time t , or $N(t) > 0$. There are two different scenarios for the device to work without failure. The probability of the two mutually exclusive scenarios must be added for every possible number of random shocks.

1) The system does not experience transition in hard failure threshold by time t , or

$X_S(t) < H_1$. Based on Eqs. (5.2) and (5.6), we have

$$\begin{aligned} & R(t|X_S(t) < H_1 \cap N(t) = i \geq 1) \\ &= R_S(t|X_S(t) < H_1 \cap N(t) = i \geq 1)R_H(t|X_S(t) < H_1 \cap N(t) = i \geq 1) \\ &= P\left(X(t) + \sum_{k=1}^i Y_k < H_0 \middle| X_S(t) < H_1\right) F_w(D_0)^i = F_w(D_0)^i. \end{aligned} \quad (5.16)$$

2) The system experiences transition in hard failure threshold due to excess of degradation over the critical value H_1 by time t , or $X_S(t) \geq H_1$. Based on Eqs. (5.2) and (5.6), we have

$$\begin{aligned} & R(t|X_S(t) \geq H_1 \cap N(t) = i \geq 1) = R_S(t|X_S(t) \geq H_1 \cap N(t) = i \geq 1) \\ & \times R_H(t|X_S(t) \geq H_1 \cap N(t) = i \geq 1) = \sum_{j=0}^i \frac{P\left(H_1 \leq X(t) + \sum_{k=1}^i Y_k < H_0\right)}{P(X_S(t) \geq H_1|N(t) = i \geq 1)} \\ & \times F_w(D_0)^j F_w(D_1)^{i-j} \left(\int_0^t P(N(\theta) = j) f_{\Theta}(\theta|N(\theta) = j) d\theta \right). \end{aligned} \quad (5.17)$$

Now by summing them all, the system reliability at time t is expressed as:

$$\begin{aligned} R(t) &= R(t|N(t)=0)P(N(t)=0) \\ &+ \sum_{i=1}^{\infty} R(t|X_S(t) < H_1 \cap N(t) = i)P(X_S(t) < H_1|N(t) = i)P(N(t) = i) \\ &+ \sum_{i=1}^{\infty} R(t|X_S(t) \geq H_1 \cap N(t) = i)P(X_S(t) \geq H_1|N(t) = i)P(N(t) = i) \end{aligned}$$

$$\begin{aligned}
&= P(X(t) < H_0) e^{-\lambda t} + \sum_{i=1}^{\infty} F_W(D_0)^i P\left(X(t) + \sum_{k=1}^i Y_k < H_1\right) \frac{e^{-\lambda t} (\lambda t)^i}{i!} \\
&+ \sum_{i=1}^{\infty} \sum_{j=0}^i P\left(H_1 \leq X(t) + \sum_{k=1}^i Y_k < H_0\right) F_W(D_0)^j F_W(D_1)^{i-j} \\
&\times \int_0^t \frac{\exp(-\lambda(\theta+t)) \lambda^{i+j} \theta^j t^i}{j! i!} f_{\Theta}(\theta | N(\theta) = j) d\theta.
\end{aligned} \tag{5.18}$$

In the specific case where φ is a constant, W_k , Y_k , and β are normally distributed, the reliability function can be derived as

$$\begin{aligned}
R(t) &= \Phi\left(\frac{H_0 - (\varphi + \mu_{\beta} t)}{\sqrt{\sigma_{\beta}^2 t^2 + \sigma^2}}\right) e^{-\lambda t} + \sum_{i=1}^{\infty} \Phi\left(\frac{H_1 - (\varphi + \mu_{\beta} t + i \mu_Y)}{\sqrt{\sigma_{\beta}^2 t^2 + \sigma^2 + i \sigma_Y^2}}\right) F_W(D_0)^i \frac{e^{-\lambda t} (\lambda t)^i}{i!} \\
&+ \sum_{i=1}^{\infty} \sum_{j=0}^i \left[\Phi\left(\frac{H_0 - (\varphi + \mu_{\beta} t + i \mu_Y)}{\sqrt{\sigma_{\beta}^2 t^2 + \sigma^2 + i \sigma_Y^2}}\right) - \Phi\left(\frac{H_1 - (\varphi + \mu_{\beta} t + i \mu_Y)}{\sqrt{\sigma_{\beta}^2 t^2 + \sigma^2 + i \sigma_Y^2}}\right) \right] F_W(D_0)^j F_W(D_1)^{i-j} \\
&\times \int_0^t \frac{\exp(-\lambda(\theta+t)) \lambda^{i+j} \theta^j t^i}{j! i!} \phi\left(\frac{H_1 - (\varphi + \mu_{\beta} \theta + j \mu_Y)}{\sqrt{\sigma_{\beta}^2 \theta^2 + \sigma^2 + j \sigma_Y^2}}\right) \\
&\times \left(\frac{\mu_{\beta} (\sigma_{\beta}^2 \theta^2 + \sigma^2 + j \sigma_Y^2) + \sigma_{\beta}^2 \theta (H_1 - (\varphi + \mu_{\beta} \theta + j \mu_Y))}{(\sigma_{\beta}^2 \theta^2 + \sigma^2 + j \sigma_Y^2)^{\frac{3}{2}}} \right) d\theta.
\end{aligned} \tag{5.19}$$

Case 2: Continuous reduction in hard failure

The threshold for hard failure decreases continuously depending on the degradation. By considering the following situations, the reliability function is derived further.

i) When no shocks occur by time t , or $N(t) = 0$,

$$R(t | N(t) = 0) = R_s(t | N(t) = 0) R_H(t | N(t) = 0) = P(X(t) < H_0). \tag{5.20}$$

ii) At least one shock occurs by time t , or $N(t) > 0$,

$$\begin{aligned}
R(t|N(t)=i \geq 1) &= R_S(t|N(t)=i \geq 1)R_H(t|N(t)=i \geq 1) \\
&= \int_{t_{i-1}}^t \cdots \int_0^t \left(\prod_{k=1}^i F_{\bar{W}_k}(D_0) f_{T_k}(t_k) dt_k \right) P\left(X(t) + \sum_{k=1}^i Y_k < H_0\right). \quad (5.21)
\end{aligned}$$

By combining these two different situations, the system reliability at time t is derived to be

$$\begin{aligned}
R(t) &= R(t|N(t)=0)P(N(t)=0) + \sum_{i=1}^{\infty} R(t|N(t)=i)P(N(t)=i) = P(X(t) < H_0)e^{-\lambda t} \\
&\quad + \sum_{i=1}^{\infty} \int_{t_{i-1}}^t \cdots \int_0^t P\left(\prod_{k=1}^i F_{\bar{W}_k}(D_0) \frac{\exp(-\lambda(t_k+t)) \lambda^{i+k} t_k^{k-1} t^i}{(k-1)! i!} dt_k\right) \left(X(t) + \sum_{k=1}^i Y_k < H_0\right). \quad (5.22)
\end{aligned}$$

The reliability function for the specific case where φ is a constant, W_k , Y_k , and β are normally distributed can be expressed as

$$\begin{aligned}
R(t) &= \Phi\left(\frac{H_0 - (\varphi + \mu_\beta t)}{\sqrt{\sigma_\beta^2 t^2 + \sigma^2}}\right) e^{-\lambda t} + \sum_{i=1}^{\infty} \Phi\left(\frac{H_0 - (\varphi + \mu_\beta t + i\mu_Y)}{\sqrt{\sigma_\beta^2 t^2 + \sigma^2 + i\sigma_Y^2}}\right) \\
&\quad \times \int_{t_{i-1}}^t \cdots \int_0^t \left(\prod_{k=1}^i \Phi\left(\frac{D_0 - (\mu_W + \alpha(\mu_\beta t_k + k\mu_Y))}{\sqrt{\sigma_W^2 + \alpha^2(\sigma_\beta^2 t_k^2 + k\sigma_Y^2)}}\right) \frac{\exp(-\lambda(t_k+t)) \lambda^{i+k} t_k^{k-1} t^i}{(k-1)! i!} dt_k \right). \quad (5.23)
\end{aligned}$$

5.3. Condition-based Maintenance Based on Failure Limit Policy

In this section, we consider a CBM policy developed based on FLP. The basic assumptions for this maintenance policy include:

1. The device is inspected at periodic intervals τ .
2. At inspection, if the device is failed, corrective replacement takes place; if the degradation is beyond the cut-off limit H_R , a preventive replacement will be implemented; if the device is still functioning and the degradation is less than H_R (safe region), no action takes place.
3. If the device fails, it is not self-announcing, and remains failed until the next inspection.

Figure 5.3 depicts how the proposed maintenance model is implemented. In this example, the first unit is preventively replaced at the third inspection, because the degradation exceeded the cut-off limit although the device is still operating. The second unit is correctively replaced due to hard failure at the sixth inspection. For the purpose of illustrating the proposed CBM model, Figure 5.3 shows the decreasing hard failure threshold related to Case 1.

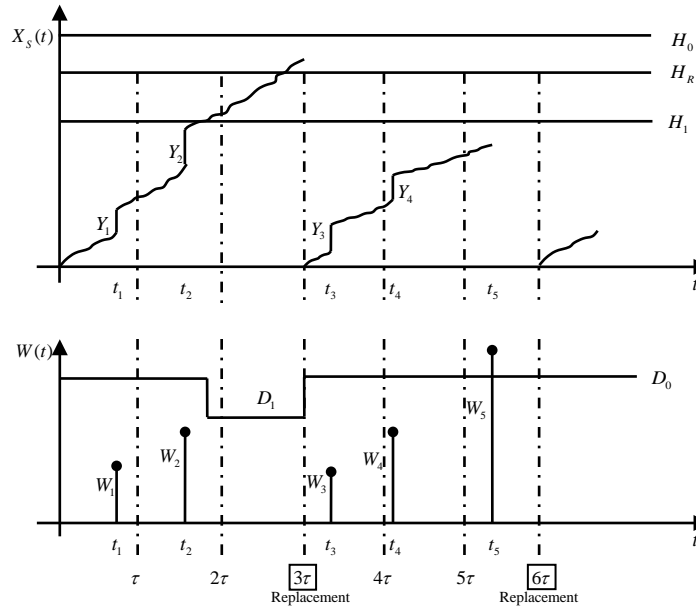


Figure 5.3: Condition-based maintenance policy

By minimizing the average maintenance cost rate, two decision variables are determined: cut-off limit on degradation for preventive replacement H_R , and inspection interval τ . From basic renewal theory, the average long run maintenance cost per unit of time can be calculated as follows:

$$C_A(\tau, H_R) = \lim_{t \rightarrow \infty} (C(t)/t) = \frac{\text{Expected maintenance cost incurred in a renewal cycle}}{\text{Expected length of a renewal cycle}} = \frac{E[C_T]}{E[L]}. \quad (5.24)$$

A renewal cycle is defined as the time from the installation to the first replacement, or the time between two successive replacements. The total maintenance cost, C_T , includes the inspection cost, replacement cost, and penalty cost due to failure, which is partially based on the lost profit during down time. Therefore, the expected total maintenance cost is formulated to be

$$E[C_T] = C_I E[N_I] + C_F E[\rho] + C_R. \quad (5.25)$$

The probability of performing preventive replacement at the k^{th} inspection, $P(N_{PR} = k)$, that ensures the system does not experience hard failure and the degradation is within (H_R, H_0) at the k^{th} inspection can be derived as:

$$\begin{aligned} P(N_{PR} = k) &= \sum_{i=0}^{\infty} R_H(k\tau | N(k\tau) = i) P(H_R \leq X_S(k\tau) < H_0 | N(k\tau) = i) P(N(k\tau) = i) \\ &= \sum_{i=0}^{\infty} R_H(k\tau | N(k\tau) = i) P(X_S(k\tau) < H_0 | N(k\tau) = i) P(N(k\tau) = i) \\ &\quad - \sum_{i=0}^{\infty} R_H(k\tau | N(k\tau) = i) P(X_S(k\tau) < H_R | N(k\tau) = i) P(N(k\tau) = i) \\ &= R(k\tau | H_0) - R(k\tau | H_R), \end{aligned} \quad (5.26)$$

where $R(t | H)$ is the probability that system is still functioning by time t given the threshold of H . The probability of performing corrective replacement at the k^{th} inspection, $P(N_{CR} = k)$, i.e., the probability that the system fails between the $(k-1)^{th}$ and k^{th} inspections, can be derived as:

$$P(N_{CR} = k) = R((k-1)\tau | H_0) - R(k\tau | H_0). \quad (5.27)$$

The number of inspections in a renewal cycle, N_I , is determined by the time of replacement, which takes place when we have to perform either preventive replacement or corrective replacement. Therefore, the probability mass function of N_I is given as

$$P(N_I = k) = P(N_{PR} = k) + P(N_{CR} = k) = R((k-1)\tau | H_0) - R(k\tau | H_R). \quad (5.28)$$

Then the expected number of inspections in a renewal cycle is derived as

$$E[N_I] = \sum_{k=1}^{\infty} k P(N_I = k) = \sum_{k=1}^{\infty} k \left(R((k-1)\tau | H_0) - R(k\tau | H_R) \right). \quad (5.29)$$

The expected length of renewal cycle is subsequently determined as

$$E[L] = \sum_{k=1}^{\infty} E[L | N_I = k] P(N_I = k) = \sum_{k=1}^{\infty} k\tau \left(R((k-1)\tau | H_0) - R(k\tau | H_R) \right). \quad (5.30)$$

The downtime is the time from a failure to the next inspection, or $\rho = N_I \tau - T$. Then the expected length of downtime is given as

$$\begin{aligned} E[\rho] &= \sum_{k=1}^{\infty} E[\rho | N_I = k] P(N_I = k) \\ &= \sum_{k=1}^{\infty} \left(\int_{(k-1)\tau}^{k\tau} (t - k\tau) dR(t | H_0) \right) \left(R((k-1)\tau | H_0) - R(k\tau | H_R) \right). \end{aligned} \quad (5.31)$$

Based on Eqs. (5.24) to (5.31), the average long run maintenance cost rate as a function of τ and H_R is derived as

$$C_A(\tau, H_R) = \frac{\sum_{k=1}^{\infty} \left(k C_I + \int_{(k-1)\tau}^{k\tau} (t - k\tau) dR(t | H_0) C_F \right) \left(R((k-1)\tau | H_0) - R(k\tau | H_R) \right) + C_R}{\sum_{k=1}^{\infty} k\tau \left(R((k-1)\tau | H_0) - R(k\tau | H_R) \right)}. \quad (5.32)$$

We obtain the optimal time interval for periodic inspection, and the cut-off limit on degradation by minimizing $C_A(\tau, H_R)$ using Nelder-Mead algorithm in the numerical examples (Lagarias et al. 1998). Optimum Results along with sensitivity analysis are presented in Section 5.4.3.

5.4. Numerical Examples

Numerical examples were solved to demonstrate the models and equations that were presented in the chapter. The corresponding values for the parameters in reliability

analysis are given in Table 5.1, where some parameters are adopted from literature and others are assumptions based on typical and plausible values.

5.4.1. Reliability Analysis for Case 1

For the described system when the hard failure threshold decreases to a lower level after the degradation exceeds a critical level, the reliability function $R(t)$ in (5.19) is plotted in Figure 5.4, and a sensitivity analysis was performed to measure the effect of the changing ratio D_1 / D_0 on the reliability function (Figure 5.5). As shown in Figure 5.5, the ratio between the reduced hard failure threshold and initial threshold (D_1 / D_0) has significant impact on the reliability of the device. By increasing the ratio (D_0 is fixed at 1.5Gpa, and D_1 increases from 1.2Gpa to 1.5Gpa), the $R(t)$ shifts to right. It can be inferred that by approaching D_1 to D_0 , the reliability improves and the model becomes the basic model without the decreasing hard failure threshold.

Table 5.1: Parameter values

Parameters	Values	Sources
H_0	$0.00125\mu\text{m}^3$	(Tanner & Dugger 2003)
H_1	$0.000875\mu\text{m}^3$	Assumption
D_0	1.5Gpa	(Tanner & Dugger 2003)
D_1	1.2Gpa	Assumption
φ	0	(Tanner & Dugger 2003)
μ_β	$8.4823 \times 10^{-9}\mu\text{m}^3$	(Tanner & Dugger 2003)
σ_β	$6.0016 \times 10^{-10}\mu\text{m}^3$	(Tanner & Dugger 2003)
μ_W	1.2Gpa	Assumption
σ_W	0.2Gpa	Assumption
μ_Y	$1.0 \times 10^{-4}\mu\text{m}^3$	Assumption
σ_Y	$2 \times 10^{-5}\mu\text{m}^3$	Assumption
σ	$10^{-10}\mu\text{m}^3$	Assumption
α	300Gpa / μm^3	Assumption
λ	5×10^{-5} / revolutions	Assumption

5.4.2. Reliability Analysis for Case 2

Figure 5.6 shows the reliability function in (5.23 for Case 2, when the hard failure threshold constantly decreases due to the degrading of the device. Figure 5.7 shows a sensitivity analysis performed to study how the parameter α affects system reliability.

The coefficient in hard failure threshold impacts the reliability function significantly (Figure 5.7). By changing α from $0\text{GPa} / \mu\text{m}^3$ to $400\text{GPa} / \mu\text{m}^3$, the $R(t)$ shifts to the left. It indicates that reliability performance is better for the smaller value of α . When $\alpha = 0$, the hard failure threshold remains a constant.

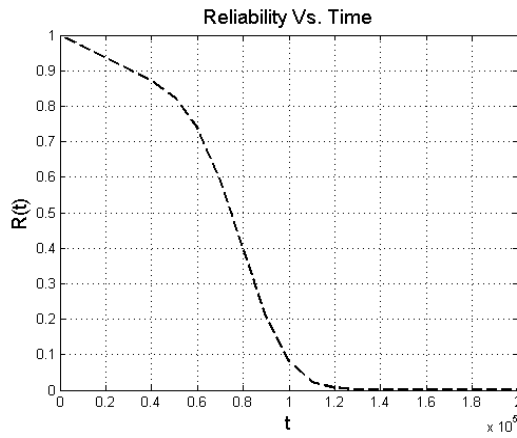


Figure 5.4: Plot of $R(t)$ for Case 1

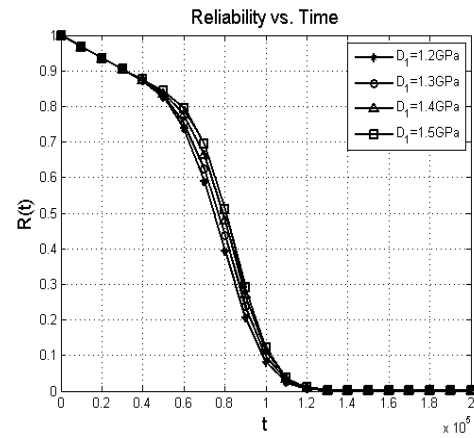


Figure 5.5: Sensitivity analysis of $R(t)$ on D_1 / D_0 for Case 1

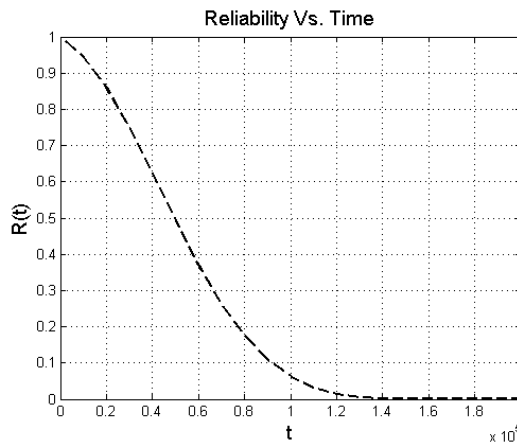


Figure 5.6: Plot of $R(t)$ for Case 2

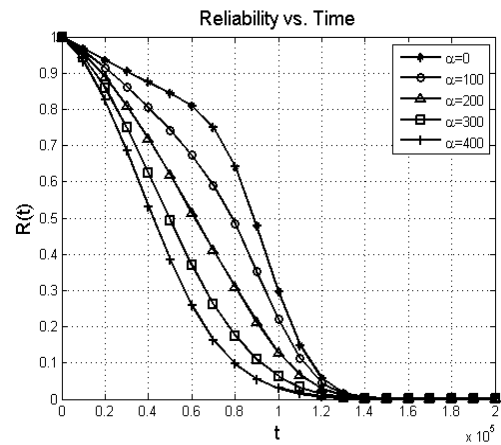


Figure 5.7: Sensitivity analysis of $R(t)$ on α for Case 2

5.4.3. Optimal Maintenance Policy

By minimizing $C_A(\tau, H_R)$ in (5.32), we can obtain the optimal time interval for periodic inspection τ , and cut-off limit H_R , in the proposed CBM policy. Since the objective function is a highly nonlinear function with two decision variables, it is challenging to find the optimum solution for the maintenance model. Therefore, we used Nelder-Mead simplex algorithm that is an effective nonlinear optimization method for problems in which derivatives may not be known. This technique can be used to approximate a local optimum of a problem with multiple variables when the objective function changes smoothly (Lagarias et al. 1998). Nelder-Mead algorithm is based on evaluating a function of N variables at the $N + 1$ vertices of a simplex to find a local minimum. In the long-run average cost rate function with two variables, the inspection interval and cut-off limit, a simplex is a triangle, and the algorithm is a pattern search that compares the cost rate values for the three vertices of a triangle. In each iteration a triangle is generated, for which the $C_A(\tau, H_R)$ values at the vertices become smaller. The i^{th} iteration starts by ordering the function values for three vertices, such that

$$C_{A1}^{(i)} \leq C_{A2}^{(i)} \leq C_{A3}^{(i)}. \quad (5.33)$$

The worst vertex, $C_{A3}^{(i)}$, where the value of $C_A(\tau, H_R)$ is the largest, is replaced by a new vertex with an improved function value to form a new triangle, and the search is continued. The value for the updated vertex is computed by using reflection, expansion, contraction, and reduction rules. Matlab is used to solve this nonlinear optimization problem. To demonstrate the optimization of the average long run cost rate, example values are assigned to the cost parameters: $C_I = \$1$, $C_F = \$50$, and $C_R = \$10$. For Case 1, the minimum average long-run maintenance cost rate is \$4.3888/cycle, which is obtained at τ^*

$= 1.125 \times 10^5$, the optimal number of revolutions per inspection period, and $H_R^* = 0.00097 \mu\text{m}^3$ (Figure 5.8). For Case 2, the minimum average long-run maintenance cost rate is \$5.1964 / cycle, which occurs at $\tau^* = 1.026 \times 10^5$ and $H_R^* = 0.00093 \mu\text{m}^3$ (Figure 5.9). Figures 5.8 and 5.9 depict $C_A(\tau, H_R)$ as a function of τ and H_R for Case 1 and 2, respectively. It can be observed from the figures how τ and H_R affect the long-run average cost rate. From Figures 5.8 and 5.9, we can see that $C_A(\tau, H_R)$ is not very sensitive to changes in H_R , compared to changes in τ .

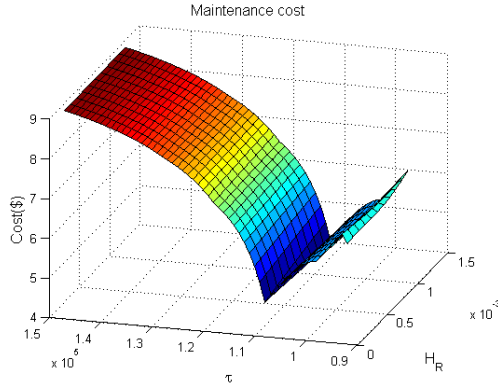


Figure 5.8: Plot of $C_A(\tau, H_R)$ on H_R and τ for Case 1

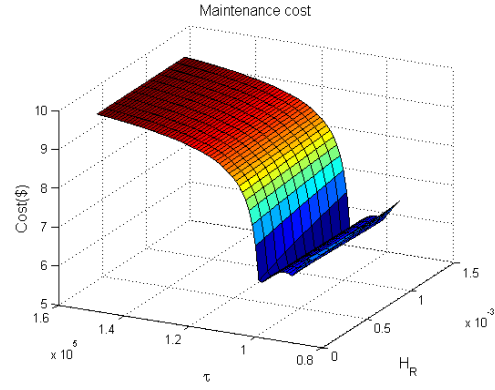


Figure 5.9: Plot of $C_A(\tau, H_R)$ on H_R and τ for Case 2

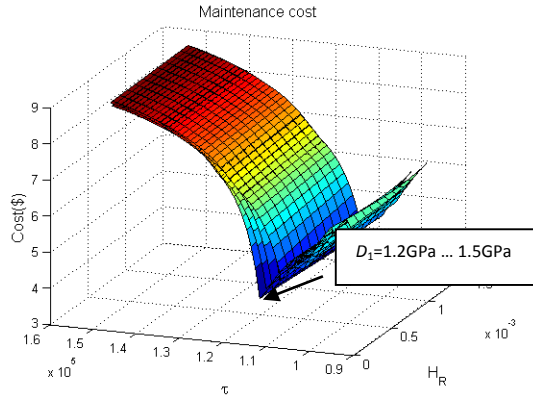


Figure 5.10: Sensitivity analysis of $C_A(\tau, H_R)$ on D_1 for Case 1

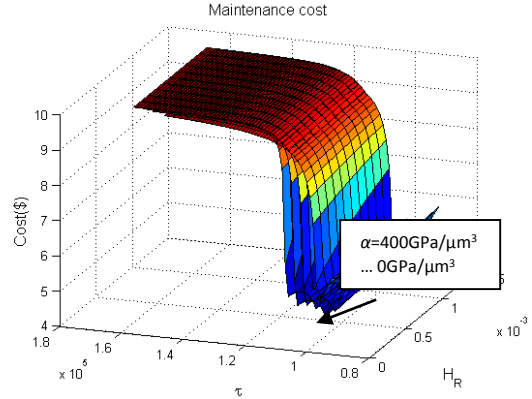


Figure 5.11: Sensitivity analysis of $C_A(\tau, H_R)$ on α for Case 2

We perform a sensitivity analysis for both cases to study the effects of certain parameters on $C_A(\tau, H_R)$. In Case 1, D_1 changes from 1.2Gpa to 1.5Gpa; and in Case 2, α

varies from $0\text{Gpa} / \mu\text{m}^3$ to $400\text{Gpa} / \mu\text{m}^3$. As shown in both Figure 5.10, and Figure 5.11, when the reliability function improves, i.e., in Case 1 by increasing ratio D_1 / D_0 , and in Case 2 by decreasing parameter α , the optimum inspection interval becomes longer and the minimum average long-run maintenance cost rate decreases.

5.5. Conclusion

In this chapter, we propose new reliability models and CBM policy for a device subject to DCFP of degradation and random shocks, with a decreasing hard failure threshold according to the change of degradation. The two dependent failure processes are degradation and random shocks. The degradation process can cause soft failure and random shocks can cause hard failure. Soft failure occurs when the degradation, accumulated by continuous wear degradation and instantaneous damage caused by random shocks, exceeds the soft failure threshold value. Hard failure occurs if the size of a shock is beyond the hard failure threshold level. A device fails as soon as either one of the failure mechanism occurs. These two failure processes are competing yet dependent, because arriving random shocks affect both failure processes and the degradation impacts on the hard failure threshold.

Two cases of dependency between the hard failure threshold and the degradation are studied: 1) the hard failure threshold has an initial value and it reduces to a lower level as soon as the overall degradation reaches a critical value, and 2) the threshold decreases continuously, but the amount of reduction in the threshold is proportional to changes in degradation. We also develop a maintenance strategy based on FLP to ensure the device functioning under a certain level of degradation. The average long-run maintenance cost rate based on the reliability model is a multivariate nonlinear function with two decision variables of cut-off limit on degradation, and inspection interval. Then the developed

reliability models are demonstrated for these two cases by using a micro-engine example. There are several interesting future research directions. One is to develop a reliability model for systems of multiple components, where each component is subject to DCFP with decreasing hard failure threshold.

Chapter 6

Condition-based Replacement Analysis for Multi-stent Systems

In this chapter, we develop a condition-based replacement (CBR) model for a multi-component system of stents implanted in human arteries that is subject to both delayed and instantaneous failures, based on the system-level reliability model developed by Feng et al. (2014) for such a system. In the proposed CBR, the replacement is either a preventive or corrective action performed depending on the condition of the system. Numerical examples using data from the literature are presented to investigate the effectiveness of the proposed CBR policy for implanted multi-stent systems.

6.1. Introduction

The high occurrence of cardiovascular diseases and the rapid evolution of bio-structure devices have elevated the maintenance study of biomedical devices from being a feature to a necessity. This issue becomes even more challenging as the failure may not be self-announcing in most cases, and hence, requires a well-studied predictive approach. Stent, a small scaffold, is one of such evolving bio-structures that is implanted in human arteries to counteract the effects of atherosclerosis (preventing the artery wall from collapsing). As reported in 2005, over one million stents are implanted in human arteries each year, and the market for endo- and cardiovascular stents was estimated to exceed \$7 billion annually (Marrey et al., 2006). Although stents have been an effective substitute for practice of vascular intrusions, the potential *in-vivo* failure of this device should never be neglected. Applied stresses in manufacturing, implantation, and operation of stents subject them to a variety of overloads and cyclic stresses, which can cause two dominating failure

modes of stents: *instantaneous failures* due to single-event overloads, and *delayed failures* or crack growth due to cyclic stresses (Robertson & Ritchie 2007).

In this chapter, we extend the previous research work presented in Keedy and Feng (2013) to a multi-stent system by proposing a CBR strategy to minimize the impact of unforeseen failures of stents and facilitate continued advancement of the implant devices. Almost none of previous studies on replacement scheduling of single or multiple stents conducted by medical and engineering research communities have considered the probabilistic nature of stent failure. The only research work addressing this issue is presented in Keedy and Feng (2013) that incorporated reliability models in the optimization of a unique two-phase maintenance policy to achieve the optimal follow-up schedule. However, their study does not address the issue of multiple stents implanted in patient arteries, which is the case in many stent implantation surgeries. The stochastic, economical, and structural dependencies and interconnection of multiple stents implanted in human arteries significantly affect the system-level reliability of stents resulting in different follow-up schedules, which has motivated us to carry out this research work.

The rest of the chapter is organized as follows. In Sections 6.2 and 6.3, the analysis of failure processes and the reliability modeling for a multiple-stent system developed by Feng et al. (2014) is presented. Their proposed reliability model is used for the mathematical formulation of the condition-based replacement (CBR) developed in Section 6.4. In Section 6.5, numerical results and discussions are presented. Finally, concluding remarks are made in Section 6.6.

Notation

$N(t)$	Number of shocks by time t
λ	Shock arrival rate Average

$a_{(i)}$	Crack length of stent i
$a_{th(i)}$	Failure threshold value of crack length for stent i
H_{ij}	Shock damage size on crack length from the j^{th} shock on stent i
K_{ij}	Fracture toughness value caused by the j^{th} shock on stent i
K_i'	Crack initiation toughness of stent i
W_i	Threshold on expected fracture toughness value for stent i
τ	Length of inspection interval
$C_A(\tau)$	Average long run maintenance cost rate
$C(t)$	Cumulative maintenance cost by time t
C_T	Total maintenance cost incurred in a renewal cycle
L	Length of a renewal cycle
$R(t a_1, \dots, a_n)$	Reliability function given the delayed failure threshold for a set of stents is (a_1, \dots, a_n)
$f_T(t a_1, \dots, a_n)$	pdf of the failure time given the delayed failure threshold for a set of stents is (a_1, \dots, a_n)
N_{PR}	Inspection count at which the preventive replacement is performed
N_{CR}	Inspection count at which the corrective replacement is performed
N_I	Number of inspection before replacement
C_I	Inspection cost
C_{PR}	Preventive replacement cost
C_{CR}	Corrective replacement cost ($C_{PR} \ll C_{CR}$)

6.2. Analysis of Two Failure Processes for Stents

There are two dominating failure modes of stents that have been identified and experimentally studied in the literature: *instantaneous fracture* due to single-event overloads and *delayed failure* or crack growth due to cyclic stresses (Robertson & Ritchie 2007). Stents in a multi-stent system may fail due to instantaneous fracture when a large single-event overload or shock arrives. The fracture toughness value of the j^{th} shock on stent i by K_{ij} , and the crack-initiation toughness of stent i by K_i' . An instantaneous fracture

occurs at the j^{th} shock when K_{ij} is greater than K_i' . Single-event overloads or shocks arrive in random interval of time that can be modeled by a Poisson process with arrival rate of λ . The experimental results from Daly et al. (2007) indicate that the fracture toughness values K_{ij} are *i.i.d.* normal random variables, $K_{ij} \sim N(\mu_{K_i}, \sigma_{K_i}^2)$. Furthermore, the crack-initiation toughness for stent i is normally distributed, $K_i' \sim N(\mu_{K_i'}, \sigma_{K_i'}^2)$. Therefore, the survival probability of stent i for each random shock is

$$P_I = P(K_{ij} < K_i') = \Phi\left(\frac{\mu_{K_i'} - \mu_{K_i}}{\sqrt{\sigma_{K_i'}^2 + \sigma_{K_i}^2}}\right), \text{ for } j=1, 2, \dots \quad (6.1)$$

where $\Phi(\cdot)$ is the cdf of the standard normal random variable.

Stents may also fail due to delayed failure, when the crack length of stent i , denoted by $a_i(t)$ as a function of loading cycles, reaches a critical threshold value of crack length for stent i denoted by $a_{th(i)}$. Using Paris power law, the crack propagation of Nitinol stents has been formulated as (Keedy & Feng, 2013; Marrey et al., 2006; Robertson & Ritchie, 2007):

$$a_i(t) = \theta_i t^{\alpha_i}, \quad (6.2)$$

where t is the number of loading cycles, and $\theta_i \sim N(\mu_{\theta_i}, \sigma_{\theta_i}^2)$, and α_i is an experimentally determined parameter for stent i . A standard Brownian motion $B_i(t) \sim N(0, \sigma_{B_i}^2 t)$ is used to represent the stochastic nature of crack propagation over time. The model is modified as

$$a_i(t) = \theta_i t^{\alpha_i} + B_i(t), \quad (6.3)$$

where $B_i(t)$ and θ_i are assumed to be independent.

These two failure processes can be dependent or associated when the shock magnitude is large enough to cause an instantaneous step increase on the crack propagation (Keedy & Feng, 2013).

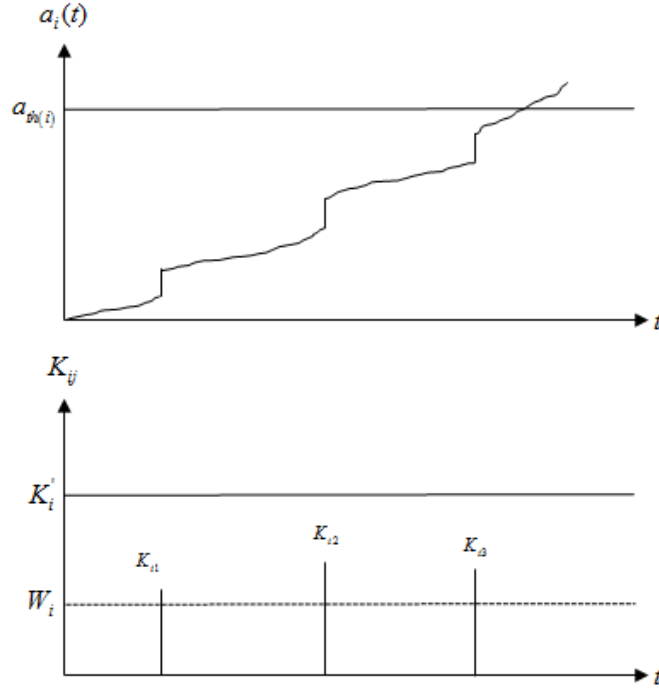


Figure 6.1. Two failure processes of degradation and random shocks

6.3. Reliability Function of Multi-stent Systems

As shown in Figure 6.1, each single-event overload j can result in an abrupt increase in the crack length. These abrupt increases in crack length denoted by H_{ij} are assumed to be independent and identically distributed following a normal distribution, $H_{ij} \sim N(\mu_{Hi}, \sigma_{Hi}^2)$, for $j = 1, 2, \dots$. It is reasonable to assume that the mean of abrupt increase in crack length due to overloads, μ_{Hi} , is proportional to the difference between the mean shock magnitude, $E[K_{ij}]$, and the threshold value, W_i . Mathematically,

$$\mu_{H_i} = E[H_i] \propto E[K_{ij}] - W_i \quad (6.4a)$$

or

$$\mu_{H_i} = b(E[K_{ij}] - W_i), \quad (6.4b)$$

where b is a predetermined constant. The cumulative damage size due to single-event overloads by time t for stent i is

$$S_i(t) = \sum_{j=1}^{N(t)} H_{ij}, \quad (6.5)$$

where $N(t)$ is the number of shocks by time t . Therefore, the total crack length $a_{S(i)}(t)$ is due to both cyclic loads, and the cumulative shock damage size. Mathematically we have

$$a_{S(i)}(t) = a_i(t) + S_i(t). \quad (6.6)$$

The delayed failure occurs when $a_{S(i)} > a_{th(i)}$. The probability that stent i does not fail due to the delayed failure is

$$\begin{aligned} P(a_{S(i)} < a_{th(i)}) &= \sum_{m=0}^{\infty} P(a_i(t) + S_i(t) < a_{th(i)} \mid N(t) = m) P(N(t) = m) \\ &= P(a_i(t) < a_{th(i)}, N(t) = 0) + \sum_{m=1}^{\infty} P\left(a_i(t) + \sum_{j=1}^{N(t)} H_{ij} < a_{th(i)}, N(t) = m\right) \\ &= \Phi\left(\frac{a_{th(i)} - \mu_{\theta_i} t^{\alpha_i}}{\sqrt{\sigma_{\theta_i}^2 t^{2\alpha_i} + \sigma_{B_i}^2 t}}\right) e^{-\lambda t} + \sum_{m=1}^{\infty} \Phi\left(\frac{a_{th(i)} - \mu_{\theta_i} t^{\alpha_i} - m b_i (\mu_{K_i} - W_i)}{\sqrt{\sigma_{\theta_i}^2 t^{2\alpha_i} + \sigma_{B_i}^2 t + m \sigma_{H_i}^2}}\right) \frac{e^{-\lambda t} (\lambda t)^m}{m!}. \end{aligned} \quad (6.7)$$

The reliability of a multi-component system of n stents at time t , is the probability that all of stents survive the $N(t)$ shocks, and the total crack length of any single stent i due to both cyclic loads and abrupt increase in crack length as a result of single-event overloads is less than its critical crack length threshold as well. Therefore, the system reliability for a multi-stent system implanted is

$$\begin{aligned} R(t) &= P(a_1(t) < a_{th(1)}, \dots, a_n(t) < a_{th(n)}) P(N(t) = 0) \\ &\quad + \sum_{m=1}^{\infty} \prod_{i=1}^n P\left[K_{i1} < K'_i, \dots, K_{im} < K'_i, a_i(t) + \sum_{j=1}^m H_{ij} < a_{th(i)}\right] P(N(t) = m) \end{aligned} \quad (6.8a)$$

or

$$R(t) = \sum_{m=0}^{\infty} \prod_{i=1}^n P(K_i < K'_i)^m P\left[a_i(t) + \sum_{j=0}^m H_{ij} < a_{th(i)}\right] P(N(t) = m). \quad (6.8b)$$

By plugging Equations (6.1) and (6.7) in (6.8b), the reliability function for a multi-component system of stents implanted in patient's arteries is expressed as follows:

$$R(t) = \sum_{m=0}^{\infty} \prod_{i=1}^n \left[\Phi \left(\frac{\mu_{K'_i} - \mu_{K_i}}{\sqrt{\sigma_{K'_i}^2 + \sigma_{K_i}^2}} \right) \right]^m \Phi \left(\frac{a_{th(i)} - \mu_{\theta_i} t^{\alpha_i} - mb_i (\mu_{K_i} - W_i)}{\sqrt{\sigma_{\theta_i}^2 t^{2\alpha_i} + \sigma_{B_i}^2 t + m\sigma_{H_i}^2}} \right) \frac{e^{-\lambda t} (\lambda t)^m}{m!}. \quad (6.9)$$

Using data from Keedy and Feng (2012) and Robertson and Ritchie (2007), along with some reasonable assumptions, the parameters for reliability analysis provided in Feng et al. (2014) study, is shown in Table 6.1.

Table 6.1. Parameter values for multi-component system reliability analysis

Parameters	Value	Source
$a_{th(i)}$	$5 \mu m$	Robertson and Ritchie (2007)
λ	0.3, 1, and 3/year	Assumption
$\mu_{K'_i}$	$27 MPa\sqrt{m}$	Robertson and Ritchie (2007)
$\sigma_{K'_i}^2$	$(0.167 MPa\sqrt{m})^2$	Keedy and Feng (2013)
μ_{K_i}	$6.25 MPa\sqrt{m}$	Robertson and Ritchie (2007)
$\sigma_{K_i}^2$	$(0.325 MPa\sqrt{m})^2$	Keedy and Feng (2013)
μ_{θ_i}	8.36×10^{-17}	Robertson and Ritchie (2007)
$\sigma_{\theta_i}^2$	4.18×10^{-18}	Keedy and Feng (2013)
$\sigma_{B_i}^2$	6.25×10^{-16}	Assumption
$\sigma_{H_i}^2$	$(0.00001 \mu m)^2$	Assumption
W_i	1.33	Robertson and Ritchie (2007)
α_i	-1.3986	Robertson and Ritchie (2007)
b	$0.01504 (mm / MPa\sqrt{m})$	Robertson and Ritchie (2007)

6.4. Condition-based Replacement with Warning Limit

The implementation of follow-up after multiple stenting is still in the case-by-case recommendation phase according to the physician's perception. It is imperative to implement reliability-based maintenance policies to minimize the impact of unforeseen failures. We develop a replacement policy derived from the CBR for multi-stent systems.

After the first survey paper on maintenance policies for multi-component systems conducted by Thomas (1986), this topic has attracted increasing attention. Cho and Parlar (1991) conducted a comprehensive survey on maintenance models for multi-component systems, including group, block, and opportunistic models. Another survey paper on this topic is provided by Dekker et al. (1997) with a focus on economic dependence.

In our practical case, failure of stents can put the life of patients in danger. Therefore, the cost associated to system failure is significantly higher than the cost to preventively replace the system when it is in the critical condition. Preventive replacement according to its condition is a form of CBR that is an effective option to reduce unexpected failure of degrading systems when the failure cost is relatively high. We can discover whether a system is in a critical condition by conducting periodic inspections or follow-ups. During an inspection, we correctively replace the whole multi-stent system if it has already failed; or we replace the system preventively if we find that the crack length on *all* stents is above a warning limit. The warning limit is a critical threshold predetermined by manufacturers, exceeding from which indicates that a stent is more likely to fail within a short period. It is important to determine the inspection intervals, because short inspection intervals can lead to more frequent inspection actions and increase the inspection cost, and long inspection intervals can increase the chance of unexpected system failure. Our proposed CBR model intends to determine the inspection interval by minimizing the long run replacement cost.

In the model, the entire multi-stent system is inspected periodically at interval τ . The required action is determined based on the system status detected during the inspection: *i*) if the system is still functioning and the crack length on at least one stent is

less than its warning limit, $a_{war(i)}$, no action is necessary to be taken, *ii*) if the system is still operating, but the crack length on each of all n stents is beyond its warning limit, $a_{war(i)}$, we need to preventively replace the whole system, and *iii*) if the system has already failed due to either instantaneous failure or delayed failure of at least one stent, we need to correctively replace the entire system. We assume the failure of a multi-stent system does not show significant symptom and only can be discovered during the inspection (hidden failure).

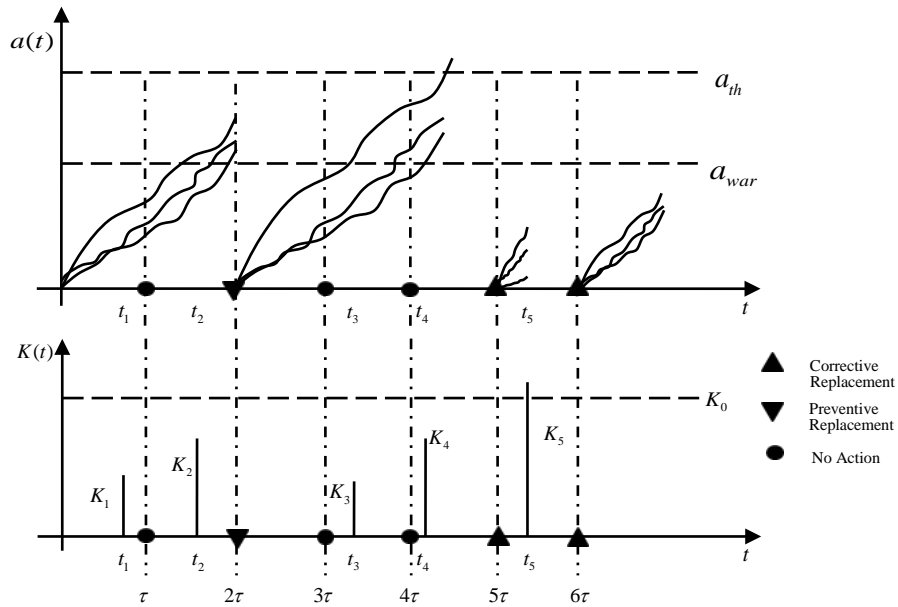


Figure 6.2: Condition-based replacement policy

Figure 6.2 depicts how the proposed CBR model is implemented for a system of three stents. In this example, the first system of three stents is preventively replaced at the second inspection, because the degradation for all stents exceeds the warning limit although the device is still operating. The second system is correctively replaced at the fifth inspection due to delayed failure of one stent. Finally, the third system is replaced correctively due to instantaneous failure.

By minimizing the average long run maintenance cost rate, the optimum value for the decision variable, τ , can be determined. From the basic renewal theory, the average long run maintenance cost per unit of time can be calculated as follows:

$$C_A(\tau) = \lim_{t \rightarrow \infty} (C(t)/t) = \frac{\text{Expected replacement cost incurred in a renewal cycle}}{\text{Expected length of a renewal cycle}} = \frac{E[C_T]}{E[L]}. \quad (6.10)$$

The total maintenance cost in a renewal cycle, C_T , includes the inspection cost, preventive replacement cost and corrective replacement cost. Therefore, the expected total maintenance cost is given as

$$E[C_T] = E \left[\begin{array}{c} \text{Inspection} \\ \text{Cost} \end{array} \right] + E \left[\begin{array}{c} \text{Preventive} \\ \text{Replacement Cost} \end{array} \right] + E \left[\begin{array}{c} \text{Corrective} \\ \text{Replacement Cost} \end{array} \right]. \quad (6.11)$$

The probability of performing a preventive replacement at the k^{th} inspection, $P(N_{PR} = k)$, i.e., the probability that the degradation of each of all n stents is within $(a_{war(i)}, a_{th(i)})$ while the system is still functioning by time $k\tau$, can be derived as

$$P(N_{PR} = k) = R(k\tau | a_{th(1)}, \dots, a_{th(n)}) - R(k\tau | a_{war(1)}, \dots, a_{war(n)}). \quad (6.12)$$

The probability of performing a corrective replacement at the k^{th} inspection, $P(N_{CR} = k)$, i.e., the probability that the system fails between the $(k-1)^{th}$ and k^{th} inspections, can be derived as:

$$P(N_{CR} = k) = R((k-1)\tau | a_{th(1)}, \dots, a_{th(n)}) - R(k\tau | a_{th(1)}, \dots, a_{th(n)}). \quad (6.13)$$

The number of inspections in a renewal cycle, N_I , is determined by the time of a preventive or corrective replacement that terminates a renewal cycle. Therefore, the probability mass function of N_I is given as

$$\begin{aligned}
P(N_I = k) &= P(N_{PR} = k \cup N_{CR} = k) = P(N_{PR} = k) + P(N_{CR} = k) \\
&= R\left((k-1)\tau \middle| a_{th(1)}, \dots, a_{th(n)}\right) - R\left(k\tau \middle| a_{war(1)}, \dots, a_{war(n)}\right).
\end{aligned} \tag{6.14}$$

We replace the system with a new one if we find the system has failed or it is in a critical condition where the crack length of each of all stents is above its warning limit. Therefore, the expected number of inspections, $E(N_I)$, is

$$E(N_I) = \sum_{k=1}^{\infty} k P(N_I = k) = \sum_{k=1}^{\infty} k \left[R\left((k-1)\tau \middle| a_{th(1)}, \dots, a_{th(n)}\right) - R\left(k\tau \middle| a_{war(1)}, \dots, a_{war(n)}\right) \right]. \tag{6.15}$$

The renewal cycle is defined as the time from the installation to the first replacement, or the time between two successive replacements that takes a value of a multiple of τ is determined as

$$\begin{aligned}
E[L] &= \sum_{k=1}^{\infty} E[L | N_I = k] P(N_I = k) = \sum_{k=1}^{\infty} k \tau P(N_I = k) \\
&= \sum_{k=1}^{\infty} k \tau \left[R\left((k-1)\tau \middle| a_{th(1)}, \dots, a_{th(n)}\right) - R\left(k\tau \middle| a_{war(1)}, \dots, a_{war(n)}\right) \right].
\end{aligned} \tag{6.16}$$

There is a cost associated with inspection when an inspection is performed. The expected inspection cost during a renewal cycle depends on the number of inspections and can be derived as

$$\begin{aligned}
E[\text{Inspection Cost}] &= C_I E[N_I] = \sum_{k=1}^{\infty} k C_I P(N_I = k) \\
&= \sum_{k=1}^{\infty} k C_I \left[R\left((k-1)\tau \middle| a_{th(1)}, \dots, a_{th(n)}\right) - R\left(k\tau \middle| a_{war(1)}, \dots, a_{war(n)}\right) \right].
\end{aligned} \tag{6.17}$$

The replacement can be either corrective or preventive, and the expected cost for replacement can be derived as

$$\begin{aligned}
E[\text{Corrective Replacement Cost}] &= \sum_{k=1}^{\infty} C_{CR} P(N_{CR} = k) \\
&= \sum_{k=1}^{\infty} C_{CR} \left[R\left((k-1)\tau \middle| a_{th(1)}, \dots, a_{th(n)}\right) - R\left(k\tau \middle| a_{war(1)}, \dots, a_{war(n)}\right) \right]
\end{aligned} \tag{6.18}$$

and

$$\begin{aligned}
E[\text{Preventive Replacement Cost}] &= \sum_{k=1}^{\infty} C_{PR} P(N_{PR} = k) \\
&= \sum_{k=1}^{\infty} C_{PR} \left[R\left((k-1)\tau \middle| a_{th(1)}, \dots, a_{th(n)}\right) - R\left(k\tau \middle| a_{war(1)}, \dots, a_{war(n)}\right) \right].
\end{aligned} \tag{6.19}$$

Based on Equations (6.10) to (6.19), the average long run maintenance cost rate as a function of τ is derived as

$$C_A(\tau) = \frac{\sum_{k=1}^{\infty} k C_I P(N_I = k) + \sum_{k=1}^{\infty} C_{CR} P(N_{CR} = k) + \sum_{k=1}^{\infty} C_{PR} P(N_{PR} = k)}{\sum_{k=1}^{\infty} k \tau P(N_I = k)}. \tag{6.20}$$

An analytical solution for this problem can be obtained by calculating the first derivative of the objective function in Equation (6.20). We can find the optimal time interval of periodic inspection by setting $C'_A(\tau)$ equal to zero, as given as below:

$$C'_A(\tau) = \frac{v(du/d\tau) - u(dv/d\tau)}{v^2} = 0, \tag{6.21}$$

where

$$\begin{aligned}
u &= \sum_{k=1}^{\infty} k C_I P(N_I = k) + \sum_{k=1}^{\infty} C_{CR} P(N_{CR} = k) + \sum_{k=1}^{\infty} C_{PR} P(N_{PR} = k) \\
&= \sum_{k=1}^{\infty} (k C_I + C_{CR}) R\left((k-1)\tau \middle| a_{th(1)}, \dots, a_{th(n)}\right) + \sum_{k=1}^{\infty} (C_{PR} - C_{CR}) R\left(k\tau \middle| a_{th(1)}, \dots, a_{th(n)}\right) \\
&\quad - \sum_{k=1}^{\infty} (C_{PR} + k C_I) R\left(k\tau \middle| a_{war(1)}, \dots, a_{war(n)}\right),
\end{aligned} \tag{6.22a}$$

$$v = \sum_{k=1}^{\infty} k \tau P(N_I = k) = \sum_{k=1}^{\infty} k \tau R\left((k-1)\tau \middle| a_{th(1)}, \dots, a_{th(n)}\right) - \sum_{k=1}^{\infty} k \tau R\left(k\tau \middle| a_{war(1)}, \dots, a_{war(n)}\right), \tag{6.22b}$$

$$\begin{aligned}
\frac{du}{d\tau} &= \sum_{k=1}^{\infty} k (C_{PR} + k C_I) f_T\left(k\tau \middle| a_{war(1)}, \dots, a_{war(n)}\right) - \sum_{k=1}^{\infty} k (C_{PR} - C_{CR}) f_T\left(k\tau \middle| a_{th(1)}, \dots, a_{th(n)}\right) \\
&\quad - \sum_{k=1}^{\infty} (k-1) (k C_I + C_{CR}) f_T\left((k-1)\tau \middle| a_{th(1)}, \dots, a_{th(n)}\right),
\end{aligned} \tag{6.22c}$$

$$\begin{aligned} \frac{dv}{d\tau} = & \sum_{k=1}^{\infty} kR \left((k-1)\tau \middle| a_{th(1)}, \dots, a_{th(n)} \right) - \sum_{k=1}^{\infty} kR \left(k\tau \middle| a_{war(1)}, \dots, a_{war(n)} \right) \\ & + \sum_{k=1}^{\infty} k^2 \tau f_T \left(k\tau \middle| a_{war(1)}, \dots, a_{war(n)} \right) - \sum_{k=1}^{\infty} k(k-1)\tau f_T \left((k-1)\tau \middle| a_{th(1)}, \dots, a_{th(n)} \right). \end{aligned} \quad (6.22d)$$

6.5. Numerical Examples

To obtain the optimal interval for periodic inspection, we need to minimize the average long-run maintenance cost rate, $C_A(\tau)$, by using analytical or numerical methods. We use the simplex search method of Lagarias et al. (1998) that is a direct search method without using numerical or analytic gradients. For an example of $C_I=\$1$, $C_{PR}=\$10$ and $C_{CR}=\$100$, the average long-run maintenance cost rate is $\$388.7032$, that can be obtained at $\tau^*=7.0 \times 10^6$, the optimum number of revolutions for inspection interval. These optimal solutions are verified through numerical calculation. Figure 6.3 presents $C_A(\tau)$ as a function of τ .

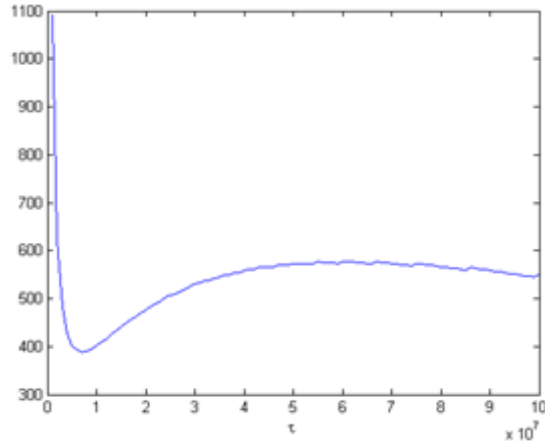


Figure 6.3: $C_A(\tau)$ versus τ

We also perform sensitivity analyses to capture the impact of the model parameters on the optimal solutions. These model parameters are the delayed failure threshold, a_{th} , and the warning limit, a_{war} . To avoid unnecessary complexity, we assume that these parameters are the same for all the components in a multi-stent system. As shown in Figure 6.4, when

the warning limit for doing the preventive replacement increases, the average long-run maintenance cost rate also increases, because the system is replaced less often preventively resulting in a higher probability of unexpected system failure and a higher maintenance cost. At the same time, the inspection interval is decreasing to reduce the risk of system failure.

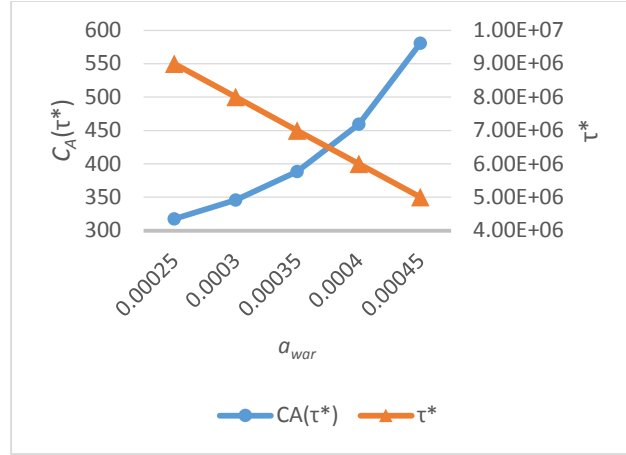


Figure 6.4: Sensitivity analysis of $C_A(\tau^*)$ and τ^* on a_{war}

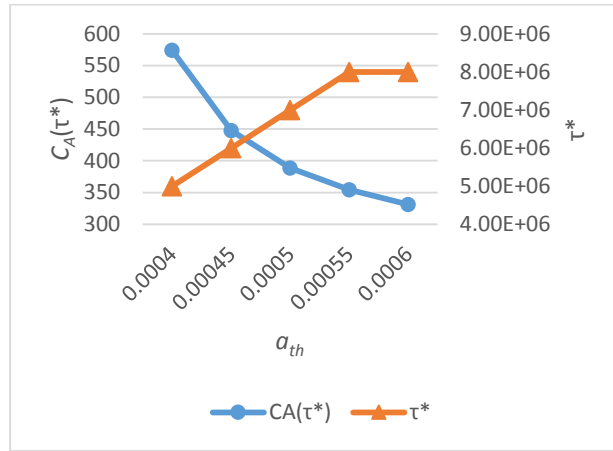


Figure 6.5: Sensitivity analysis of $C_A(\tau^*)$ and τ^* on a_{th}

Figure 6.5 illustrates that increasing the delayed failure threshold a_{th} causes the average long-run maintenance cost rate to be lowered, because it is less likely for the system to fail. At the same time, the inspection interval increases.

6.6. Conclusion

In this chapter, reliability models were used as a foundation for the follow-up or maintenance of a multi-stent system. We proposed the replacement policy derived from CBR to reduce unexpected system failure by preventively replacing the whole system if we discover that the system degradation exceeds the warning limit during the inspection. The frequency of system inspection is a decision variable, and the optimum inspection interval has been obtained by minimizing the average long-run maintenance cost rate.

Chapter 7

A Condition-based Maintenance Strategy for Repairable Deteriorating Systems subject to Generalized Mixed Shock Model

In this chapter, a new generalized mixed shock model is proposed to describe the failure process due to external shocks, and it is a mixture of three classic shock models, i.e., extreme shock model, run shock model, and δ -shock model. Based on reliability analysis for a system subject to dependent competing risks of internal degradation and external shocks, we propose a CBM policy considering imperfect repair. Under the proposed CBM policy, the system is inspected at fixed time intervals and a decision for an appropriate maintenance action (i.e., no action, imperfect repair, preventive or corrective replacement) is made based on the actual health condition of the system detected through inspection. The objective is to determine the optimal inspection interval that minimizes the expected long-run average maintenance cost rate. A MEMS example is used to evaluate the efficiency of developed reliability and condition-based maintenance model.

7.1. Introduction

In this chapter, we attempt to generalize the traditional mixed shock model by incorporating three, rather than two, classic shock models (i.e. extreme shock model, run shock model, and δ -shock model). We assume that a system fails because of a single large shock, a series of consecutive shocks, or a short time lag between successive shocks, depending on which critical level is attained first. An example to illuminate this new generalized shock model is in boxing, where a knockout can happen due to a single powerful punch, a series of moderate punches, or two immediate punches.

External shocks are not the only reason causing the system failure. It is well known that systems degrade over time due to different factors such as erosion, corrosion, wear out, fatigue and crack growth. Even new technologies cannot protect modern systems from degradation. Such systems can be critical engineering systems (e.g., a reactor fuel core in a nuclear power plant), a giant structure (e.g., a bridge), or a complex device (e.g., a MEMS device). Degradation processes can be modeled using different approaches, such as a stochastic process (Kharoufeh & Cox, 2005), or a random coefficient model (Bae & Kvam, 2004). A system fails when the overall degradation level exceeds a critical threshold.

In this chapter, we develop a new CBM policy considering imperfect repair, based on the reliability modeling for systems subject to dependent competing risks of degradation and generalized mixed shock model. What distinguishes this model from others (Tan et al. 2010; Fouladirad & Grall 2011; van & Bérenguer 2012) is that we incorporate various actions in the maintenance model: imperfect repair, preventive replacement, and corrective replacement. The imperfect repair impacts the system by lowering the degradation level to a certain level.

The remainder of this chapter is structured as follows. Section 7.2 discusses the modeling of different competing failure processes of the system. The maintenance strategy is described in details in Section 7.3. Section 7.4 presents a numerical example to illustrate the reliability modeling and the maintenance strategy, and finally Section 7.5 provides summary and conclusions.

Notation

$X(t)$	Amount of continuous degradation at time t
$N(t)$	Number of random shocks by time t
D_e	Failure threshold for the extreme shock model
D_r	Failure threshold for the run shock model

δ	Minimum time lag between two successive shocks for the δ -shock model
S	Fatal shock count
S_e	Fatal shock count due to the extreme shock model
S_δ	Fatal shock count due to the δ -shock model
S_r	Fatal shock count due to the run shock model
B_k	Interval time between the $(k-1)^{th}$ and k^{th} shocks
W_k	Magnitude of the k^{th} shock load
$F_W(w)$	Cumulative distribution function (cdf) of W_k
τ	Length of inspection interval
H	Threshold for degradation-based failure
H_p	Critical degradation level for preventive replacement
H_w	Critical degradation level for imperfect repair
H_r	Restored degradation level after imperfect repair
L	Length of renewal cycle
N_I	Number of inspection before replacement
N_{PR}	Inspection count at which a preventive replacement is performed
N_{CR}	Inspection count at which a corrective replacement is performed
N_{IR}	Inspection count at which an imperfect repair is performed
T_w	Time when the degradation reaches H_w , given the initial degradation level equals 0
T_p	Time when the degradation reaches H_p , given the initial degradation level equals H_r
C_I	Cost to inspect the system
C_{IR}	Cost to perform imperfect repair
C_{PR}	Cost to perform preventive replacement
C_{CR}	Cost to perform corrective replacement

7.2. System Failure Modeling

Consider a repairable system whose failure is due to the competing risks of degradation and shocks. The system is considered as failed when the degradation level exceeds a critical threshold or when a fatal shock arrives, or a DTS model. Figure 7.1 illustrates an example of the two dependent failure processes: *degradation-based failure* and *shock-based failure* for a deteriorating system subject to the generalized mixed shock model. As shown in Figure 7.1, the first failure the system experiences is a *shock-based failure* when the magnitude of the shock arrived at time t_2 is greater than the critical level

for the extreme shock model ($W_2 > D_e$). The system experiences the second failure at time t_3 when B_3 is less than the threshold δ (δ -shock model). The third failure is a *degradation-based failure* because the accumulated degradation level exceeds the threshold H . The last failure occurs at time t_3 as soon as there are two successive shocks with their magnitudes greater than the critical level for the run shock model ($W_2, W_3 > D_r$). Because the system is replaced after each failure, the shock count and time origin have been reset after each failure as shown in Figure 7.1.

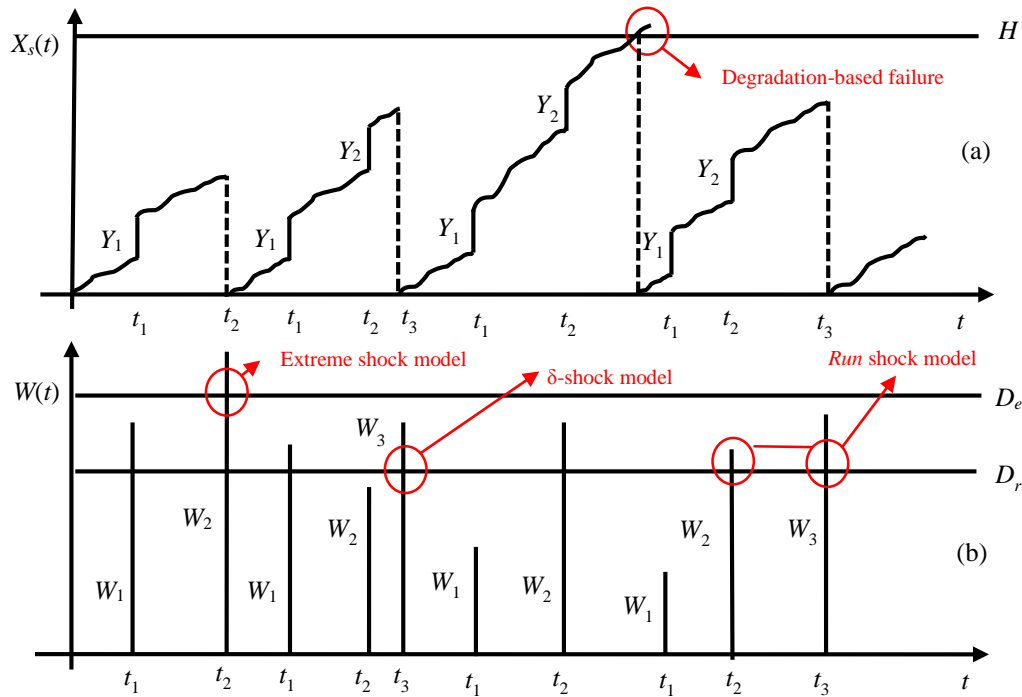


Figure 7.1: Two dependent competing failure processes:

(a) degradation-based failure, (b) shock-based failure

7.2.1. Degradation-based Failure Modeling

We assume that the system is subject to a monotonically increasing degradation over time due to use, which is denoted by $X(t)$ with $X(0) = \varphi$, where φ is the initial degradation level that is a random variable (due to variability in manufacturing and delivering processes). If no maintenance is performed, the continuous degradation by time

t is expressed as $X(t) = \varphi + \beta t + \varepsilon$, where β is the degradation rate that is a random variable and varies from part to part, and ε is the random error term following a normal distribution $\varepsilon \sim N(0, \sigma^2)$. This linear path function can be applied to a wide range of degradation phenomena, such as wear degradation.

When a non-fatal shock arrives, we assume that it damages the system by increasing the degradation level. We denote the damage caused by the k^{th} shock by Y_k for $k = 1, 2, \dots$, where Y_k is an *i.i.d.* non-negative random variable. The accumulated degradation including both continuous degradation and instantaneous damage induced by non-fatal shocks can be expressed as

$$X_s(t) = X(t) + Z(t) = X(t) + \sum_{k=1}^{N(t)} Y_k, \quad (7.1)$$

where $Z(t)$ represents the cumulative damage by non-fatal random shocks, and $N(t)$ is the number of shocks by time t . In order for the system to survive the *degradation-based failure*, the accumulated degradation level must be less than the threshold H . Therefore, the probability of no *degradation-based failure* by time t is

$$P(X_s(t) < H) = \sum_{i=0}^{\infty} P\left(X(t) + \sum_{k=1}^{N(t)} Y_k < H \mid N(t) = i\right) P(N(t) = i). \quad (7.2)$$

We assume that shocks arrive according to a homogenous Poisson process with a constant rate of λ . If we consider $F_X(x; \varphi, t)$ to be the cdf of continuous degradation, $X(t)$, and $f_Z(z)$ to be the pdf of the accumulated damage caused by shocks, $Z(t)$, then the cdf of $X_s(t)$, $F_{X_s}(x; \varphi, t)$, can be derived using a convolution integral:

$$F_{X_s}(x; \varphi, t) = P(X_s(t) < x) = F_X(x; \varphi, t) e^{-\lambda t} + \sum_{i=1}^{\infty} \left(\int_0^x F_X(x-u; \varphi, t) f_Z(u) du \right) \frac{e^{-\lambda t} (\lambda t)^i}{i!}. \quad (7.3)$$

The model in (7.3) is general and can accommodate different distributional assumptions. In a specific case, we assume that φ is a constant, β and Y_k are normally distributed, i.e., $\beta \sim N(\mu_\beta, \sigma_\beta^2)$ and $Y_k \sim N(\mu_Y, \sigma_Y^2)$. For this specific case, the resulting total degradation, $X_S(t)$, follows a normal distribution. Then the probability in (7.2) can be expressed as

$$F_{X_S}(H; \varphi, t) = \sum_{i=0}^{\infty} \Phi \left(\frac{H - (\varphi + \mu_\beta t + i\mu_Y)}{\sqrt{\sigma_\beta^2 t^2 + \sigma^2 + i\sigma_Y^2}} \right) \frac{e^{-\lambda t} (\lambda t)^i}{i!}. \quad (7.4)$$

7.2.2. Shock-based Failure Modeling

Only one shock model (e.g., extreme shock model, δ -shock model) is typically considered to result in an immediate failure. We introduce a generalized mixed shock model, a combination of three shock models including extreme shock model, δ -shock model, and run shock model, as the direct cause for the *shock-based failure*. The system suffers shock-based failure as soon as the condition for one of the three shock models is realized: 1) the magnitude of one shock is above the critical value D_e (extreme shock model), 2) the time lag between two sequential shocks is less than the threshold δ (δ -shock model), or 3) a set of n consecutive shocks with magnitudes that are greater than the critical level D_r ($D_r < D_e$) occurs (run shock model). These three classic shock models are competing against each other, and whichever occurs first causes the system to experience shock-based failure.

Depending on which shock model is the reason for the system failure, different scenarios can occur. In the following, we discuss each scenario along with the correspondent probability that the system survives by the i^{th} shock.

Scenario (1): If the magnitude of the i^{th} shock is greater than the critical threshold D_e , the system fails according to the extreme shock model, and the i^{th} shock is the fatal shock. We use S_e to denote the *fatal shock count* due to the extreme shock model, which is a random variable. The probability that the system does not experience extreme shock model by the i^{th} shock is derived to be

$$P(S_e > N(t) | N(t) = i) = P\left(\bigcap_{k=1}^i \{W_k < D_e\}\right) = F_W(D_e)^i, \quad (7.5)$$

where W_k is the magnitude of the k^{th} shock load, an *i.i.d.* non-negative random variable, and $F_W(w)$ is the cdf of W_k .

Scenario (2): If the time interval between the $(i - 1)^{th}$ shock and the i^{th} shock is less than the threshold δ , the system breaks down and the i^{th} shock is considered as the fatal shock. We use S_δ to denote the *fatal shock count* due to the δ -shock model, which is a random variable. The probability that the system does not fail according to the δ -shock model by the i^{th} shock is derived to be

$$P(S_\delta > N(t) | N(t) = i) = P\left(\bigcap_{k=1}^i \{B_k > \delta\}\right) = e^{-i\lambda\delta}, \quad (7.6)$$

where B_k is the arrival time of the first shock or the time interval between the $(k - 1)^{th}$ and k^{th} shocks, an *i.i.d.* non-negative random variable. For the homogenous Poisson process, B_k follows an exponential distribution with a rate of λ .

Scenario (3): If the first run of n consecutive shocks that are greater than the critical level D_r occurs by the i^{th} shock, it causes the system to break down according to the run shock model. The i^{th} shock is considered to be the fatal shock. We use S_r to denote the *fatal shock count* due to the run shock model, which is a random variable.

In general, if we define V_m to be the probability that no run of n consecutive successes (in our case, a success is defined as a shock greater than D_r) occurs in a set of m shocks, it has been shown to satisfy the recursive equation (Krieger 1984):

$$V_m = qV_{m-1} + \dots + p^{n-1}qV_{m-n}, \quad \text{for } m > n, \quad (7.7)$$

with the initial conditions $V_k = 1$ when $1 \leq k \leq n - 1$, and $V_n = 1 - p^n$, where p is the probability of success, and $q = 1 - p$. Based on Eq. (7.7), the probability that no run of n consecutive shocks greater than D_r happens by time t , or the probability that the fatal shock count due to the run shock model, S_r , is larger than $N(t)$, is derived to be

$$\begin{aligned} P(S_r > N(t) | N(t) = i > n) &= P(W_i < D_r) P(S_r > N(t) - 1 | N(t) = i) + \dots \\ &+ P(W_{i-n+1} < D_r) P\left(\bigcap_{k=i-n+2}^i \{W_k \geq D_r\}\right) P(S_r > N(t) - n | N(t) = i) \\ &= F_W(D_r) P(S_r > N(t) - 1 | N(t) = i) + \dots \\ &+ F_W(D_r) (1 - F_W(D_r))^{n-1} P(S_r > N(t) - n | N(t) = i), \end{aligned} \quad (7.8)$$

with the initial conditions $P(S_r > N(t) | N(t) = i \leq n - 1) = 1$, and

$$P(S_r > N(t) | N(t) = n) = 1 - P\left(\bigcap_{k=1}^n \{W_k \geq D_r\}\right) = 1 - (1 - F_W(D_r))^n. \quad (7.9)$$

□

For a system not to experience a *shock-based failure*, the condition for the above three scenarios should not be met. Therefore, the probability that a system does not experience the *shock-based failure* by time t , i.e., the fatal shock count is greater than $N(t)$, is derived as follows:

$$\begin{aligned} P(S > N(t) | N(t) = i) &= P(S_e > N(t) \cap S_\delta > N(t) \cap S_r > N(t) | N(t) = i) \\ &= P(S_r > N(t) | S_e > N(t) = i) P(S_e > N(t) | N(t) = i) P(S_\delta > N(t) | N(t) = i), \end{aligned} \quad (7.10)$$

where $P(S_r > N(t) | S_e > N(t) = i)$ is the probability that no run of n consecutive shocks greater than D_r occurs by time t given that the magnitudes of all shocks are less than D_e .

By considering the following situations, the probability of no *shock-based failure* by time t is derived further:

i) When the number of shocks by time t is less than n , or $N(t) \leq n-1$, based on Eqs. (7.5), (7.6) and (7.10), we have

$$P(S > N(t) | N(t) = i \leq n-1) = 1 \times F_W(D_e)^i e^{-i\lambda\delta}. \quad (7.11)$$

ii) When the number of shocks by time t is equal to n , or $N(t) = n$, based on Eqs. (7.5), (7.6), (7.9) and (7.10), we have

$$P(S > N(t) | N(t) = n) = \left(1 - \left(\frac{F_W(D_e) - F_W(D_r)}{F_W(D_e)} \right)^n \right) F_W(D_e)^n e^{-n\lambda\delta}. \quad (7.12)$$

iii) When the number of shocks by time t is larger than n , or $N(t) > n$, based on Eqs. (7.5), (7.6), (7.8) and (7.10), we have

$$\begin{aligned} P(S > N(t) | N(t) = i > n) &= F_W(D_r) P(S_r > i-1 | S_e > i-1) F_W(D_e)^i e^{-i\lambda\delta} + \dots \\ &+ \frac{F_W(D_r)}{F_W(D_e)} \left(\frac{F_W(D_e) - F_W(D_r)}{F_W(D_e)} \right)^{n-1} P(S_r > i-n | S_e > i-n) F_W(D_e)^i e^{-i\lambda\delta}. \end{aligned} \quad (7.13)$$

Now by summing them all, we finally have the probability that a system does not experience the *shock-based failure* by time t , i.e., the fatal shock count is greater than $N(t)$:

$$\begin{aligned} P(S > N(t)) &= \sum_{i=1}^{n-1} F_W(D_e)^i \frac{e^{-\lambda(i\delta+t)} (\lambda t)^i}{i!} + \left(1 - \left(\frac{F_W(D_e) - F_W(D_r)}{F_W(D_e)} \right)^n \right) \\ &\times F_W(D_e)^n \frac{e^{-\lambda(n\delta+t)} (\lambda t)^n}{n!} + \sum_{i=n+1}^{\infty} F_W(D_r) P(S_r > i-1 | S_e > i-1) F_W(D_e)^i \frac{e^{-\lambda(i\delta+t)} (\lambda t)^i}{i!} + \dots \\ &+ \frac{F_W(D_r)}{F_W(D_e)} \left(\frac{F_W(D_e) - F_W(D_r)}{F_W(D_e)} \right)^{n-1} P(S_r > i-n | S_e > i-n) F_W(D_e)^i \frac{e^{-\lambda(i\delta+t)} (\lambda t)^i}{i!}. \end{aligned} \quad (7.14)$$

7.2.3. System Reliability Function

For a system to survive by time t in this DTS model, we need to ensure that *degradation-based failure* and *shock-based failure* do not occur by time t . The reliability function for such a system using Eqs. (7.2) and (7.14) is derived as

$$R(t) = \sum_{i=0}^{\infty} P(S > i) P\left(X(t) + \sum_{k=1}^i Y_k < H\right) \frac{e^{-\lambda t} (\lambda t)^i}{i!}. \quad (7.15)$$

Given the number of shocks by time t , *degradation-based failure* and *shock-based failure* are conditionally independent, due to the assumption that the shock damage size Y_k is independent of the shock load W_k .

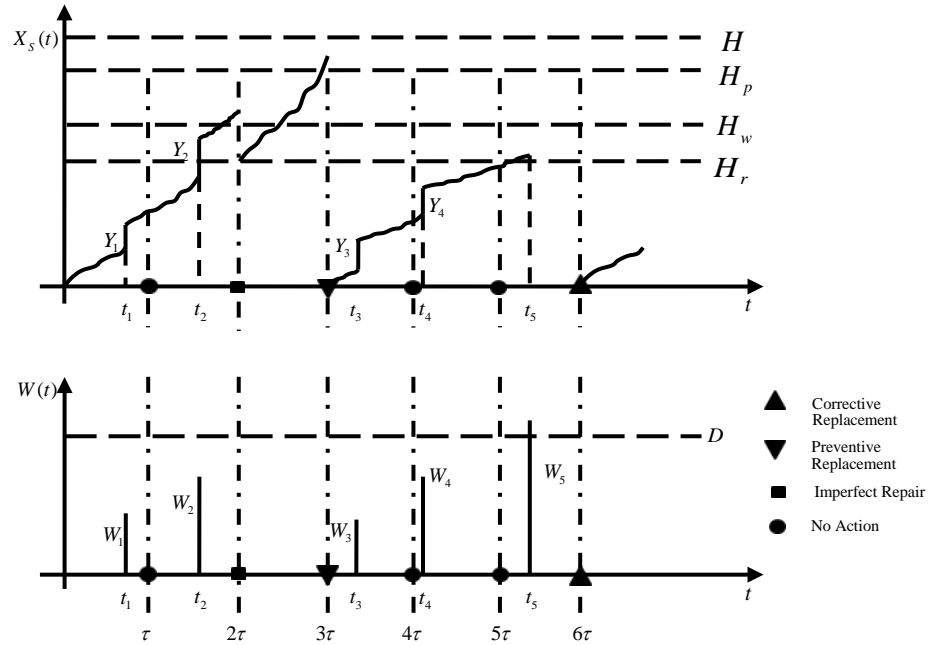


Figure 7.2: Proposed condition-based maintenance policy

7.3. Condition-based Maintenance Strategy

In this section, we propose a condition-based maintenance model with periodic inspection for a repairable system subject to two competing failure processes. The proposed CBM takes into account corrective replacement, preventive replacement, and imperfect

repair actions. The maintenance actions take place according to the detected condition of the system through inspections. The proposed condition-based maintenance model is illustrated in Figure 7.2, which presents the critical level for preventive replacement, H_p , the critical level for imperfect repair, H_w , and the restored level from imperfect repair, H_r .

Assumptions

1. The repairable system is inspected at a periodic interval, τ .
2. If the system fails, it is not self-announcing and remains failed until the next inspection.
3. At an inspection,
 - a. If the system is detected to be failed due to shock-based or degradation-based failure, a *corrective replacement* is performed;
 - b. If the degradation is beyond the cut-off limit, H_p , a *preventive replacement* is implemented even though the device is still functioning;
 - c. If the degradation exceeds the warning limit value H_w , but is not beyond H_p , an *imperfect repair* takes place that restores the degradation level to some younger system status, H_r , $H_r < H_w < H_p < H$;
 - d. If the system is operating and the degradation level is less than the warning limit, H_w , *no action* is needed.
4. The repair action can be performed only once during a renewal cycle, which is defined as the time from the installation to the first replacement, or the time between two successive replacements.

From the basic renewal theory, the average long run maintenance cost per unit of time can be calculated as follows:

$$C_A(\tau) = \lim_{t \rightarrow \infty} (C(t)/t) = \frac{\text{Expected maintenance cost incurred in a renewal cycle}}{\text{Expected length of a renewal cycle}} = \frac{E[C_T]}{E[L]}. \quad (7.16)$$

By minimizing the average maintenance cost rate, the decision variable is determined: the inspection interval τ . The expected renewal cycle length, $E[L]$, is formulated as follows

$$E[L] = \sum_{i=1}^{\infty} E[L | N_I = i] P(N_I = i) = \sum_{i=1}^{\infty} i\tau P(N_I = i), \quad (7.17)$$

where N_I is the number of inspections taking place in a renewal cycle. The probability for the number of inspection is derived according to the replacement actions taken, either preventively or correctively:

$$P(N_I = i) = P(N_{PR} = i \cup N_{CR} = i) = P(N_{PR} = i) + P(N_{CR} = i), \quad (7.18)$$

where N_{PR} and N_{CR} , the inspection counts at which we perform preventive replacement and corrective replacement, respectively, are random variables.

7.3.1. Probability of Performing Imperfect Repair

During the j^{th} inspection, if the degradation level is within the interval of $[H_w, H_p)$ for the first time, i.e., the time that the degradation reaches H_w is between the $j - 1^{th}$ inspection and the j^{th} inspection, an imperfect repair is performed at the j^{th} inspection that brings the degradation to the restored level of H_r . We define N_{IR} to be the inspection count at which a repair action is performed. The probability of performing a repair at the j^{th} inspection is

$$\begin{aligned}
P(N_{IR} = j) &= \sum_{k=0}^{\infty} P(S > k) P(X_S((j-1)\tau) < H_w < X_S(j\tau) \leq H_p) P(N(j\tau) = k) \\
&= \sum_{k=0}^{\infty} P(S > k) P(X_S(j\tau - T_w) \leq H_p - H_w | (j-1)\tau < T_w < j\tau) P(N(j\tau) = k) \quad (7.19) \\
&= \sum_{k=0}^{\infty} \int_{(j-1)\tau}^{j\tau} P(S > k) P(X_S(j\tau - t_w) \leq H_p - H_w) P(N(j\tau) = k) dF_{T_w},
\end{aligned}$$

where T_w , the first time that the degradation reaches H_w given the initial degradation level equals 0, is a random variable defined as

$$T_w = \inf \{t : X_S(t) \geq H_w\}. \quad (7.20)$$

The pdf for T_w is to be provided in Section 7.3.4.

7.3.2. Probability of Performing Preventive Replacement

The system is preventively replaced when the overall degradation is greater than H_p , but the system is still functioning. The probability of performing a preventive replacement at the i^{th} inspection depends on whether the system has already undergone a repair action during the renewal cycle. Two scenarios may occur before the preventive replacement is performed.

Scenario 1: No repair is recorded by the i^{th} inspection.

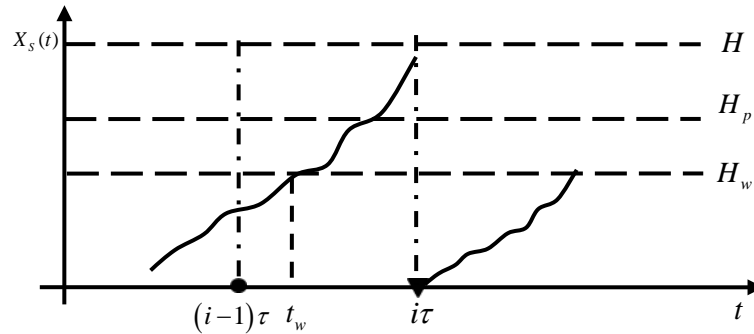


Figure 7.3: Scenario 1 for performing preventive replacement at the i^{th} inspection

Figure 7.3 shows an example of Scenario 1 where the degradation level is less than the warning limit H_w at time $(i-1)\tau$, and it is within the interval of $[H_p, H)$ at time $i\tau$

leading to a preventive replacement. Let $P(N_{PR} = i \mid N_{IR} > i-1)$ denote the probability of performing a preventive replacement at time $i\tau$, given the system has not been repaired yet, and it is derived as follows:

$$\begin{aligned}
& P(N_{PR} = i \mid N_{IR} > i-1) \\
&= \sum_{k=0}^{\infty} P(S > k) \frac{P(X_S((i-1)\tau) < H_w, H_p \leq X_S(i\tau) < H)}{P(X_S((i-1)\tau) < H_w)} P(N(i\tau) = k) \\
&= \sum_{k=0}^{\infty} P(S > k) \frac{P(H_p - H_w \leq X_S(i\tau - T_w) < H - H_w \mid (i-1)\tau < T_w < i\tau)}{P(X_S((i-1)\tau) < H_w)} P(N(i\tau) = k) \quad (7.21) \\
&= \sum_{k=0}^{\infty} \int_{(i-1)\tau}^{i\tau} P(S > k) \frac{P(H_p - H_w \leq X_S(i\tau - t_w) < H - H_w)}{P(X_S((i-1)\tau) < H_w)} P(N(i\tau) = k) dF_{T_w}.
\end{aligned}$$

Scenario 2: One repair action is performed by the i^{th} inspection.

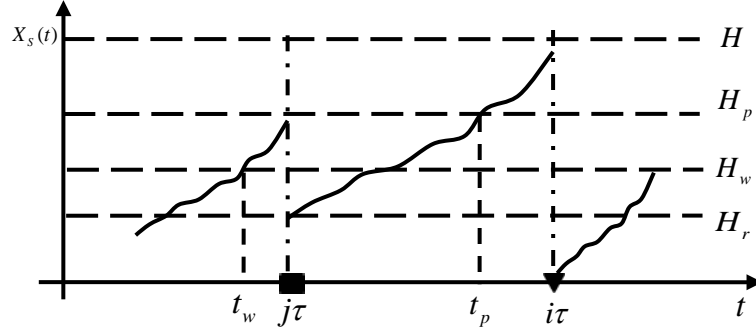


Figure 7.4: Scenario 2 for performing preventive replacement at the i^{th} inspection

Figure 7.4 depicts an example of Scenario 2 where the degradation is within $[H_w, H_p)$ at time $j\tau$, and therefore, an imperfect repair action is taken to restore the degradation level to H_r at the j^{th} inspection. The system is continuously operating and the degradation level reaches the interval $[H_p, H)$ at time $i\tau$, i.e. the time that the degradation reaches H_p is between the $i - 1^{th}$ inspection and the i^{th} inspection, leading to a preventive replacement. Let $P(N_{PR} = i \mid N_{IR} = j)$ denote the probability of performing the preventive replacement at the i^{th} inspection given the system has been repaired at the j^{th} inspection, $j < i$, and we have

$$\begin{aligned}
P(N_{PR} = i | N_{IR} = j) &= \sum_{k=0}^{\infty} P(X_S((i-j-1)\tau) < H_p - H_r \leq X_S((i-j)\tau) < H - H_r) \\
&\times P(S > k) P(N((i-j)\tau) = k) \\
&= \sum_{k=0}^{\infty} \int_{(i-j-1)\tau}^{(i-j)\tau} P(X_S((i-j)\tau - t_p) \leq H - H_p) P(S > k) P(N((i-j)\tau) = k) dF_{T_p},
\end{aligned} \tag{7.22}$$

where T_p , the first time that the degradation reaches H_p given the initial degradation level equals H_r , is a random variable defined as

$$T_p = \inf \{t : X_S(t) \geq H_p - H_r\}. \tag{7.23}$$

The pdf for T_p is to be provided in Section 7.3.4. Considering the above two scenarios, the probability of performing a preventive replacement at the i^{th} inspection is

$$P(N_{PR} = i) = \sum_{j=1}^{i-1} P(N_{PR} = i | N_{IR} = j) P(N_{IR} = j) + P(N_{PR} = i | N_{IR} > i-1) P(N_{IR} > i-1). \tag{7.24}$$

7.3.3. Probability of Performing Corrective Replacement

The system is correctively replaced when it fails due to either internal degradation process or external shock process. The probability that a corrective replacement is performed at the i^{th} inspection depends on whether the system is already repaired or not during the renewal cycle. Two scenarios may happen before the corrective replacement takes place.

Scenario 1: No repair is recorded by the i^{th} inspection.

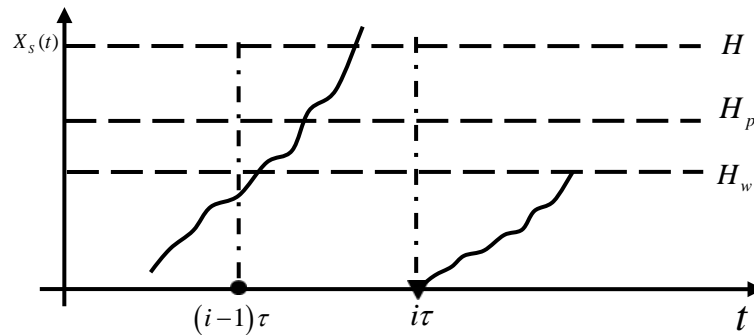


Figure 7.5: Scenario 1 for performing corrective replacement at the i^{th} inspection

Figure 7.5 shows an example of Scenario 1 where the degradation level is less than the warning limit H_w at time $(i-1)\tau$, and the system is failed at time $i\tau$ due to degradation-based failure, leading to corrective replacement. Let $P(N_{CR} = i | N_{IR} > i-1)$ denote the probability of performing the corrective replacement at time $i\tau$, given the system has not been repaired yet:

$$P(N_{CR} = i | N_{IR} > i-1) = F_T(i\tau | \varphi = 0) - F_T((i-1)\tau | \varphi = 0), \quad (7.25)$$

where $F_T(t | \varphi = 0)$ is the cdf of the time to failure given the initial degradation equals to zero, and it can be calculated using the reliability function in (7.15).

Scenario 2: One repair action is performed by the i^{th} inspection. Figure 7.6 depicts an example of Scenario 2 where the degradation is within $[H_w, H_p)$ at time $j\tau$, and therefore, an imperfect repair action is taken to restore the degradation level to H_r . The system is continuously operating and the degradation level is beyond H at time $i\tau$ leading to a corrective replacement. Let $P(N_{CR} = i | N_{IR} = j)$ denote the probability of performing the corrective replacement at the i^{th} inspection given the system was repaired at the j^{th} inspection, and we have

$$P(N_{CR} = i | N_{IR} = j) = F_T((i-j)\tau | \varphi = H_r) - F_T((i-j-1)\tau | \varphi = H_r), \quad (7.26)$$

where $F_T(t | \varphi = H_r)$ is the cdf of the time to failure for a system that has been undergone a repair action, i.e., the initial degradation equals to H_r .

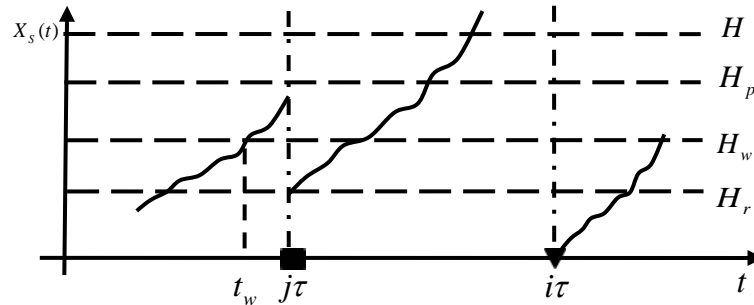


Figure 7.6: Scenario 2 for performing corrective replacement at the i^{th} inspection

Considering the above two scenarios, the probability of performing a corrective replacement at the i^{th} inspection is

$$P(N_{CR} = i) = \sum_{j=1}^{i-1} P(N_{CR} = i | N_{IR} = j) P(N_{IR} = j) + P(N_{CR} = i | N_{IR} > i-1) P(N_{IR} > i-1). \quad (7.27)$$

7.3.4. Probability Density Functions of T_w and T_p

To derive the probability density functions of T_w and T_p to be used in calculating the probabilities of different actions, we use Θ to denote the time that the degradation reaches a threshold H_1 given the initial degradation is equal to φ . We employ the cdf of $X_S(t)$ in (7.3) to find the cdf of Θ , $F_\Theta(\theta)$:

$$F_\Theta(\theta) = 1 - F_X(H_1; \varphi, \theta) e^{-\lambda\theta} - \sum_{l=1}^{\infty} \left(\int_0^\theta F_X(H_1 - u; \varphi, \theta) f_Z(u) du \right) \frac{e^{-\lambda\theta} (\lambda\theta)^l}{l!}. \quad (7.28)$$

Then the pdf of Θ for the specific case when β and $Z(t)$ follow normal distributions is derived as follows:

$$\begin{aligned} f_\Theta(\theta) &= \frac{dF_\Theta(\theta)}{d\theta} = -\frac{dF_{X_S}(H_1; \varphi, \theta)}{d\theta} = -\sum_{l=0}^{\infty} \phi \left(\frac{H_1 - (\varphi + \mu_\beta \theta + l\mu_Y)}{\sqrt{\sigma_\beta^2 \theta^2 + \sigma^2 + l\sigma_Y^2}} \right) \frac{e^{-\lambda\theta} (\lambda\theta)^l}{l!} \\ &\quad \times \left(\frac{-\mu_\beta (\sigma_\beta^2 \theta^2 + \sigma^2 + l\sigma_Y^2) - \sigma_\beta^2 \theta (H_1 - (\varphi + \mu_\beta \theta + l\mu_Y))}{(\sigma_\beta^2 \theta^2 + \sigma^2 + l\sigma_Y^2)^{\frac{3}{2}}} \right) \\ &\quad - \sum_{l=0}^{\infty} \Phi \left(\frac{H_1 - (\varphi + \mu_\beta \theta + l\mu_Y)}{\sqrt{\sigma_\beta^2 \theta^2 + \sigma^2 + l\sigma_Y^2}} \right) \frac{\lambda e^{-\lambda\theta} (\lambda\theta)^{l-1} (l - \lambda\theta)}{l!}, \end{aligned} \quad (7.29)$$

where $\phi(\cdot)$ is the pdf of a standard normal random variable. By using $(\varphi = 0, H_1 = H_w)$ and $(\varphi = H_r, H_1 = H_p)$, we can find the pdf of T_w and T_p , respectively.

7.3.5. Expected Cost Rate

As part of the average maintenance cost rate in (7.16), the expected total cost in a renewal cycle includes the expected values of the inspection, one time imperfect repair, preventive replacement, and corrective replacement costs:

$$E(C_T) = E \left[\begin{array}{c} \text{Inspection} \\ \text{Cost} \end{array} \right] + E \left[\begin{array}{c} \text{Imperfect} \\ \text{Repair Cost} \end{array} \right] + E \left[\begin{array}{c} \text{Preventive} \\ \text{Replacement Cost} \end{array} \right] + E \left[\begin{array}{c} \text{Corrective} \\ \text{Replacement Cost} \end{array} \right]. \quad (7.30)$$

Every time that the system is inspected, a fixed inspection cost is imposed to the system. The expected inspection cost in a renewal cycle is calculated as

$$E \left[\begin{array}{c} \text{Inspection} \\ \text{Cost} \end{array} \right] = C_I E[N_I] = C_I \sum_{i=1}^{\infty} i P(N_I = i). \quad (7.31)$$

The imperfect repair cost incurs when the system is repaired before replacement.

The expected imperfect repair cost during a renewal cycle is derived to be

$$E \left[\begin{array}{c} \text{Imperfect} \\ \text{Repair Cost} \end{array} \right] = C_{IR} \sum_{i=2}^{\infty} \sum_{j=1}^{i-1} P(N_{IR} = j) P(N_I = i). \quad (7.32)$$

The expected preventive replacement cost is formulated as

$$E \left[\begin{array}{c} \text{Preventive} \\ \text{Replacement Cost} \end{array} \right] = C_{PR} \sum_{i=1}^{\infty} P(N_{PR} = i). \quad (7.33)$$

Finally, the expected corrective replacement cost is

$$E \left[\begin{array}{c} \text{Corrective} \\ \text{Replacement Cost} \end{array} \right] = C_{CR} \sum_{i=1}^{\infty} P(N_{CR} = i). \quad (7.34)$$

We assume that $C_{CR} > C_{PR} > C_{IR} > C_I$.

7.4. Illustrative Examples

Numerical examples are presented to illustrate the reliability and maintenance models that were developed. The corresponding values for the parameters in reliability analysis are given in Table 7.1, where some parameters are adopted from the literature and others are assumptions based on typical and plausible values.

Table 7.1. Parameter values

Parameters	Values	Sources
H	$0.00125 \mu\text{m}^3$	(Tanner & Dugger 2003)
H_p	$0.00100 \mu\text{m}^3$	Assumption
H_w	$0.00075 \mu\text{m}^3$	Assumption
H_r	$0.00050 \mu\text{m}^3$	Assumption
D_e	1.55 Gpa	(Tanner & Dugger 2003)
D_r	1.20 Gpa	Assumption
φ	0	(Tanner & Dugger 2003)
μ_β	$8.4823 \times 10^{-9} \mu\text{m}^3$	(Tanner & Dugger 2003)
σ_β	$6.0016 \times 10^{-10} \mu\text{m}^3$	(Tanner & Dugger 2003)
μ_w	1.2 Gpa	Assumption
σ_w	0.2 Gpa	Assumption
μ_Y	$1.0 \times 10^{-4} \mu\text{m}^3$	Assumption
σ_Y	$2 \times 10^{-5} \mu\text{m}^3$	Assumption
σ	$10^{-10} \mu\text{m}^3$	Assumption
δ	2×10^3 revolutions	Assumption
λ	5×10^{-5} / revolutions	Assumption

For the described system, the reliability function $R(t)$ in (7.15) is plotted in Figure 7.7, and sensitivity analyses was performed to measure the effect of the changing parameters D_e , D_r , and δ on the reliability function (Figure 7.8-7.10). As shown in Figure 7.8, by increasing D_e , the critical level for the extreme shock model, from 1.55 Gpa to 1.65 Gpa, the $R(t)$ shifts to right. It can be inferred that by increasing the value of D_e , the reliability improves. Figure 7.9 shows that system reliability is sensitive to the parameter D_r , the critical level for the run shock model. Increasing D_r from 1.2 Gpa to 1.4 Gpa, causes

$R(t)$ to shift to right. As can be observed in Figure 7.10, the inter-arrival time threshold δ affects the reliability function. By increasing δ from 1.0×10^3 revolutions to 3.0×10^3 revolutions, the $R(t)$ shifts slightly to the left. It indicates that reliability performance is better for the smaller value of δ .

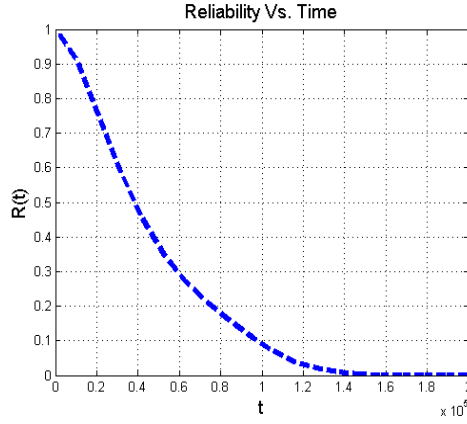


Figure 7.7: Plot of $R(t)$

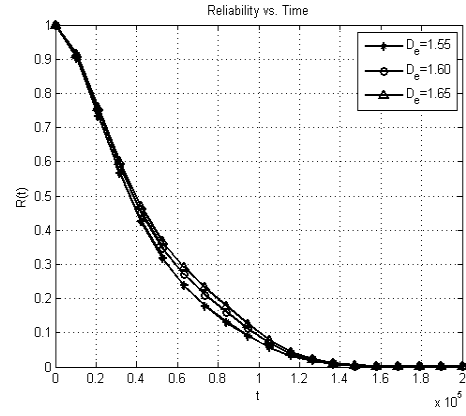


Figure 7.8: Sensitivity analysis of $R(t)$ on D_e

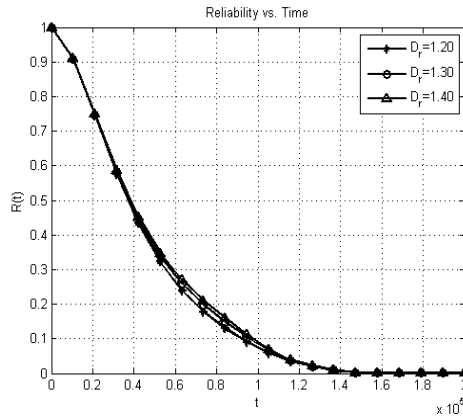


Figure 7.9: Sensitivity analysis of $R(t)$ on D_r

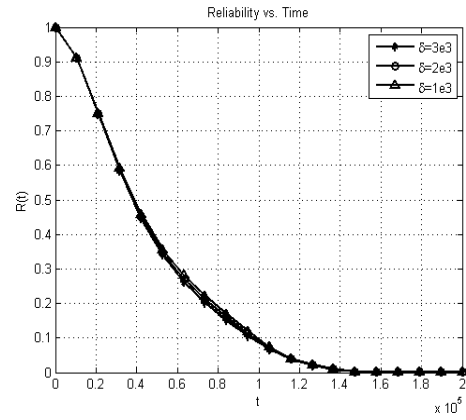


Figure 7.10: Sensitivity analysis of $R(t)$ on δ

To obtain the optimal time interval for the periodic inspection, we need to minimize the average long-run maintenance cost rate, $C_A(\tau)$ in (7.16). We use the simplex search method of Lagarias et al. (1998) that is a direct search method without using numerical or analytic gradients. For an example of $C_I = \$10$, $C_{IR} = \$50$, $C_{PR} = \$100$ and $C_{CR} = \$500$, the minimum average long-run maintenance cost rate is \$57.1585 that is obtained at $\tau^* =$

7.59×10^4 revolutions, the optimum inspection interval. Figure 7.11 presents $C_A(\tau)$ as a function of τ , obtained by using Matlab to solve this optimization problem. We also performed sensitivity analyses to capture the impact of the model parameters (H , H_p , H_w , and H_r) on the optimal solutions (Figures 7.12-7.15).

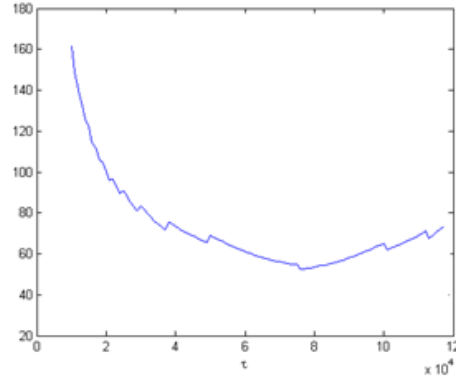


Figure 7.11: Average long-run maintenance cost rate versus inspection interval

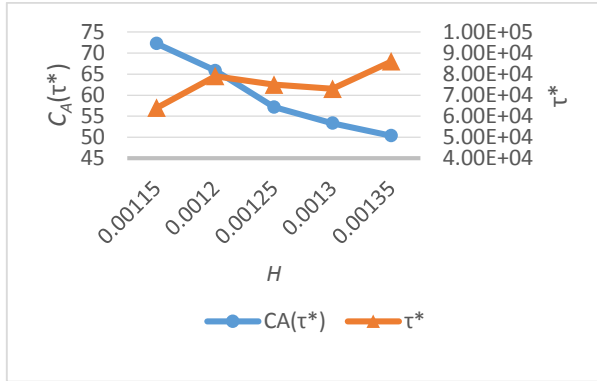


Figure 7.12: Sensitivity analysis of $C_A(\tau^*)$ and τ^* on H

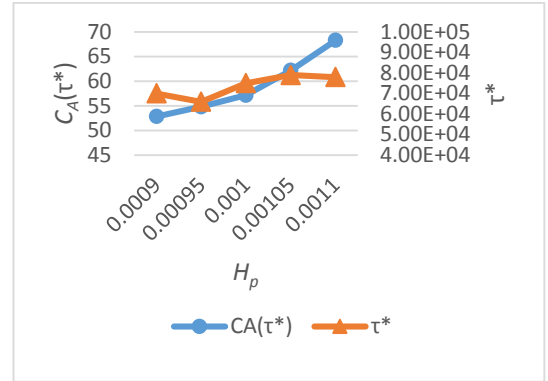


Figure 7.13: Sensitivity analysis of $C_A(\tau^*)$ and τ^* on H_p

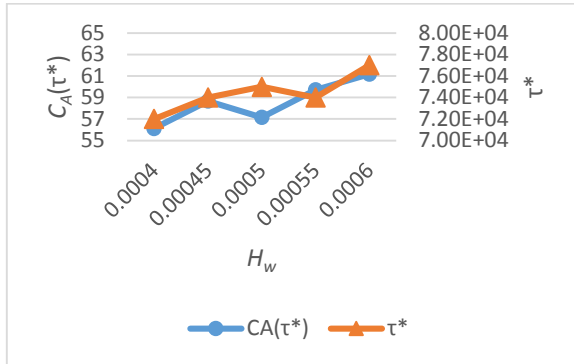


Figure 7.14: Sensitivity analysis of $C_A(\tau^*)$ and τ^* on H_w

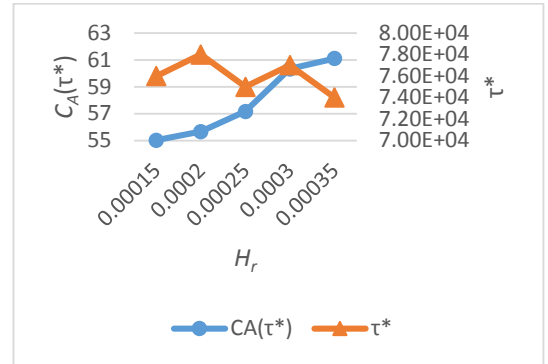


Figure 7.15: Sensitivity analysis of $C_A(\tau^*)$ and τ^* on H_r

7.5. Conclusions

In this chapter, we investigate the reliability modeling for a complex system subject to dependent competing risks of degradation-based failure and shock-based failure. The system experiences degradation-based failure when the overall degradation exceeds the critical threshold for degradation process. The shock-based failure occurs when the condition for the generalized mixed shock model is satisfied. The generalized mixed shock model is the combination of three classic shock models: extreme shock model, run shock model and δ -shock model. These three classic shock models are competing against each other, whichever occurs first can cause the system to fail.

We also develop a condition-based maintenance policy based on the reliability analysis. The proposed maintenance strategy incorporates various maintenance actions: imperfect repair, preventive replacement and corrective replacement. The decision regarding the appropriate maintenance action is made based on the information gathered about the real-time condition of the system through inspection. The maintenance strategy is analyzed through the numerical search of the optimal inspection interval that minimizes the cost rate of maintenance.

Chapter 8

Conclusions and Summary

Novel and evolving technologies such as MEMS, biomedical implant devices and other new device types continue to achieve innovative and impressive new features and capabilities. These new technologies are to be transitioned from low volume production or relatively simple design applications. However, there must also be associated new research focusing on reliability to develop new models and analysis tools that can assist manufacturing and maintenance of these evolving devices, and also to offer fundamentally new insights on the application of effective reliability analyses for technologies that have unique manufacturing challenges.

This research aims to develop new methodologies to model the system reliability by relaxing the assumption of independency between competing risks of degradation and random shocks to have more accurate estimation of system reliability. We also investigate various CBM policies for repairable systems to reduce maintenance cost by eliminating unnecessary replacement actions. Case studies on complex systems, e.g., MEMS, and biomedical implant systems, are provided to implement and demonstrate this new probabilistic and stochastic methodology to estimate system reliability and evaluate optimum maintenance policies.

In Chapter 3, we develop reliability models by considering the increasing degradation rate affected by the shock process. The degradation process can accelerate when the system becomes more susceptible to fatigue and deteriorates faster, as a result of withstanding shocks. We consider four classic shock models, including extreme shock model, δ -shock model, m -shock model, and run shock model that can cause the degradation

rate to transition. Then numerical results for MEMS are presented to illustrate the developed reliability models.

In Chapter 4, we study a system subject to dependent competing risks under the impact from a generalized mixed shock model. Random shocks imposed on a complex system can affect the system in three different ways simultaneously: 1) damage the unit by increasing the degradation level instantaneously; 2) speed up the deterioration process by accelerating the degradation rate; and 3) weaken the unit by reducing the hard failure threshold. While the first impact of non-fatal shocks comes from individual shocks, the other two impacts are realized when the condition for a generalized mixed shock model, a combination of three classic shock models, is satisfied. Based on degradation and random shock modeling, we present a reliability model by incorporating all these impacts due to the shock process in one extended model. An example using MEMS devices illustrates the effectiveness of the proposed model with sensitivity analysis.

In Chapter 5, we model reliability for complex systems subject to shifting hard failure threshold due to changes in degradation. In reality, a degraded system is more vulnerable to force and stress during operation. We assume the initial hard failure threshold value may reduce to a lower level as soon as the overall degradation reaches a critical value, or it may decrease continuously and the amount of reduction is proportional to the change in degradation. In addition, a new CBM model derived from FLP is also applied to ensure a device is functioning under a certain level of degradation. A numerical example based on MEMS example is used to demonstrate the developed reliability and maintenance models, along with sensitivity analysis.

In Chapter 6, based on reliability analysis for a multi-component system subject to both delayed and instantaneous failures, we extend the CBM policy presented in Chapter 5 for single-unit systems to be applied for multiple component systems. As a case study, the replacement policy for the multi-component system of stents implanted in human arteries is investigated.

In Chapter 7, we attempt to generalize the traditional mixed shock model by incorporating three, rather than two, classic shock models (i.e., extreme shock model, run shock model, and δ -shock model). We also propose a CBM policy considering imperfect repair for a system subject to dependent competing risks of internal degradation and such a generalized mixed shock process. Under the proposed CBM policy, the system is inspected at fixed time intervals and a decision for an appropriate maintenance action is made based on the actual health condition of the system detected through inspection. The objective is to determine the optimal inspection interval that minimizes the expected long-run average maintenance cost rate.

Several future research directions can be pursued to extend our reliability modeling considering dependence relationship between degradation process and shock process. Systems subject to multiple dependent degradation processes can be considered in future reliability modeling using stochastic processes. In our CBM policies, modern concepts associated with multi-objective optimization can be applied. Besides the real-world applications of MEMS and stents in this research, our integrated methodology can also be applied directly or customized for many other complex systems to optimize their operation and maintenance processes, such as power grids and oil pipelines.

References

- [1]. Abdel-Hameed, M. S., & Proschan, F. (1973), "Nonstationary shock models," *Stochastic Processes and Their Applications*, 1, 383–404.
- [2]. Abdel-Hameed, M. S., & Proschan, F. (1975), "Shock models with underlying birth process," *Journal of Applied Probability*, 12(1), 18–28.
- [3]. Agrafiotis, G. K., & Tsoukalas, M. Z. (1995), "On excess-time correlated cumulative processes," *The Journal of the Operational Research Society*, 46(10), 1269–1280.
- [4]. Bae, S. J., Kuo, W., & Kvam, P. H. (2007), "Degradation models and implied lifetime distributions," *Reliability Engineering & System Safety*, 92(5), 601–608.
- [5]. Bae, S. J., & Kvam, P. H. (2004) "A nonlinear random-coefficients model for degradation testing," *Technometrics*, 46(4), 460–469.
- [6]. Bai, J.-M., Li, Z.-H., & Kong, X.-B. (2006) "Generalized shock models based on a cluster point process," *IEEE Transactions on Reliability*, 55(3), 542–550.
- [7]. Bai, J.-M., Zhang, Z. G., & Li, Z.-H. (2014), "Lifetime properties of a cumulative shock model with a cluster structure," *Annals of Operations Research*, 212(1), 21–41.
- [8]. Bergman, B. (1978), "Optimal replacement under a general failure model," *Advances in Applied Probability*, 10(2), 431–451.
- [9]. Cha, J. H., & Finkelstein, M. (2009), "On a terminating shock process with independent wear increments," *Journal of Applied Probability*, 46(2), 353–362.
- [10]. Cha, J. H., & Finkelstein, M. (2013), "On history-dependent shock models," *Operations Research Letters*, 41(3), 232–237.

- [11]. Chelbi, A., & Ait-Kadi, D. (2000), "Generalized inspection strategy for randomly failing systems subjected to random shocks," *International Journal of Production Economics*, 64(1-3), 379–384.
- [12]. Chen, L. P., Ye, Z. S., & Huang, B. (2011), "Condition-based maintenance for systems under dependent competing failures," In *IEEE MTT-S International Microwave Workshop Series on Innovative Wireless Power Transmission: Technologies, Systems, and Applications* (pp. 1586–1590).
- [13]. Chiang, J. H., & Yuan, J. (2001), "Optimal maintenance policy for a Markovian system under periodic inspection," *Reliability Engineering & System Safety*, 71(2), 165–172.
- [14]. Chien, Y.-H., Sheu, S.-H., Zhang, Z. G., & Love, E. (2006), "An extended optimal replacement model of systems subject to shocks," *European Journal of Operational Research*, 175(1), 399–412.
- [15]. Chiodo, E., & Mazzanti, G. (2006), "Indirect reliability estimation for electric devices via a dynamic “Stress-strength” model," In *International Symposium on Power Electronics, Electrical Drives, Automation and Motion (SPEEDAM)* (pp. 903–908).
- [16]. Cho, D. I., & Parlar, M. (1991), "A survey of maintenance models for multi-unit systems," *European Journal of Operational Research*, 51(1), 1–23.
- [17]. Ciampoli, M. (1998), "Time dependent reliability of structural systems subject to deterioration," *Computers & Structures*, 67(1-3), 29–35.
- [18]. Cirillo, P., & Hüsler, J. (2011), "Extreme shock models: An alternative perspective," *Statistics & Probability Letters*, 81(1), 25–30.

- [19]. Daly, S., Miller, A., Ravichandran, G., & Bhattacharya, K. (2007), "An experimental investigation of crack initiation in thin sheets of nitinol," *Acta Materialia*, 55(18), 6322–6330.
- [20]. Dekker, R., Wildeman, R. E., & Duyn Schouten, F. A. (1997), "A review of multi-component maintenance models with economic dependence," *Mathematical Methods of Operations Research*, 45(3), 411–435.
- [21]. Ebrahimi, N. (2001), "A stochastic covariate failure model for sssessing system reliability," *Journal of Applied Probability*, 38(3), 761–767.
- [22]. Elsayed, E. A. (1996), Reliability engineering. Reading, MA: Addison Wesley.
- [23]. Elsayed, E. A. (2000), "Invited paper: Perspectives and challenges for research in quality and reliability engineering," *International Journal of Production Research*, 38(9), 1953–1976.
- [24]. Eryilmaz, S. (2012a), "Generalized δ -shock model via runs," *Statistics & Probability Letters*, 82(2), 326–331.
- [25]. Eryilmaz, S. (2012b), "Life behavior of a system under discrete shock model," *Discrete Dynamics in Nature and Society*, 2012, 1–12.
- [26]. Eryilmaz, S. (2013), "On the lifetime behavior of a discrete time shock model," *Journal of Computational and Applied Mathematics*, 237(1), 384–388.
- [27]. Esary, J. D., Marshall, A. W., & Proschan, F. (1973), "Shock models and wear processes," *The Annals of Probability*, 1(4), 627–649.
- [28]. Fan, H., Hu, C., Chen, M., & Zhou, D. (2011), "Cooperative predictive maintenance of repairable systems with dependent failure modes and resource constraint," *IEEE Transactions on Reliability*, 60(1), 144–157.

- [29]. Fan, J., Ghurye, S. G., & Levine, R. A. (2000), "Multicomponent lifetime distributions in the presence of ageing," *Journal of Applied Probability*, 37(3).
- [30]. Feng, Q., Rafiee, K., Keedy, E., Arab, A., Coit, D. W., & Song, S. (2014), "Reliability and condition-based maintenance analysis for multi-stent systems with stochastic dependent competing risk processes," Submitted to *Reliability Engineering & System Safety*.
- [31]. Finkelstein, M., & Marais, F. (2010), "On terminating Poisson processes in some shock models," *Reliability Engineering & System Safety*, 95(8), 874–879.
- [32]. Finkelstein, M. S., & Zarudnij, V. I. (2001), "A shock process with a non-cumulative damage," *Reliability Engineering & System Safety*, 71(1), 103–107.
- [33]. Fouladirad, M., & Grall, A. (2011), "Condition-based maintenance for a system subject to a non-homogeneous wear process with a wear rate transition," *Reliability Engineering & System Safety*, 96(6), 611–618.
- [34]. Frostig, E., & Kenzin, M. (2009), "Availability of inspected systems subject to shocks – A matrix algorithmic approach," *European Journal of Operational Research*, 193(1), 168–183.
- [35]. Gut, A. (2001), "Mixed shock models," *Bernoulli*, 7(3), 541–555.
- [36]. Gut, A., & Hüsler, J. (2005), "Realistic variation of shock models," *Statistics & Probability Letters*, 74(2), 187–204.
- [37]. Hosseini, M. M., Kerr, R. M., & Randall, R. B. (2000), "An inspection model with minimal and major maintenance for a system with deterioration and Poisson failures," *IEEE Transactions on Reliability*, 49(1), 88–98.

- [38]. Hsieh, M.-H., Jeng, S.-L., & Shen, P.-S. (2009), "Assessing device reliability based on scheduled discrete degradation measurements," *Probabilistic Engineering Mechanics*, 24(2), 151–158.
- [39]. Huang, W., & Askin, R. G. (2004), "A generalized SSI reliability model considering stochastic loading and strength aging degradation," *IEEE Transactions on Reliability*, 53(1), 77–82.
- [40]. Huang, W., & Dietrich, D. L. (2005), "An alternative degradation reliability modeling approach using maximum likelihood estimation," *IEEE Transactions on Reliability*, 54(2), 310–317.
- [41]. Huang, Y., Sai Sarathi Vasani, A., Doraiswami, R., Osterman, M., & Pecht, M. (2012), "MEMS reliability review," *IEEE Transactions on Device and Materials Reliability*, 12(2), 482–493.
- [42]. Huynh, K. T., Barros, A., Bérenguer, C., & Castro, I. T. (2011). "A periodic inspection and replacement policy for systems subject to competing failure modes due to degradation and traumatic events," *Reliability Engineering & System Safety*, 96(4), 497–508.
- [43]. Huynh, K. T., Castro, I. T., Barros, A., & Bérenguer, C. (2012), "Modeling age-based maintenance strategies with minimal repairs for systems subject to competing failure modes due to degradation and shocks," *European Journal of Operational Research*, 218(1), 140–151.
- [44]. Jardine, A. K. S., Lin, D., & Banjevic, D. (2006), "A review on machinery diagnostics and prognostics implementing condition-based maintenance," *Mechanical Systems and Signal Processing*, 20(7), 1483–1510.

- [45]. Jiang, L., Feng, Q., & Coit, D. W. (2012), "Reliability and maintenance modeling for dependent competing failure processes with shifting failure thresholds," *IEEE Transactions on Reliability*, 61(4), 932–948.
- [46]. Keedy, E., & Feng, Q. (2012), "A physics-of-failure based reliability and maintenance modeling framework for stent deployment and operation," *Reliability Engineering & System Safety*, 103, 94–101.
- [47]. Keedy, E., & Feng, Q. (2013), "Reliability analysis and customized preventive maintenance policies for stents with stochastic dependent competing risk processes," *IEEE Transactions on Reliability*, 62(4), 887–897.
- [48]. Kharoufeh, J. P. (2003), "Explicit results for wear processes in a Markovian environment," *Operations Research Letters*, 31(3), 237–244.
- [49]. Kharoufeh, J. P., & Cox, S. M. (2005), "Stochastic models for degradation-based reliability," *IIE Transactions*, 37(6), 533–542.
- [50]. Klutke, G.-A., & Yang, Y. (2002), "The availability of inspected systems subject to shocks and graceful degradation," *IEEE Transactions on Reliability*, 51(3), 371–374.
- [51]. Krieger, A. (1984), "On the probability of n consecutive successes out of N tries," *IEEE Transactions on Aerospace and Electronic Systems*, AES-20(6), 835–835.
- [52]. Lagarias, J. C., Reeds, J. a., Wright, M. H., & Wright, P. E. (1998), "Convergence properties of the nelder-mead simplex method in low dimensions," *SIAM Journal on Optimization*, 9(1), 112–147.
- [53]. Le, M. D., & Tan, C. M. (2013), "Optimal maintenance strategy of deteriorating system under imperfect maintenance and inspection using mixed inspectionscheduling," *Reliability Engineering & System Safety*, 113, 21–29.

- [54]. Lehmann, A. (2009), "Joint modeling of degradation and failure time data," *Journal of Statistical Planning and Inference*, 139(5), 1693–1706.
- [55]. Li, W., & Pham, H. (2005), "Reliability modeling of multi-state degraded systems with multi-competing failures and random shocks," *IEEE Transactions on Reliability*, 54(2), 297–303.
- [56]. Li, W., & Pham, H. (2011), "A condition-based maintenance model for periodically inspected systems subjected to competing failure processes," *International Journal of System Assurance Engineering and Management*, 2(3), 226–233.
- [57]. Li, Z., & Kong, X. (2007), "Life behavior of δ -shock model," *Statistics & Probability Letters*, 77(6), 577–587.
- [58]. Li, Z., & Zhao, P. (2007), "Reliability analysis on the δ -shock model of complex systems," *IEEE Transactions on Reliability*, 56(2), 340–348.
- [59]. Liao, H., Elsayed, E. a., & Chan, L.-Y. (2006), "Maintenance of continuously monitored degrading systems," *European Journal of Operational Research*, 175(2), 821–835.
- [60]. Liao, W., Pan, E., & Xi, L. (2009), "Preventive maintenance scheduling for repairable system with deterioration," *Journal of Intelligent Manufacturing*, 21(6), 875–884.
- [61]. Liu, X., Li, J., Al-Khalifa, K. N., Hamouda, A. S., Coit, D. W., & Elsayed, E. A. (2013), "Condition-based maintenance for continuously monitored degrading systems with multiple failure modes," *IIE Transactions*, 45(4), 422–435.
- [62]. Lu, C. J., & Meeker, W. Q. (1993), "Using degradation measures to estimate a time-to-failure distribution," *Technometrics*, 35(2), 161–174.

- [63]. Mallor, F., & Omei, E. (2001), "Shocks, runs and random sums," *Journal of Applied Probability*, 38(2), 438–448.
- [64]. Mallor, F., Omei, E., & Santos, J. (2006), "Asymptotic results for a run and cumulative mixed shock model," *Journal of Mathematical Sciences*, 138(1), 5410–5414.
- [65]. Mallor, F., & Santos, J. (2003), "Classification of shock models in system reliability," *Monografías Del Semin. Matem. Garcia de Galdeano*, 27, 405–412.
- [66]. Marrey, R. V., Burgermeister, R., Grishaber, R. B., & Ritchie, R. O. (2006), "Fatigue and life prediction for cobalt-chromium stents: A fracture mechanics analysis," *Biomaterials*, 27(9), 1988–2000.
- [67]. Meeker, W. Q., & Hamada, M. (1995), "Statistical tools for the rapid development and evaluation of high-reliability products," *IEEE Transactions on Reliability*, 44(2), 187–198.
- [68]. Meeker, W. Q., & LuValle, M. J. (1995), "An accelerated life test model based on reliability kinetics," *Technometrics*, 37(2), 133–146.
- [69]. Miller, S. L., Rodgers, M. S., LaVigne, G., Sniegowski, J. J., Clews, P., Tanner, D. M., & Peterson, K. a. (1998), "Failure modes in surface micromachined microelectromechanical actuators," In *IEEE International Reliability Physics Symposium Proceedings 36th Annual* (pp. 17–25).
- [70]. Montoro-Cazorla, D., & Pérez-Ocón, R. (2006), "A deteriorating two-system with two repair modes and sojourn times phase-type distributed," *Reliability Engineering & System Safety*, 91(1), 1–9.

- [71]. Nicolai, R. P., Dekker, R., & van Noortwijk, J. M. (2007), "A comparison of models for measurable deterioration: An application to coatings on steel structures," *Reliability Engineering & System Safety*, 92(12), 1635–1650.
- [72]. Pandey, M. D., Yuan, X.-X., & van Noortwijk, J. M. (2005), "Gamma process model for reliability analysis and replacement of aging structural components," In *Nineth International Conference on Structural Safety and Reliability* (pp. 2439–2444).
- [73]. Peng, H., Feng, Q., & Coit, D. W. (2009), "Simultaneous quality and reliability optimization for microengines subject to degradation," *IEEE Transactions on Reliability*, 58(1), 98–105.
- [74]. Peng, H., Feng, Q., & Coit, D. W. (2010), "Reliability and maintenance modeling for systems subject to multiple dependent competing failure processes," *IIE Transactions*, 43(1), 12–22.
- [75]. Qian, C., Nakamura, S., & Nakagawa, T. (2003), "Replacement and minimal repair policies for a cumulative damage model with maintenance," *Computers & Mathematics with Applications*, 46(7), 1111–1118.
- [76]. Rafiee, K., Feng, Q., & Coit, D. W. (2014a), "Reliability analysis and condition-based maintenance for failure processes with degradation-dependent hard failure threshold," Submitted to *IIE Transactions*.
- [77]. Rafiee, K., Feng, Q., & Coit, D. W. (2014b), "Reliability modeling for dependent competing failure processes with changing degradation rate," *IIE Transactions*, 46(5), 483–496.

- [78]. Robertson, S. W., & Ritchie, R. O. (2007), "In vitro fatigue-crack growth and fracture toughness behavior of thin-walled superelastic Nitinol tube for endovascular stents: A basis for defining the effect of crack-like defects," *Biomaterials*, 28(4), 700–9.
- [79]. Robinson, M. E., & Crowder, M. J. (2000), "Bayesian methods for a growth-curve degradation model with repeated measures," *Lifetime Data aAnalysis*, 6(4), 357–74.
- [80]. Saassouh, B., Dieulle, L., & Grall, A. (2007), "Online maintenance policy for a deteriorating system with random change of mode," *Reliability Engineering & System Safety*, 92(12), 1677–1685.
- [81]. Satow, T., Teramoto, K., & Nakagawa, T. (2000), "Optimal replacement policy for a cumulative damage model with time deterioration," *Mathematical and Computer Modelling*, 31(10-12), 313–319.
- [82]. Shanthikumar, J. G., & Sumita, U. (1983), "General shock models associated with correlated renewal sequences," *Journal of Applied Probability*, 20(3), 600–614.
- [83]. Sheu, S.-H., Chang, C.-C., Zhang, Z. G., & Chien, Y.-H. (2012), "A note on replacement policy for a system subject to non-homogeneous pure birth shocks," *European Journal of Operational Research*, 216(2), 503–508.
- [84]. Sim, S. H., & Endrenyi, J. (1993), "A failure-repair model with minimal and major maintenance," *IEEE Transactions on Reliability*, 42(1), 134–140.
- [85]. Singpurwalla, N. D. (1995), "Survival in dynamic environments," *Statistical Science*, 10(1), 86–103.
- [86]. Skoulakis, G. (2000), "A general shock model for a reliability system," *Journal of Applied Probability*, 37(4), 925–935.

- [87]. Sumita, U., & Shanthikumar, G. (1985), "A class of correlated cumulative shock models," *Advances in Applied Probability*, 17(2), 347–366.
- [88]. Suzuki, K., Maki, K., & Yokogawa, S. (1993), "An analysis of degradation data of a carbon film and properties of the estimators," *Statistical Sciences and Data Analysis*, 501–511.
- [89]. Taghipour, S., & Banjevic, D. (2012), "Optimal inspection of a complex system subject to periodic and opportunistic inspections and preventive replacements," *European Journal of Operational Research*, 220(3), 649–660.
- [90]. Taguchi, G. (1986), Introduction to quality engineering: designing quality into products and processes, Asian Productivity Organization.
- [91]. Taguchi, G. (1987). System of experimental design: engineering methods to optimize quality and minimize costs, (D. Clausing, Ed.), New York: UNIPUB/Kraus International Publications.
- [92]. Tan, L., Cheng, Z., Guo, B., & Gong, S. (2010), "Condition-based maintenance policy for gamma deteriorating systems," *Journal of Systems Engineering and Electronics*, 21(1), 57–61.
- [93]. Tanner, D. M. (2009), "MEMS reliability: Where are we now?" *Microelectronics Reliability*, 49(9-11), 937–940.
- [94]. Tanner, D. M., & Dugger, M. (2003a), "Wear mechanisms in a reliability methodology," In *Proceedings of SPIE* (Vol. 4980, pp. 22–40).
- [95]. Tanner, D. M., & Dugger, M. T. (2003b), "Wear mechanisms in a reliability methodology," In R. Ramesham & D. M. Tanner (Eds.), *Reliability, Testing, and Characterization of MEMS/MOEMS II* (Vol. 4980, pp. 22–40).

- [96]. Tanner, D. M., Walraven, J. a., Helgesen, K., Irwin, L. W., Brown, F., Smith, N. F., & Masters, N. (2000), "MEMS reliability in shock environments," In *IEEE International Reliability Physics Symposium Proceedings. 38th Annual (Cat. No.00CH37059)* (pp. 129–138).
- [97]. Thomas, L. C. (1986), "A survey of maintenance and replacement models for maintainability and reliability of multi-item systems," *Reliability Engineering*, 16(4), 297–309.
- [98]. Van der Weide, J. A. M., Pandey, M. D., & van Noortwijk, J. (2010), "Discounted cost model for condition-based maintenance optimization," *Reliability Engineering & System Safety*, 95(3), 236–246.
- [99]. Van, P. Do, & Bérenguer, C. (2012), "Condition-based maintenance with imperfect preventive repairs for a deteriorating production system," *Quality and Reliability Engineering International*, 28(6), 624–633.
- [100]. Van Noortwijk, J. M., Cooke, R. M., & Kok, M. (1995), "A Bayesian failure model based on isotropic deterioration," *European Journal of Operational Research*, 82(2), 270–282.
- [101]. Van Noortwijk, J. M., & Pandey, M. D. (2003), "A stochastic deterioration process for time-dependent reliability analysis," In *The Eleventh IFIP WG 7.5 Working Conference on Reliability and Optimization of Structural Systems* (pp. 259–265).
- [102]. Van Noortwijk, J. M., van der Weide, J. A. M., Kallen, M. J., & Pandey, M. D. (2007), "Gamma processes and peaks-over-threshold distributions for time-dependent reliability," *Reliability Engineering & System Safety*, 92(12), 1651–1658.

- [103]. Wang, G. J., & Zhang, Y. L. (2005), "A shock model with two-type failures and optimal replacement policy," *International Journal of Systems Science*, 36(4), 209–214.
- [104]. Wang, H. (2002), "A survey of maintenance policies of deteriorating systems," *European Journal of Operational Research*, 139(3), 469–489.
- [105]. Wang, Y., & Pham, H. (2011a), "A multi-objective optimization of imperfect preventive maintenance policy for dependent competing risk systems with hidden failure," *IEEE Transactions on Reliability*, 60(4), 770–781.
- [106]. Wang, Y., & Pham, H. (2011b), "Imperfect preventive maintenance policies for two-process cumulative damage model of degradation and random shocks," *International Journal of System Assurance Engineering and Management*, 2(1), 66–77.
- [107]. Wang, Y., & Pham, H. (2012), "Modeling the dependent competing risks with multiple degradation processes and random shock using time-varying copulas," *IEEE Transactions on Reliability*, 61(1), 13–22.
- [108]. Wang, Z., Huang, H.-Z., Li, Y., & Xiao, N.-C. (2011), "An approach to reliability assessment under degradation and shock process," *IEEE Transactions on Reliability*, 60(4), 852–863.
- [109]. Wang, Z.-L., Du, L., & Huang, H.-Z. (2008), "Reliability modeling for dependent competitive failure processes," In *Annual Reliability and Maintainability Symposium* (pp. 278–282).

- [110]. Wortman, M. a., Klutke, G. -a., & Ayhan, H. (1994), "A maintenance strategy for systems subjected to deterioration governed by random shocks," *IEEE Transactions on Reliability*, 43(3), 439–445.
- [111]. Wu, S., & Shao, J. (1999), "Reliability analysis using the least squares method in nonlinear mixed-effect degradation models," *Statistica Sinica*, 9, 855–877.
- [112]. Xue, J., & Yang, K. (1995), "Dynamic reliability analysis of coherent multistate systems," *IEEE Transactions on Reliability*, 44(4), 683–688.
- [113]. Ye, Z. S., Tang, L. C., & Xu, H. Y. (2011), "A distribution-based systems reliability model under extreme shocks and natural degradation," *IEEE Transactions on Reliability*, 60(1), 246–256.
- [114]. Ye, Z.-S., Shen, Y., & Xie, M. (2012), "Degradation-based burn-in with preventive maintenance," *European Journal of Operational Research*, 221(2), 360–367.
- [115]. Yuan, X.-X., & Pandey, M. D. (2009), "A nonlinear mixed-effects model for degradation data obtained from in-service inspections," *Reliability Engineering & System Safety*, 94(2), 509–519.
- [116]. Zhao, X., Fouladirad, M., Bérenguer, C., & Bordes, L. (2010), "Condition-based inspection/replacement policies for non-monotone deteriorating systems with environmental covariates," *Reliability Engineering & System Safety*, 95(8), 921–934.
- [117]. Zhu, Y., Elsayed, E. A., Liao, H., & Chan, L. Y. (2010), "Availability optimization of systems subject to competing risk," *European Journal of Operational Research*, 202(3), 781–788.

Appendices

Appendix I: The Probability of no Hard Failure given $S_1 \leq N(t) = i$ in Section 4.2.3

Given the shock count for the first transition is less than or equal to $N(t)$, $S_1 = s_1 \leq N(t) = i$, we have

$$\begin{aligned}
 R_H(t | S_1 = s_1 \leq N(t) = i) &= \sum_{s_l=1}^{I_l} \cdots \sum_{s_2=1}^{I_2} \sum_{l=1}^L R_H \left(t | \bigcap_{j=1}^l \{S_j = s_j\}, S_{l+1} > I_{l+1} \right) \\
 &\times P \left(S_{l+1} > I_{l+1} | \bigcap_{j=1}^l \{S_j = s_j\} \right) \left[\prod_{j=2}^l P \left(S_j = s_j | \bigcap_{k=1}^{j-1} \{S_k = s_k\} \right) \right] \\
 &= \sum_{s_l=1}^{i_l} \cdots \sum_{s_2=1}^{i_2} \sum_{l=1}^L P \left(\bigcap_{j=1}^l \bigcap_{z=1}^{s_j} \{W_z < D_j\}, \bigcap_{z=1}^{i_{l+1}} \{W_z < D_{l+1}\} \right) P(S_{l+1} > i_{l+1}) \left[\prod_{j=2}^l P(S_j = s_j) \right] \\
 &= \sum_{s_l=1}^{i_l} \cdots \sum_{s_2=1}^{i_2} \sum_{l=1}^L \left[\prod_{j=1}^l F_W(D_j)^{s_j} \right] F_W(D_{l+1})^{i_{l+1}} P(S_{l+1} > i_{l+1}) \left[\prod_{j=2}^l P(S_j = s_j) \right].
 \end{aligned} \tag{A.1}$$

This formula derives the probability of no hard failure when the system experiences at least one transition by time t , i.e., the shock count for the $l + 1^{th}$ transition is greater than the number of remaining shocks after the l^{th} transition, $S_{l+1} > I_{l+1}$.

Appendix II: The Probability of no Soft Failure given $S_1 \leq N(t) = i$ in Section 4.2.4

Similar to the derivation in Appendix I, the following derivation takes into account when there is at least one transition by time t , i.e., the shock count for the $l + 1^{th}$ transition is greater than the number of remaining shocks after the l^{th} transition, $S_{l+1} > I_{l+1}$:

$$\begin{aligned}
 R_S(t | S_1 = s_1 \leq N(t) = i) &= \sum_{s_l=1}^{I_l} \cdots \sum_{s_2=1}^{I_2} \sum_{l=1}^L P \left(X_S(t) < H | \bigcap_{j=1}^l \{S_j = s_j\}, S_{l+1} > I_{l+1} \right) \\
 &\times P \left(S_{l+1} > I_{l+1} | \bigcap_{j=1}^l \{S_j = s_j\} \right) \left[\prod_{j=2}^l P \left(S_j = s_j | \bigcap_{k=1}^{j-1} \{S_k = s_k\} \right) \right] \\
 &= \sum_{s_l=1}^{i_l} \cdots \sum_{s_2=1}^{i_2} \sum_{l=1}^L P \left(\varphi + \sum_{j=1}^l \beta_j T_j + \beta_{l+1} T_{l+1} + \sum_{z=1}^i Y_z < H \right) P(S_{l+1} > i_{l+1}) \left[\prod_{j=2}^l P(S_j = s_j) \right].
 \end{aligned} \tag{A.2}$$

Appendix III: List of Publications

Refereed Journal Papers

- [1]. Rafiee, K., Feng, Q. & Coit, D.W. (2014), “Reliability modeling for dependent competing failure processes with changing degradation rate,” *IIE Transactions*, 46(5), 483-496. (Featured in the IE Magazine)

Submitted Journal Papers

- [1]. Rafiee, K., Feng, Q. & Coit, D.W. (2014), “Reliability analysis and condition-based maintenance for failure processes under degradation-dependent hard failure threshold,” *IIE Transactions*.
- [2]. Rafiee, K., Feng, Q. & Coit, D. W. (2014), “Reliability assessment of competing risks with generalized mixed shock model,” *IEEE Transactions on Reliability*.
- [3]. Rafiee, K., Feng, Q., Arab, A. & Coit, D. W. (2014), “Reliability analysis and condition-based maintenance for implanted multi-stent systems with stochastic dependent competing risk processes,” *Reliability Engineering & System Safety*.
- [4]. Rafiee, K. & Feng, Q. (2014), “Periodic condition-based maintenance with imperfect repair for deteriorating systems subject to generalized mixed shock model,” *IEEE Transactions on Reliability*.

Refereed Conference Proceedings

- [1]. Rafiee, K., Feng, Q. & Coit, D. W., “Reliability assessment of dependent competing risks with mixed shock model,” Industrial and Systems Engineering Research Conference (*ISERC*), San Juan, Puerto Rico, May 2013 (Honorable Mention).

Conference Presentations

- [1]. Rafiee, K., Feng, Q. & Coit, D. W., “Reliability analysis for failure processes under degradation-dependent hard failure threshold,” *INFORMS* Annual Meeting, Minneapolis, MN, October 2013.
- [2]. Rafiee, K., Feng, Q. & Coit, D. W., “Reliability analysis for dependent competing risk processes with degradation rate transition,” *INFORMS* Annual Meeting, Minneapolis, MN, October 2013.
- [3]. Rafiee, K., Feng, Q. & Coit, D. W., “Reliability assessment of dependent competing risks with mixed shock model,” Industrial and Systems Engineering Research Conference (*ISERC*), San Juan, Puerto Rico, May 2013.

Poster Presentation

- [1]. Rafiee, K., “Reliability analysis of deteriorating systems subject to generalized mixed shock model,” Doctoral Colloquium Session - Industrial and Systems Engineering Research Conference (*ISERC*), San Juan, Puerto Rico, May 2013.